Development of Sulfolane Modified Electrode Sensor for the Determination of Vitamin-B_6, Vitamin-C and Uric Acid

by

Shahin Ara Mitu

A thesis submitted in partial fulfillment of the requirements for the degree of

Master of Science in Chemistry

Khulna University of Engineering & Technology

Khulna 9203, Bangladesh.

May 2017

Declaration

This is to certify that the thesis work entitled "Development of Sulfolane Modified Electrode Sensor for the Determination of Vitamin-B_6, Vitamin-C and Uric acid" has been carried out by Shahin Ara Mitu in the Department of Chemistry, Khulna University of Engineering & Technology, Khulna, Bangladesh. The above thesis work has not been submitted anywhere for the award of any degree or diploma.

Signature of Supervisor

Signature of Candidate

Acknowledgements

The author is extremely indebted to the Almightily Allah for the successful completion of the research work and the preparation of this dissertation.

The author expresses her deepest sense of gratitude and indebtedness to her respective and honorable supervisor **Dr. Md. Abdul Motin**, Professor and Head, Department of Chemistry, Khulna University of Engineering & Technology, Khulna for providing me the opportunity of working under his kind supervision. He had helped me at each and every point of the thesis work with his dedication, comments, suggestions and guidance which put me on the right path to fulfill the requirement, without which this situation was impossible to overcome. I learnt a lot of things from him, not only the academic knowledge, but also the way of research. This will be precious wealth in all my future academic life. Our communication is always flexible and efficient. He also friendly supported me a lot in my daily life which I am truly comprehended.

Again the author bestows thanks to her respective teacher **Md. Abdul Hafiz Mia**, Lecturer, Department of Chemistry, Khulna University of Engineering & Technology, Khulna for his lucid cooperation and necessary advice during the period of study.

The author wishes to offer deepest appreciation to all her friends and well-wishers especially **Md. Bodrul Alom** and **Md. Nazim Uddin** for their continuous support and help.

The author feels proud to express her sincere appreciation and indebtedness to her parents, family members who always blessed, inspired and sacrificed a lot in the long process of building her academic career which can never be repaid.

Shahin Ara Mitu

Abstract

Vitamin-B_6 (VB_6) and Vitamin-C (VC) are important biomolecules and are widely used as food additives or antioxidants and for the treatment of anemia, depression, acute seizures, scurvy, cold problems etc. Uric acid (UA) is the primary end product of purine metabolism. UA also coexists with VB_6 and VC in biological fluids such as blood and urine. In this study, a simple and sensitive modified electrode sensor has been developed using Sulfolane (SFL) as a trifunctional electrochemical sensor for the determination of VB_6, VC and UA. Cyclic voltammetry (CV), Differential pulse voltammetry (DPV) and UV-Visible spectroscopy were performed as detection techniques.

In this work, glassy carbon (GC), gold (Au) and platinum (Pt) electrodes were used as the working electrode. The electrodes were modified with SFL by applying continuous potential cycle for 15 scans at a range of -1.0 to 2.0 V at 100 mV s^{-1}. Then the electrodes were activated in phosphate buffer solution (PBS) (pH 7) by applying continuous potential cycle for 5 scans at a range of -0.5 V to 1.2 V. A ternary solution of VB_6, VC and UA was prepared and the CV and DPV were taken at the modified (GC, Au and Pt) electrodes. It is seen that the performance of modified GC electrode is better than the modified Au and Pt electrodes.

The influence of pH has been studied by varying pH from 3 to 9. The detection was mostly favorable at pH 7. The effect of different scan rates has been discussed and the variation of peak current was plotted with square root of scan rate. The peak current increases with the increase of square root of scan rates. The nearly proportionality of the peak current suggests that the peak current of the reactant at each redox reaction is controlled by diffusion process with some chemical complications.

The effect of bare and modified GC electrode on single, binary and ternary solution of VB_6, VC and UA have been studied. CVs of the single solution of VC, UA and VB_6 at bare GC electrode shows the oxidation peaks at 0.34 V, 0.35 V and 0.74 V respectively. But at modified GC electrode VC, UA and VB_6 gives the oxidation peaks at 0.15 V, 0.33V and 0.72 V respectively. At bare GC electrode, the ternary mixture of VC, UA and VB_6

shows two oxidation peaks at 0.5 V and 0.74 V. But SFL modified GC electrode shows three separated and well defined oxidation peaks at 0.18 V, 0.34 V and 0.79 V respectively. The peak intensity of SFL modified electrode was high compared with the bare GC electrode. Similar behavior have been seen in the DPV technique.

Quantitative analysis of VB_6, VC and UA have been carried out by DPV using SFL modified GC electrode in a single, binary and ternary solution. In every case, the peak currents of VB_6, VC and UA increased linearly with increasing their concentrations over the range of 0.5-2.5mM. The SFL modified GC electrode showed good selectivity and strong anti-interference activity for the determination of VB_6, VC and UA in binary and ternary mixture with excellent results. The limit of detection (LoD) has been calculated by signal-to-noise ratio (S/N=3). For the simultaneous concentration change, the LoD for VB_6, VC and UA at SFL modified GC electrode are 0.8 μML^{-1}, 1.0 μML^{-1} and 0.2 μML^{-1} respectively. The sensitivity of VB_6, VC and UA are 41.84 $\mu A/mM/cm^2$, 31.12 $\mu A/mM/cm^2$ and 138.14 $\mu A/mM/cm^2$ respectively at SFL modified GC electrode.

The practical application of the SFL modified electrode sensor was demonstrated by the determination of VB_6 and VC in pharmaceutical tablet samples and UA in blood sample. The results have been valided by UV-Vis spectroscopic method and pathological method. The amount of VB_6 and VC in some well-established pharmaceutical (Beximco, ACI, Square, Aristopharma, Opsonin, ACME etc) tablet samples have been found approximately same with compared to the labeled value. The single determination of VB_6, VC and UA in tablet and blood samples by SFL modified GC electrode is very consistent with the determination of VB_6, VC and UA by UV-Vis spectroscopic method and pathological method in the same samples. Thus it is suggested that the SFL modified sensor may be used in the pharmaceutical industry and pathology for the determination of VB_6, VC and UA.

Contents

LIST OF TABLES

LIST OF FIGURES

CHAPTER I

Introduction

1.1 General

Electroanalytical chemistry is an active field of modern research. It is the branch of analytical chemistry that employs electrochemical methods for the study of the separation, identification and quantification of the chemical components of natural and artificial materials. This is divided into two categories. First one, qualitative analysis that gives the indication of the identity of the chemical species in the sample and the second one, quantitative analysis that determines the amount of certain components in the substance. It is the branch of physical chemistry that studies chemical reactions which take place at the interface of an electrode, usually a solid metal or a semiconductor, and an ionic conductor, the electrolyte. These reactions involve electric charges moving between the electrodes and the electrolyte (or ionic species in a solution), the interaction between electrical energy and chemical change [1, 2].

Electroanalytical methods are the most powerful and popular techniques used in analytical chemistry [3-5]. These methods are a class of techniques in analytical chemistry which study an analyte by measuring the potential (volts) and/or current (amperes) in an electrochemical cell containing the analyte. These methods can be broken down into several categories depending on which aspects of the cell are controlled and which are measured. The three main categories are potentiometry (the difference in electrode potentials is measured), coulometry (the cell's current is measured over time), and voltammetry (the cell's current is measured while actively altering the cell's potential).

Electroanalytical chemistry can play a very important role in the protection of our environment. In particular, electrochemical sensors and detectors are very attractive in the fields of environmental conservation and monitoring, disaster and disease prevention, and industrial analysis. A typical chemical sensor is a device that transforms chemical

information in a selective and reversible way, ranging from the concentration of a specific sample component to total composition analysis, into an analytically useful signal. The interest in electrochemical sensors continues unabated today, stimulated by the wide range of potential applications. Their impact is most clearly illustrated in the widespread use of electrochemical sensors seen in daily life, where they continue to meet the expanding need for rapid, simple and economic methods of determination of numerous analytes [6-8]. A huge number of research effort has taken place over the several years to achieve electrochemical sensors. Electrochemical sensors have attractive qualities, which can boast the following advantages:

1) Low detection and determination limits,
2) high sensitivity,
3) relative simplicity and rapidity,
4) wide spectrum of the analyte (especially drug compounds),
5) insignificant effect of the matrix (from endogenous substances in biological media or from excipients in pharmaceutical dosage forms),
6) low cost of equipment.

Recent advances in electrochemical sensor technology will certainly expand the scope of these devices towards a wide range of organic and inorganic contaminants and will facilitate their role in field analysis. These advances include the introduction of modified or ultra-microelectrodes, the design of highly selective chemical or biological recognition layers, of molecular devices or sensor arrays, and developments in the areas of micro fabrication, computerized instrumentation and flow detectors [9-11].

1.2 Sensor

The development of chemical and biological sensors is currently one of the most active areas of analytical research. Sensors are small devices that incorporate a recognition element with a signal transducer. Such devices can be used for direct measurement of the analyte in the sample matrix [12]. Chemical sensors have been widely used in applications such as critical care, safety, industrial hygiene, process controls, product quality controls, human comfort controls, emissions monitoring, automotive, clinical diagnostics, home safety alarms, and, more recently, homeland security. In these applications, chemical

sensors have resulted in both economic and social benefits. A useful definition for a chemical sensor is ‘‘a small device that as the result of a chemical interaction or process between the analyte and the sensor device, transforms chemical or biochemical information of a quantitative or qualitative type into an analytically useful signal” [13]. The biosensors can be defined in terms of sensing aspects, where these sensors can sense biochemical compounds such as biological proteins, nucleotides and even tissues [14].

1.3 Types of chemical sensors

Chemical sensors are categorized into the following groups according to the transducer type.

1.3.1 Optical sensor

It relies on an optical transducer for signal measurement. In optical sensors there is a spectroscopic measurement associated with the chemical reaction. Normally it involve a two phase system in which the reagents are immobilized in or on a solid substrate such as a membrane which changes color in the presence of a solution of the analyte. Optical sensors are often referred to as ‘optodes’ and the use of optical fibres is a common feature. Absorbance, reflectance and luminescence measurements are used in the different types of optical sensors.

1.3.2 Mass sensitive sensor

These make use of the piezoelectric effect and include devices such as the surface acoustic wave (SAW) sensor and are particularly useful as gas sensors. They rely on a change in mass on the surface of an oscillating crystal which shifts the frequency of oscillation. The extent of the frequency shift is a measure of the amount of material adsorbed on the surface.

1.3.3 Heat sensitive sensor

Chemical reactions produce heat and the quantity of the heat produced depends on the amounts of the reactants. Thus, the measurement of heat of reaction can be related to the amount of a particular reactant. Measurements of the heats of reaction form the basis of the field of calorimetry and this has provided a class of chemical sensors which has gained considerable importance. Calorimetric sensors, like all other chemical sensors, have a region where a chemical reaction takes place and a transducer which responds to heat.

There are three classes of calorimetric sensors which are of particular importance. The first uses a temperature probe such as a thermistor as the transducer to sense the heat involved in a reaction on its surface. The second class of calorimetric sensors is referred to as catalytic sensors and is used for sensing flammable gases. The third class is called thermal conductivity sensors and this sense a change in the thermal conductivity of the atmosphere in the presence of a gas. This is the basis of the thermal conductivity detector which has been used for many years in gas chromatography [15].

1.3.4 Electrochemical sensor

Electrochemical sensors, in which an electrode is used as the transducer element, represent an important subclass of chemical sensors. Electrochemical sensors are essentially an electrochemical cell which employs a two or three electrode arrangement. Electrochemical sensor measurement can be made at steady-state or transient. The applied current or potential for electrochemical sensors may vary according to the mode of operation, and the selection of the mode is often intended to enhance the sensitivity and selectivity of a particular sensor.

Depending on the exact mode of signal transduction, electrochemical sensors can use a range of modes of detection such as potentiometric, voltammetric and conductimetric. Each principle requires a specific design of the electrochemical cell. Potentiometric sensors are very attractive for field operations because of their high selectivity, simplicity and low cost. They are, however, less sensitive and often slower than their voltammetric counterparts. Examples of transduction techniques include:

- Potentiometric – The measurement of the potential at zero current. The potential is proportional to the logarithm of the concentration of the substance being determined.

- Voltammetric – Increasing or decrease the potential that is applied to a cell until the oxidation or reduction of the analyte occurs. This generates a rise in current that is proportional to the concentration of the electroactive potential. Once the desired stable oxidation/reduction potential is known, stepping the potential directly to that value and observing the current is known as amperometry.

- Conductiometric – Observing changes in electrical conductivity of the solution. [16]

The selection and development of an active material is a challenge. The active sensing materials may be of any kind as whichever acts as a catalyst for sensing a particular analyte or a set of analytes. The recent development in the modified electrode sensors has paved the way for large number of new materials and devices of desirable properties which have useful functions for numerous electrochemical sensor and biosensor applications [17].

1.4 Chemically modified electrodes

Chemically modified electrodes (CMEs) comprise a relatively modem approach to electrode systems a wide spectrum of basic electrochemical investigations, including the relationship of heterogeneous electron transfer and chemical reactivity to electrode surface chemistry, electrostatic phenomena at electrode surfaces, and electron and ionic transport phenomena in polymers, and the design of electrochemical devices and systems for applications in chemical sensing, energy conversion and storage, molecular electronics, electrochromic displays, corrosion protection, and electro-organic syntheses. Compared with other electrode concepts in electrochemistry, the distinguishing feature of a CME is that a generally quite thin film (from a molecular monolayer to perhaps a few micrometers-thick multilayer) of a selected chemical is bonded to or coated on the electrode surface to endow the electrode with the chemical, electrochemical, optical,

electrical, transport, and other desirable properties of the film in a rational, chemically designed manner [18].

The range of electrode surface properties includes, but is more diverse than, that of ion-selective electrodes (ISEs) which also involve, in their highest forms, rational design of the phase-boundary, partition and transport properties of membranes on or between electrodes. While CMEs can operate both voltammetrically and potentiometrically, they are generally used voltammetrically, a redox (electron transfer) reaction being the basis of experimental measurement or study, whereas ISEs are generally used in potentiometric formats where a phase-boundary potential (interfacial potential difference) is the measured quantity [19]. Gas-sensing electrodes (e.g., for $C0_2$, NH_3, NOx) are also potentiometrically based [20] although the oxygen electrode, which functions amperometri -cally, is an exception [21]. Chemically sensitive field effect transistors (CHEMFETs) are basically non-faradaic electrode systems in which electric field variations in the semiconductor gate region control the magnitude of the source drain current [22].

1.5 General methods of modification of electrodes

The concept of chemically modified electrodes (CMEs) is one of the exciting developments in the field of electroanalytical chemistry. Many different strategies have been employed for the modification of the electrode surface. The motivations behind the modifications of the electrode surface are: (i) improved electrocatalysis, (ii) freedom from surface fouling and (iii) prevention of undesirable reactions competing kinetically with the desired electrode process [23]. The increasing demand for it has led to the development of a rapid, simple and non-separation method for the simultaneous determination of compounds where the CMEs have emerged as an efficient and versatile approach, and have attracted considerable attention over the past decades due to its advantages in terms of reduced costs, automatic and fast analysis, high sensitivity and selectivity [24-26]. There are numerous techniques that may be used to modify electrode surfaces. Among various CMEs, polymer-modified electrodes (PMEs) are promising approach to determination. Some modification processes are-

Covalent Bonding: This method employs a linking agent (e.g. an organosilane) to covalently attach one of several monomolecular layers of the chemical modifier to the electrode surface [27].

Drop-Dry Coating (or solvent evaporation): A few drops of the polymer, modifier or catalyst solution are dropped onto the electrode surface and left to stand to allow the solvent to dry out [28].

Dry-Dip Coating: The electrode is immersed in a solution of the polymer, modifier or catalyst for a period sufficient for spontaneous film formation to occur by adsorption. The electrode is then removed from solution and the solvent is allowed to dry out [29].

Composite: The chemical modifier is simply mixed with an electrode matrix material, as in the case of an electron-transfer mediator (electrocatalyst) combined with the carbon particles (plus binder) of a carbon paste electrode. Alternatively, intercalation matrices such as certain Langmuir-Blodgett films, zeolites, clays and molecular sieves can be used to contain the modifier [30].

Spin-Coating (or Spin-Casting): it is also called spin casting; a droplet of a dilute solution of the polymer is applied to the surface of a rotating electrode. Excess solution is spun off the surface and the remaining thin polymer film is allowed to dry. Multiple layers are applied in the same way until the desired thickness is obtained. This procedure typically produces pinhole-free thin films for example; oxide xerogel film electrodes prepared by spin-coating a viscous gel on an indium oxide substrate [31].

Electrodeposition: In this technique the electrode is immersed in a concentrated solution ($\sim 10^{-3}$ $molL^{-1}$) of the polymer, modifier or catalyst followed by repetitive voltammetry scans. The first and second scans are similar, subsequent scans decrease with the peak current. For example, electrochemical deposition of poly (o-toluidine) on activated carbon fiber [32].

Electropolymerization: A solution of monomer is oxidized or reduced to an activated form that polymerizes to form a polymer film directly on the electrode surface. This

procedure results in few pinholes since polymerization would be accentuated at exposed (pinhole) sites at the electrode surface. Unless the polymer film itself is redox active, electrode passivation occurs and further film growth is prevented.

In this technique the electrode is immersed in a polymer, modifier or catalyst solution and layers of the electropolimerized material builds on the electrode surface. Generally, the peak current increases with each voltammetry scan such that there is a noticeable difference between the first and final scans indicating the presence of the polymerized material. For example, electropolymerization of aniline on platinum electrode perturbations.

1.6 Determination of compounds by modified electrodes

The determination of analytes is an interesting subject in electroanalytical chemistry. The increasing demand for it has led to the development of a rapid, simple and non-separation method for the determination of analytes where the chemically modified electrodes (CMEs) have emerged as an efficient and versatile approach and have attracted considerable attention over the past decades due to its advantages in terms of reduced costs, automatic and fast analysis, high sensitivity and selectivity [24, 33-34]. This type of chemically modified electrode sensors are well known for the measurement of multiple analytes in a mixture.

In this work, a novel modified electrode sensor is developed using Sulfolane **(**Tetrahydrothiophene-1,1-dioxide) as a trifunctional electrochemical sensor for the determination of Vitamin-B_6 (VB_6), Vitamin-C (VC) (Ascorbic acid) and Uric acid (UA). These compounds (VC and UA) go through redox reaction on the electrode surface within the same potential range which causes an overlapping oxidation peak at bare electrode. The electro activeness of such compounds depends upon the pH of the medium, nature of the electrode and active moiety present in their structures.

1.7 Prospect of Modified Electrode Sensor for the Determination of VB_6, VC and UA

Electrochemical detection of VB_6, VC and UA by modified electrode sensor is a preferred method, because they are electrochemically active [35] and they have basic structures that might be electrochemically oxidized at a gold, platinum or carbon electrodes [36]. But there are many difficulties for the determination of VB_6, VC and UA. At bare Glassy Carbon (GC) and other available electrodes VB_6, VC and UA are detectable quantitatively if they are investigated individually. But when investigated one in presence of other, they give one broad overlapped peak for VC and UA as they are oxidized at nearly same potential and another peak for VB_6, which results in rather poor selectivity and difficulty on the determination of concentration of each species [37, 38]. This is why modification of electrode is necessary to get corresponding, non-overlapped peaks. Recently, an enormous amount of research has been devoted to the development of new chemically modified electrodes for monitoring VB_6, VC and UA [39, 40]. Among various chemically modified electrodes, polymer-modified electrodes (PMEs) are promising approach to detect VB_6, VC and UA. Polymer-modified electrodes prepared by electropolymerization have received extensive interest in the detection of analytes because of their selectivity, sensitivity and homogeneity in electrochemical deposition, strong adherence to electrode surface and chemical stability of the films. Selectivity of PMEs as a sensor can be attained by different mechanisms such as size exclusion, ion exchange, hydrophobicity interaction and electrostatic interaction [41-45].

1.7.1 Vitamin-B_6 (Pyridoxine)

Vitamin-B_6 (VB_6) also known as Pyridoxine refers to a group of chemically very similar compounds which can be inter converted in biological systems. VB_6 is a form of vitamin B group found commonly in food and used as dietary supplement. It is widely distributed in foods in both its free and bound forms. Foods that contain large amounts of VB_6 include pork, turkey, beef, bananas, chickpeas, potatoes and pistachios. It is also found in the germ and aleurone layer of grains and milling results in the reduction of this vitamin in white flour. VB_6 is absorbed in the jejunum and ileum by passive diffusion. The products of VB_6 metabolism are excreted in the urine and a small amount of VB_6 is also excreted in the feces. VB_6 deficiency may cause weakness, depression, anemia and skin disorders [46, 47].

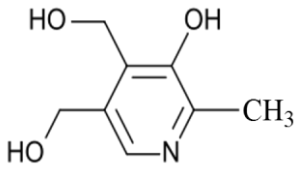

Figure 1.1: Vitamin-B_6

1.7.2 Uses of Vitamin-B_6

VB_6 is one of the most significant water-soluble vitamins that is an important biochemical active molecule. It is essential in the diet for the metabolism of amino acids and in the maintenance of body cells. It is also important for normal function of the nervous system and several hormones. Usually VB_6 use for the treatment of anemia, migraine headache, depression, acute seizures etc. Treatment of VB_6 deficiency lies with replacement, usually in the form of pyridoxine hydrochloride, orally, as a nasal spray, or for injection when in its solution form [48, 49].

1.7.3 Vitamin-C (Ascorbic acid)

Vitamin-C (VC) also known as ascorbic acid is a naturally occurring organic compound with antioxidant properties. It is a water-soluble vitamin, meaning that our body doesn't store it. We have to get what we need from food, including citrus fruits, broccoli, and tomatoes.. It helps the body to make collagen, an important protein used to make skin, cartilage, tendons, ligaments, and blood vessels. VC is needed for healing wounds, and for repairing and maintaining bones and teeth. It also helps the body to absorb iron. VC is an antioxidant, along with vitamin E, beta-carotene, and many other plant-based nutrients. Antioxidants block some of the damage caused by free radicals, substances that damage DNA. The buildup of free radicals over time may contribute to the aging process and the development of health conditions such as cancer, heart disease, and arthritis [50-52].

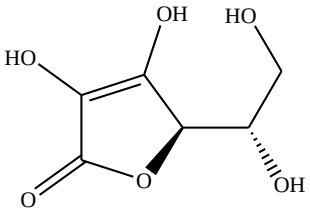

Figure 1.2: Vitamin-C

1.7.4 Uses of Vitamin-C

Ascorbic acid (Vitamin C) plays an important role in the body. Vitamin C is used to prevent or treat low levels of vitamin C in people who do not get enough of the vitamin from their diets. Most people who eat a normal diet do not need extra ascorbic acid. Low levels of vitamin C can result in a condition called scurvy. Scurvy may cause symptoms such as rash, muscle weakness, joint pain, tiredness, or tooth loss. It is needed to maintain the health of skin, cartilage, teeth, bone, and blood vessels. It is also used to protect body cells from damage. Vitamin C is also important for bones and connective tissues, muscles, and blood vessels. Vitamin C helps the body absorb iron, which is needed for red blood cell production. It is known as an antioxidant [53].

1.7.5 Uric Acid (UA)

Uric acid is a heterocyclic compound of carbon, nitrogen, oxygen, and hydrogen with the formula $C_5H_4N_4O_3$. It forms ions and salts known as urates and acid urates, such as ammonium acid urate. UA is a diprotic acid with pK_{a1} = 5.4 and pK_{a2} = 10.3. It is a product of the metabolic breakdown of purine nucleotides. The water solubility of UA and its alkali metal and alkaline earth salts is low. In humans and higher primates, uric acid is the final oxidation (breakdown) product of purine metabolism and is excreted in urine. In humans, about 70% of daily uric acid disposal occurs via the kidneys, and in 5–25% of humans, impaired renal (kidney) excretion leads to hyperuricemia. Extreme abnormalities of UA levels indicate symptoms of several diseases, such as gout, hyperuricemia, leukemia, pneumonia, and Lesch-Nyhan [54, 55].

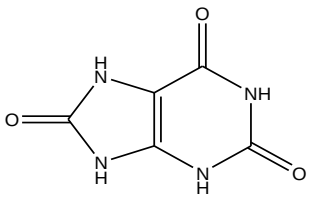

Figure 1.3: Uric Acid

1.7.6 Uses of Uric Acid

Uric acid may be a marker of oxidative stress, and may have a potential therapeutic role as an antioxidant. On the other hand, like other strong reducing substances such as ascorbate, uric acid can also act as a pro oxidant. Thus, it is unclear whether elevated levels of uric

acid in diseases associated with oxidative stress such as stroke and atherosclerosis are a protective response or a primary cause. For example, some researchers propose hyperuricemia-induced oxidative stress is a cause of metabolic syndrome. On the other hand, plasma uric acid levels correlate with longevity in primates and other mammals. This is presumably a function of urate's antioxidant properties [56, 57].

1.7.7 Sulfolane

Sulfolane (tetrahydrothiophene-1, 1-dioxide) is an organosulfur compound, formally a cyclic sulfone containing a sulfonyl functional group with the formula $(CH_2)_4SO_2$. The sulfone group is a sulfur atom doubly bonded to two oxygen atoms and singly bonded to two carbon centers. The sulfur-oxygen double bond is polar, conferring good solubility in water, while the four carbon ring provides non-polar stability. It is a colorless liquid commonly used in the chemical industry as a solvent for extractive distillation and chemical reactions. Sulfolane was originally developed by the Shell Oil Company in the 1960s as a solvent to purify butadiene.

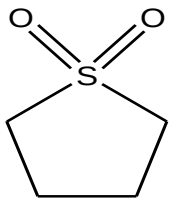

Figure 1.4: Sulfolane

1.7.8 Uses of Sulfolane

Sulfolane is widely used as an industrial solvent, especially in the extraction of aromatic hydrocarbons from hydrocarbon mixtures and to purify natural gas. It is found to be highly effective in separating high purity aromatic compounds from hydrocarbon mixtures using liquid-liquid extraction. This process is widely used in refineries and the petrochemical industry. Whereas sulfolane is highly stable and can therefore be reused many times, it does eventually degrade into acidic byproducts [58].

1.8 Electrochemistry as an analytical tool

Electrochemistry has become a powerful tool to study widely for solving the different problem in the arena of organic chemistry, biochemistry, material science, environmental science etc. Many natural and biochemical processes have redox nature. Their redox mechanisms can be easily established based on the experiment in voltammetry. For example, cyclic voltammetry is the most widely used modern electro-analytical method available for the mechanistic probing study of redox system.

1.9 Electrical double layer

Electroanalytical studies are centered on electrode, which is considered as a probe in the electrolyte. An electrode can only donate or accept electrons from a species that is present in a layer of solution that is immediately adjacent to the electrode. Thus, this layer may have a composition that differs significantly from that of the bulk of the solution. Let us consider the structure of the solution immediately adjacent to that electrode. Immediately after impressing the potential, there will be a momentary surge of current, which rapidly decays to zero if no reactive species is present at the surface of the electrode. This current is a charging current that creates an excess of negative charge at the surface of the two electrodes. As a consequence of ionic mobility, however, the layers of solution immediately adjacent to the electrodes acquire an opposing charge. This effect is illustrated in Figure 1.5. The surface of the metal electrode is shown as having an excess of positive charge as a consequence of an applied positive potential. The charged solution layer consists of two parts: (1) a compact inner layer (d_0 to d_1), in which the potential decreases linearly with distance from the electrode surface and (2) a diffuse layer (d_1 to d_2), in which the decrease is exponential. This assemblage of charge at the electrode surface and in the solution adjacent to the surface is termed as electrical double layer.

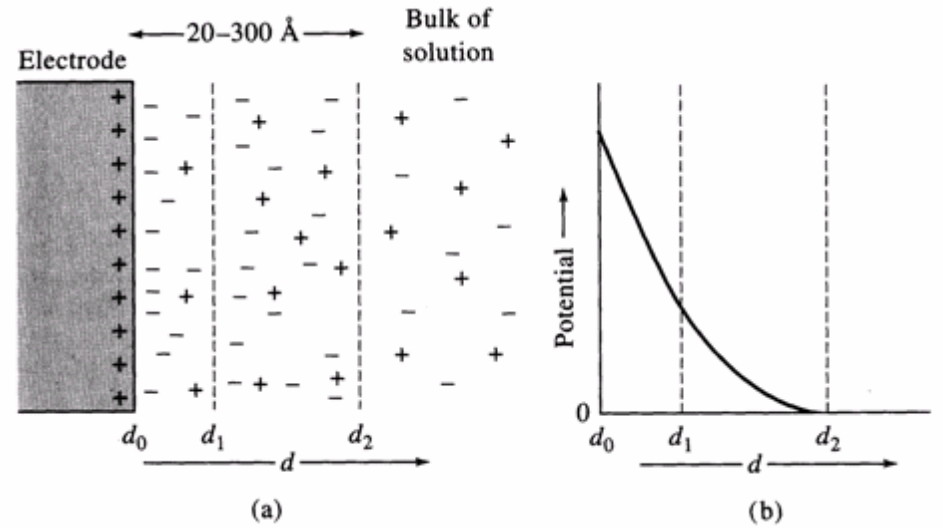

Figure 1.5: Electrical double layer formed at electrode surface as a result of an applied potential

1.10 Faradaic and nonfaradaic currents

Two types of processes can conduct currents across an electrode/solution interface. One involves a direct transfer of electrons via an oxidation reaction at one electrode and a reduction reaction at the other. Processes of this type are called faradaic processes because they are governed by Faraday's law, which states that the amount of chemical reaction at an electrode is proportional to the current; the resulting currents are called faradaic currents. Under some conditions a cell will exhibit a range of potentials where faradaic processes are precluded at one or both of the electrodes for thermodynamic or kinetic reasons. Here, conduction of continuous alternating currents can still take place. With such currents, reversal of the charge relationship occurs with each half cycle, as first negative and then positive ions are attracted alternately to the electrode surface. Electrical energy is consumed and converted to heat by friction associated with this ionic movement. Thus, each electrode surface behaves as one plate of a capacitor, the capacitance of which may be large. The capacitive current increases with frequency and with electrode area; by controlling these variables, it is possible to arrange conditions such that essentially all the alternating current in a cell is carried across the electrode interface by this nonfaradaic process [59].

Current in voltammetric experiment is a measure of the rate of the electrode process. When an electrode is placed in an electrolyte solution, different processes may occur. Steps involved in an electrode reaction are (Figure 1.6**)**.

1) Mass transfer of species between bulk solution and the electrode surface.
2) Heterogeneous electron transfer at the electrode/solution interface.
3) Chemical reactions, either preceding or following electron transfer.
4) Surface reactions such as adsorption, desorption and electrodeposition-dissolution [60].

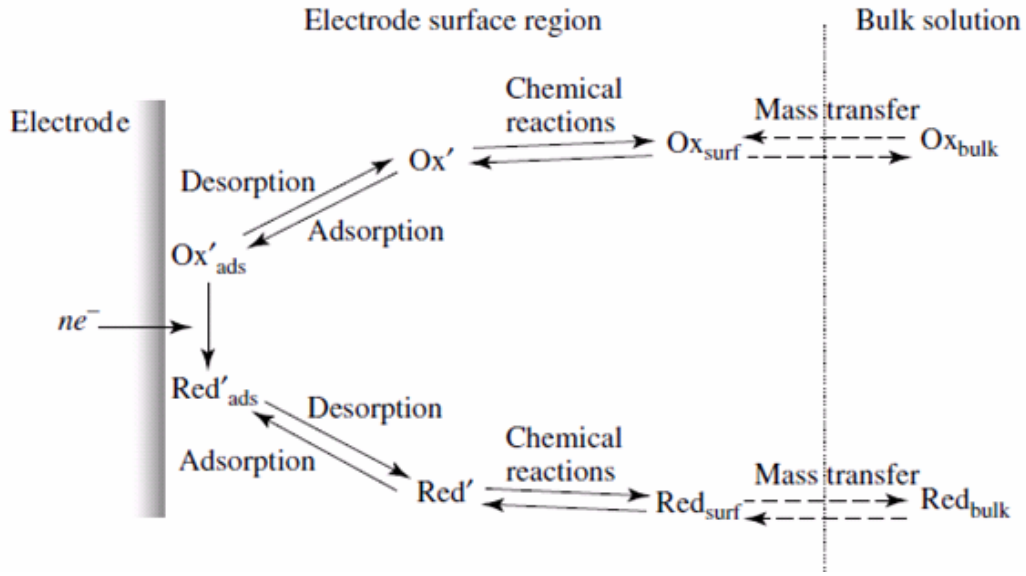

Figure 1.6: Typical steps involved in an electrode reaction

1.11 Mass transfer process in voltammetry

The movement of the electro-active substance through solution is referred as mass transfer at the electrode surface. In electrochemical systems, there are different types of mass transfer system by which a substance may be transferred to the electrode surface from bulk solution. Depended on the experimental conditions, any of these or more than one might be operating in a given experiment system.

A reacting species may be brought to an electrode surface by three types of mass transfer processes:

- Migration
- Diffusion
- Convection

1.11.1 Migration

Migration refers to movement of a charge particle in a potential field. It occurs by the movement of ions through a solution as a result of electrostatic attraction between the ions and the electrodes. In general, most electrochemical experiment it is unwanted but can be eliminated by the addition of a large excess of supporting electrolytes. In the electrolysis solution, ions will move towards the charged electrode that means cations to the cathode and anions to the anode. This motion of charged particle through solution, induced by the charges on the electrodes is called migration [61]. This charge movement constitutes a current. This current is called migration current. The fraction of the current carried by a given cation and anion is known as its transport number. The larger the number of different kinds of ions in a given solution, the smaller is the fraction of the total charge that is carried by a particular species. Electrolysis is carried out with a large excess of inert electrolyte in the solution so the current of electrons through the external circuit can be balanced by the passage of ions through the solution between the electrodes, and a minimal amount of the electroactive species will be transported by migration. Migration is the movement of charged species due to a potential gradient. In voltammetric experiments, migration is undesirable but can be eliminated by the addition of a large excess of supporting electrolytes in the electrolysis solution. The effect of migration is applied zero by a factor of fifty to hundred ions excess of an inert supporting electrolyte.

1.11.2 Diffusion

The movement of a substance through solution by random thermal motion is known as diffusion. Whereas a concentration gradient exists in a solution, that is the concentration of a substance, is not uniform throughout the solution. There is a driving force for diffusion of the substance from regions of high concentration to regions of lower concentration. In any experiment in which the electrode potential is such that the electron transfer rate is very high, the region adjacent to the electrode surface will become depleted of the electro-active species, setting up a concentration in which this species will constantly be arriving at the electrode surface by the diffusion from points further away [62]. The one kind of mode of mass transfer is diffusion to an electrode surface in an electrochemical cell. The rate of diffusion is directly proportional to the concentration difference. When the potential

is applied, the cations are reduced at the electrode surface and the concentration is decreased at the surface film. Hence a concentration gradient is produced. Finally, the result is that the rates of diffusion current become larger.

1.11.3 Convection

By mechanical way reactants can also be transferred to or from an electrode. Thus forced convection is the movement of a substance through solution by stirring or agitation. This will tend to decrease the thickness of the diffuse layer at an electrode surface and thus decrease concentration polarization. Natural convection resulting from temperature or density differences also contributes to the transport of species to and from the electrode [63]. At the same time a type of current is produced. This current is called convection current. Removing the stirring and heating can eliminate this current. Convection is a far more efficient means of mass transport than diffusion. These three kinds of mass transfer processes are shown in Figure 1.7.

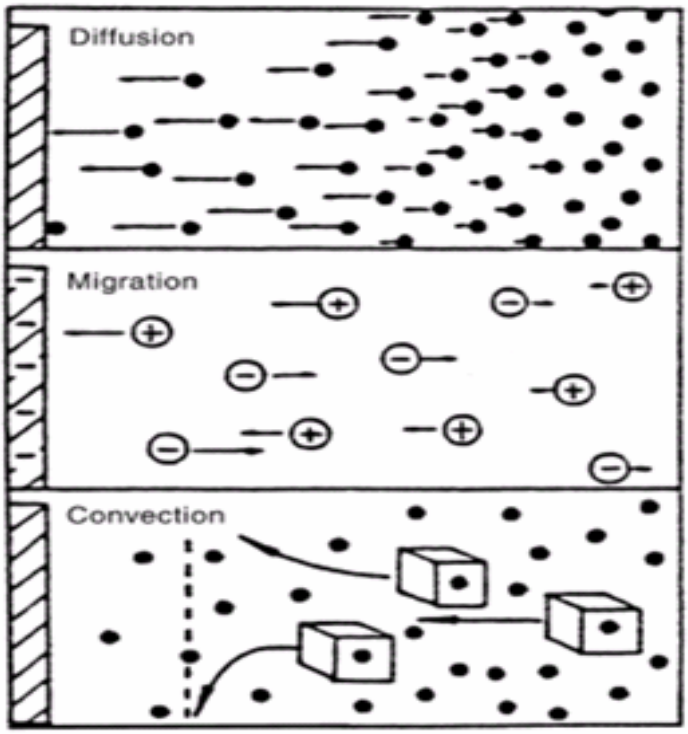

Figure 1.7: Modes of mass transfer

In this research work, various electrochemical techniques such as cyclic voltammetry (CV), differential pulse voltammetry (DPV) along with UV-visible Spectrophotometry were used for the qualitative and quantitative determination of VB_6, VC and UA.

1.12 Objectives of the research work (Within 150 words):

The objective of this research work is to develop electrochemically modified electrode for the detection of VB_6, VC and UA qualitatively and quantitatively. The specific objectives of this research work are-

i) To develop Sulfolane modified GC, Au and Pt electrodes,
ii) To compare the behavior of VB_6, VC and UA at bare and Sulfolane modified electrodes,
iii) To recognize the most favorable condition (such as pH and scan rate) for the separation of VB_6, VC and UA,
iv) To determine the quantity of VB_6 and VC in known sample and tablet samples of some Bangladeshi industry and UA in known sample as well as blood sample.

CHAPTER II

Literature Review

Many analytical techniques have been described for the determination of VB_6, VC and UA, such as spectrophotometry, high-performance liquid chromatography, and electrochemical methods. Among them, electrochemical method based on modified electrode sensor has attracted more attention for their high sensitivity, simplicity, reproducibility, on site monitoring and low cost.

Hai-Ying *et al*., 2001, reported an electrochemically pretreated glassy carbon electrode (PGCE) by anodic oxidation. The PGCE showed good activity in improving the electrochemical responses of some water-soluble Vitamins, such as Vitamin (VB_2), Vitamin (VB_6) and Vitamin (VC). VB_2, VB_6 could be adsorbed at PGCE and VC proceeded with an electrocatalytic process [64].

Marcos *et al*., 2003, used a copper (II) hexacyanoferrate (III) (CuHCF) modified carbon paste electrode for the electroanalytical determination of pyridoxine (Vitamin B_6) in pharmaceutical preparations using cyclic voltammetry. Diverse parameters were investigated for the optimization of the sensor response, such as composition of the electrode, electrolytic solution, effect of pH, scan rate of potential and interferences. The optimum conditions were found at an electrode composition of 20% CuHCF, 55% graphite and 25% mineral oil (m/m) in an acetate buffer (pH 5.5) containing 0.05 $molL^{-1}$ of NaCl. The range of determination of pyridoxine was from 1.2×10^{-6} to 6.9×10^{-4} $molL^{-1}$. The procedure was successfully applied for the determination of vitamin B_6 in formulation preparations [65].

Ahmed *et al*., 2005, developed a differential pulse voltammetric method for the analysis of ascorbic acid in acetate buffer. Hanging mercury drop electrode (HMDE) was used for the determination of ascorbic acid as working electrode. Effect of pH was studied on the determination of ascorbic acid. At higher pH sensitivity of the method increased

significantly. After developing and optimizing the method different pharmaceutical tablets were analyzed for levels of Vitamin-C. After dissolution of tablets in water aliquots were taken into acetate buffer and determined applying the standard addition method. Different types of fruit juices were also analyzed for Vitamin-C. Levels of ascorbic acid in juices were in the range of 24 to 225 µg/100 mL [66].

Zhao *et al*., 2006, studied the electrochemical behaviors of uric acid (UA) and ascorbic acid (AA) at the L-cysteine (L-Cys) self assembled monolayers modified gold electrode (L-Cys/Au electrode). The modified electrode shows an excellent electrocatalytical effect on the oxidation of UA and AA by cyclic voltammetry (CV) in 0.1 M phosphate buffer solution (pH 7.0). In differential pulse voltammetric (DPV) measurements, the L-Cys/Au electrode was able to separate the oxidation peak potentials of UA and AA present in homogeneous solution by about 236 mV though the bare electrode give a single broad response. The detection limit of UA and AA is 2.0×10^{-6} M and 1.1×10^{-5} M, respectively. The proposed method can be used for the determination of UA in urine sample. The method is simple, quick and sensitive [67].

Wu *et al*., 2008, studied the voltammetic behavior of Vitamin B_6 (VB_6) at a glassy carbon electrode in phosphate buffers using cyclic, linear sweep and differential pulse voltammetry. The oxidation process was shown to be irreversible over the entire pH range studied (4.0-10.0) and was adsorption controlled. VB_6 was determined by differential pulse voltammetry and the peak current was found linearly with its concentration in the range of 3×10^{-7} $molL^{-1}$ to 2×10^{-4} $molL^{-1}$. The detection limit was 1×10^{-7} $molL^{-1}$. The procedure was successfully applied for the assay of VB_6 in tablets [68].

Wang *et al*., 2008, constructed a glassy carbon electrode modified with hexacyanoferrate lanthanum (LaHCF) and was characterized by cyclic voltammetry (CV) and electrochemical impedance spectrum (EIS). The LaHCF modified glassy carbon electrode showed good catalytic character on uric acid (UA) and was used to detect uric acid and ascorbic acid (AA) simultaneously. The DPV peak currents increased linearly on the UA in the range of 2.0×10^{-7} to 1.0×10^{-4} mol/L with the detection limit (signal-to-noise ratio was 3) for UA 1.0×10^{-7} mol/L. The proposed method showed excellent selectivity and

stability, and the determination of UA and AA simultaneously in urine was satisfactory [69].

Yang *et al*., 2009, synthesized a Polypyrrole (PPy) nanotubes by chemical oxidative polymerization of pyrrole within the pores of polycarbonate membrane using the technology of diffusion of solutes. An amperometric uric acid sensor based on PPy NEEs has been developed and used for determination of uric acid in human serum samples. The electrode can direct response to uric acid at potential of 0.60V vs. SCE with wide linear range of 1.52×10^{-6} to 1.54×10^{-3} M. The detection limit was 3.02×10^{-7} M. This sensor was used to determine uric acid in real serum samples. PPy NEEs is thought of as a good application in the foreground [70].

Yuzhong *et al*., 2011, fabricated the gold nanoparticles (Au NPs)/multi-walled carbon nanotubes (MWCNTs) composite film modified glassy carbon electrode (GCE) and scanning electron microscopy (SEM) was used to investigate the assemble process of the composite film. In pH 7.0 PBS, an oxidation peak of the vitamin B_6 (VB_6) was only observed at composite film modified electrode. Under the optimized conditions, the current intensity was linear with the concentrations of VB_6 in the range of 1.59 to 102.74 μg mL^{-1} with a detection limit of 0.53 μg mL^{-1} (S/N = 3). The modified electrode had been applied in pharmaceutical analysis, and obtained good results [71].

Hadi *et al*., 2012, described the development, electrochemical characterization and utilization of novel modified molybdenum (VI) complex-carbon nanotube paste electrode for the electrocatalytic determination of ascorbic acid (AA). The electrochemical profile of the proposed modified electrode was analyzed by cyclic voltammetry (CV). Differential pulse voltammetry (DPV) in 0.1 M phosphate buffer solution (PBS) at pH 7.0 was performed to determine AA in the range of 0.1 M to 950.0 M, with a detection limit of 89.0 nM. Then the modified electrode was used to determine AA in an excess of uric acid (UA) by DPV. Finally, this method was used for the determination of AA in some real samples [72].

Shou-King *et al*., 2012, reported about the electron transfer between DNA and Vitamin B_6 by observing the electro-catalytic behaviors of a ssDNA-modified electrode towards

Vitamin B_6 and was determined the quantitative content of vitamin B_6 using the ssDNA-modified electrode. The peak currents depend linearly on the concentration of vitamin B_6 from 0.10 to 6.00 mM with R= 0.99952 (n=8) and SD=0.07008. The linear regression equation was C (mM) = 0.03245 × Ip (μA) - 0.04049 with the detection limit of 0.040 (±0.001) mM. The determination for the real tablets yielded a good mean recovery of 99.46% with a relative standard deviation of 5.36%. Thus, the method is expected to find its applications in monitoring the content of vitamin B_6 in medical industry [73].

Sadikoglu *et al*., 2012, prepared a stable modified glassy carbon electrode based on poly (*p*-aminobenzene sulfonic acid) (*p*-ABSA) film by electrochemical polymerization technique in phosphate buffer solution (PBS) (pH 7.0) and its electrochemical behavior were studied by cyclic voltammetry (CV). The polymer film-modified electrode was used for the dermination of uric acid (UA). The modified glassy carbon electrode had an excellent response and specificity for the electrocatalytic oxidation of UA in PBS (pH 7.0). A linear calibration curve for DPV analysis was constructed in the uric acid concentration range 1×10^{-5} M to 1×10^{-4} M. Limit of detection (LOD) and limit of quantification (LOQ) at *p*-ABSA modified electrode were obtained as 1.125×10^{-6} M and 3.750×10^{-6} M, respectively. This electrode was used for UA determinations in human urine samples satisfactorily [74].

Fritea *et al*., 2013, investigated the electrochemical behavior of ascorbic acid and uric acid on glassy carbon bare electrodes and ones modified with *β*-cyclodextrin entrapped in polyethyleneimine film using square wave voltammetry. On the modified electrodes the potential of the oxidation peak of the ascorbic acid was shifted to more negative values by over 0.3 V, while in the case of uric acid, the negative potential shift was about 0.15 V compared to the bare glassy carbon electrode. The peak intensity of the ascorbic acid was increased linearly with the concentration (r^2 = 0.996) when the concentration of uric acid remained constant and the peak intensity of the uric acid increased linearly with the concentration (r^2 = 0.992) at the constant concentration of ascorbic acid. FTIR measurements supported the formation of inclusion complexes. The modified electrodes were successfully employed for the determination of ascorbic acid in pharmaceutical formulations with a detection limit of 0.22 μM [75].

Ngai *et al*., 2013, developed a simple procedure to prepare a glassy carbon electrode (GCE) modified with single-walled carbon nanotube/zinc oxide (SWCNT/ZnO). The carbon nanotube/zinc oxide composites were immobilized on the GCE by mechanical attachment. Cyclic voltammetry study of the modified electrode indicated that the oxidation potential shifted towards a lower potential by approximately 240 mV and the peak current was enhanced by 2.0 fold in comparison to the bare GCE. The resulting modified electrode also indicated the absence of a well-defined redox couple implying that the reaction is irreversible. The electrochemical behavior was further described by characterization studies of scan rate, concentration of ascorbic acid, pH and temperature. The stability of the modified electrode was evaluated by potential cycling study. The SWCNT/ZnO-modified electrodes suggested a promising ascorbic acid sensor on the basis of these attractive results [76].

Lamari *et al*., 2013, reported the synthesis of polumer modified carbon paste electrode and its application for the electrochemical detection of ascorbic acid (AA). The cyclic voltammetry and square wave voltammetry was used for the investigations. The observed linear range for the determination of AA concentration was from 0.2 mM to 9 mM. The detection limit was estimated to be 5.48 mM [77].

Bikila *et al*., 2015, reported the determination of ascorbic acid (AA) at a glassy carbon electrode (GCE) modified with a perforated film produced by reduction of diazonium generated *in situ* from *p*-phenylenediamine (PD). Holes were intentionally created in the modifier film by stripping pre-deposited gold nanoparticles. The modified electrodes were electrochemically characterized using common redox probes: hydroquinone, ferrocyanide and hexamineruthenium (III). The bare GCE showed a linear response to AA in the concentration range of 5 mM to 45 mM with detection limit of 1.656 mM and the modified GCE showed a linear response to AA in the concentration range from 5 to 45 μM with detection limit of 0.123 μM. The modified electrode showed excellent inter-electrode reproducibility, accuracy and stability. The modified electrode was reported as a promising candidate for use in the electro-analysis of AA [78].

Afrasiabi *et al*., 2015, demonstrated that simultaneous determination of ascorbic acid (AA), uric acid (UA) and acetaminophen (ACT) can be performed on a novel single

walled carbon nanotubes (SWCNTs), chitosan (CHIT) and MCM-41 composite modified glassy carbon electrode (SWCNTs-CHIT-MCM-41/GCE). The electro-oxidations of AA, UA and ACT were investigated by using differential pulse voltammetry (DPV), chronoamperometry (CA) and electrochemical impedance spectroscopy (EIS) methods. Under optimum conditions application of DPV method showed that the linear relationship between oxidation peak current and concentration of AA, UA and ACT were 1-160 μM, 0.1-24 μM and 0.1-21 μM with detection limits of 0.41, 0.04 and 0.03 μM, respectively [79].

Eser *et al*., 2016, prepared a novel polymer film of poly(glyoxal-bis(2-hydroxyanil)) P(GBHA), by electropolymerization of glyoxal-bis(2-hydroxyanil) (GBHA) on a glassy carbon electrode (GCE). The electrochemical sensor exhibited high electrocatalytic activity towards the oxidation of AA and UA. The linear response ranges for the individual determination of AA and UA were 1.0–2000 and 1.0–200 mol L^{-1} with the detection limit of 0.26 and 0.3 mol L^{-1}, respectively. These results present that the P(GBHA) is a promising substance for the production of electrochemical sensors with high sensitivity [80].

From the above literature review, it is seen that the determination of VB_6, VC and UA individually or in a binary mixture or in a ternary mixture using sulfolane modified electrode sensor was not reported previously. Most of the work for the determination of VB_6, VC and UA has been done on carbon nanotube or carbon paste electrodes which are very costly.

In this work, Sulfolane modified electrode sensor is developed for the determination of VB_6, VC and UA. Sulfolane has choose as the sensing material because, Sulfolane is a promising material regarding its low cost and availability, high sensitivity and selectivity. The modification process of glassy carbon electrode with Sulfolane is easy compared with the carbon paste electrodes. This modified electrode sensor can also be applicable for the determination of these compounds in tablet samples (VB_6 and VC) and real samples (UA).

CHAPTER III

Experimental

The electrochemical behavior of Vitamin-B_6 (VB_6), Vitamin-C (VC) and Uric acid (UA) in buffer solution at various pH has been investigated using cyclic voltammetry (CV) and differential pulse voltammetry (DPV) at Glassy carbon (GC), Gold (Au) and Platinum (Pt) electrode. The sensitivity of electrode reactions has been improved by modifying the electrodes with Sulfolane. DPV has also been employed for the quantitative estimation of VB_6, VC and UA in known sample and real sample such as tablets and blood sample. The instrumentation is given details in the following sections. The source of different chemicals, instruments and methods are briefly given below.

3.1 Chemicals

Analytical grade chemicals and solvents have been used in electrochemical synthesis and analytical work. The used chemicals were-

Sl. No.	Chemicals	Molecular formula	Molar mass	Reported purity	Producer
1.	Pyridoxine or Vitamin-B_6	$C_8H_{11}NO_3$	169.18	99.5%	Loba Chemie Pvt. Ltd., India
2.	L-Ascorbic Acid or Vitamin-C	$C_6H_8O_6$	176.12	99%	Loba Chemie Pvt. Ltd., India
3.	Uric Acid	$C_5H_4N_4O_3$	168.11	99%	Damstadt, Germany
4.	Sulfolane	$C_4H_8O_2S$	120.17	99.5%	E-Merck, Germany
5.	Glacial Acetic Acid	CH_3COOH	60.05	99.5%	Loba Chemie Pvt. Ltd., India

Sl. No.	Chemicals	Molecular formula	Molar mass	Reported purity	Producer
6.	Sodium Acetate	$CH_3COONa.3H_2O$	136.08	99%	Merk Specialities Pvt. Ltd., India
7.	Potassium Chloride	KCl	74.60	99%	E-Merck, Germany
8.	Sodium Di-hydrogen Orthophosphate	$NaH_2PO_4.2H_2O$	156.01	98%	Loba Chemie Pvt. Ltd., India
9.	Di-sodium Hydrogen Orthophosphate	$Na_2HPO_4.2H_2O$	177.99	97%	Loba Chemie Pvt. Ltd., India
10.	Sodium Hydroxide	NaOH	40.0	97%	E-Merck, Germany
11.	Sodium Bicarbonate	$NaHCO_3$	84.0	99%	E-Merck, Germany

3.2 Equipments

During this research work the following instruments were used-

- The electrochemical studies (CV, DPV) were performed with a computer controlled potentiostats/ galvanostats (μstat 400, Drop Sens, Spain)
- A Pyrex glass micro cell with 26eflon cap
- Glassy carbon (GC)/ Gold (Au)/ Platinum (Pt)as working electrode (BASi, USA)
- Ag/AgCl as reference electrode (BASi, USA)
- Liquid micro size (0.05um) polishing alumina (BAS Inc. Japan)
- Pt wire as counter electrode (Local market, Dhaka, Bangladesh)
- A HR 200 electronic balance with an accuracy of ± 0.0001g was used for weighting and
- A pH meter (pH Meter, Hanna Instruments, Italy) was employed for maintaining the pH of the solutions.
- The UV-Vis spectroscopic analysis was performed by a computer controlled spectrophotometer (Thermo Scientific, USA).

3.3 Cyclic Voltammetry (CV)

There are many well developed electro-analytical techniques are used for the study of electrochemical reactions. Among these we have selected the CV technique to study and analyze the redox reactions occurring at the polarizable electrode surface. This technique provides suitable information to understand the mechanism of electron transfer reaction of the compounds as well as the nature of adsorption of reactants or products on the electrode surface. CV is often the first experiment performed in an electrochemical study. CV consists of imposing an excitation potential nature on an electrode immersed in an unstirred solution and measuring the current and its potential ranges varies from a few millivolts to hundreds of millivolts per second in a cycle. This variation of anodic and cathodic current with imposed potential is termed as voltammogram [81].

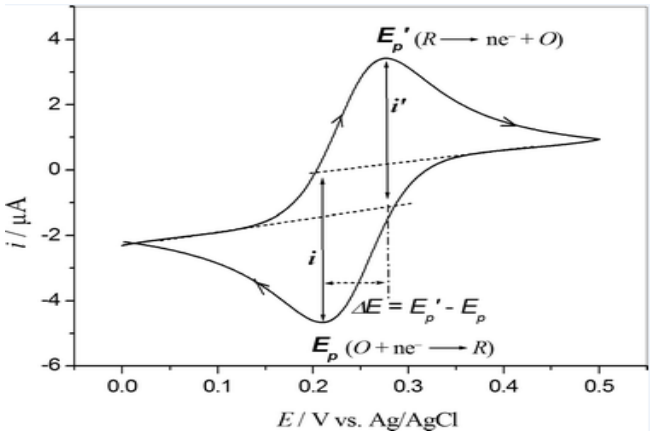

Figure 3.1: The expected response of a reversible redox couple during a single potential cycle

This technique is based on varying the applied potential at a working electrode in both forward and reverse directions while monitoring the current. Simply stated, in the forward scan, the reaction is $O + e^- \rightarrow R$, R is electrochemically generated as indicated by the cathodic current. In the reverse scan, $R \rightarrow O + e^-$, R is oxidized back to O as indicated by the anodic current. The CV is capable of rapidly generating a new species during the forward scan and then probing its fate on the reverse scan. This is a very important aspect of the technique [82].

In CV the current function can be measured as a function of scan rate. The potential of the working electrode is controlled vs a reference electrode such as Ag/AgCl electrode. The

electrode potential is ramped linearly to a more negative potential and then ramped is reversed back to the starting voltage. The forward scan produces a current peak for any analyte that can be reduced through the range of potential scan. The current will increase as the current reaches to the reduction potential of the analyte [83].

The current at the working electrode is monitored as a triangular excitation potential is applied to the electrode. The resulting voltammogram can be analyzed for fundamental information regarding the redox reaction. The potential at the working electrode is controlled vs a reference electrode, Ag/AgCl (standard NaCl) electrode. The excitation signal varies linearly with time. First scan positively and then the potential is scanned in reverse, causing a negative scan back to the original potential to complete the cycle. Signal on multiple cycles can be used on the scan surface. A cyclic voltammogram is plot of response current at working electrode to the applied excitation potential.

3.4 Important features of CV

An electrochemical system containing species 'O' capable of being reversibly reduced to 'R' at the electrode is given by,

$$O + ne^- = R \quad \ldots\ldots\ldots\ldots\ldots\ldots\ldots\ldots 3.1$$

Nernst equation for the system is

$$E = E^0 + \frac{0.059}{n} \log \frac{C_0^s}{C_R^s} \quad \ldots\ldots\ldots\ldots\ldots\ldots\ldots 3.2$$

Where,

E = Potential applied to the electrode

E^0 = Standard reduction potential of the couple versus reference electrode

n = Number of electrons in Equation (3.1)

C_0^s = Surface concentration of species 'O'

C_R^s = Surface concentration of species 'R'

A redox couple that changes electrons rapidly with the working electrode is termed as electrochemically reverse couple. The relation gives the peak current i_{pc}

$$i_{pc} = 0.4463\ nFA\ (D\alpha)^{1/2}C \quad \ldots\ldots\ldots\ldots\ldots\ldots 3.3$$

$$\alpha = \left(\frac{nFv}{RT}\right) = \left(\frac{nv}{0.026}\right)$$

Where,

i_{pc} = peak current in amperes

F= Faraday`s constant (approximately 96500)

A = Area of the working electrode in cm^2

v= Scan rate in volt/ sec

C= Concentration of the bulk species in mol/L

D= Diffusion coefficient in cm^2 /sec

In terms of adjustable parameters, the peak current is given by the Randless- Sevcik equation,

$$i_{pc}=2.69\times10^5\times n^{3/2}AD^{1/2}Cv^{1/2} \quad \ldots\ldots\ldots\ldots\ldots\ldots\ldots 3.4$$

The peak potential E_p for reversible process is related to the half wave potential $E_{1/2}$, by the expression,

$$E_{pc} = E_{1/2} - 1.11\left(\frac{RT}{nF}\right), \quad \text{at } 25^0\text{C} \ldots\ldots\ldots\ldots\ldots\ldots 3.5$$

$$E_{pc} = E_{1/2} - \left(\frac{0.0285RT}{n}\right) \ldots\ldots\ldots\ldots\ldots\ldots\ldots\ldots 3.6$$

The relation relates the half wave potential to the standard electrode potential

$$E_{1/2} = E^0 - \frac{RT}{nF}\ln\frac{f_{red}}{f_{ox}}\left(\frac{D_{ox}}{D_{ox}}\right)^{1/2}$$

$$E_{1/2} = E^0 - \frac{RT}{nF}\ln\left(\frac{D_{ox}}{D_{red}}\right)^{1/2} \ldots\ldots\ldots\ldots\ldots\ldots\ldots 3.7$$

Assuming that the activity coefficient f_{ox} and f_{red} are equal for the oxidized and reduced species involved in the electrochemical reaction.

From Equation (3.6), we have,

$$E_{pa} - E_{pc} = 2.22\left(\frac{RT}{nF}\right) \text{ at } 25^0\text{C} \ldots\ldots\ldots\ldots\ldots\ldots 3.8$$

$$\text{Or, } E_{pa} - E_{pc} = \left(\frac{0.059}{n}\right) \quad \text{at } 25^0\text{C} \ldots\ldots\ldots\ldots\ldots 3.9$$

This is a good criterion for the reversibility of electrode process. The value of i_{pa} should be close for a simple reversible couple,

$$i_{pa}/i_{pc} = 1 \quad \text{.....3.10}$$

And such a system $E_{1/2}$ can be given by,

$$E_{1/2} = \frac{E_{pa} + E_{pc}}{2} \quad \text{.....3.11}$$

For irreversible processes (those with sluggish electron exchange), the individual peaks are reduced in size and widely separated, Totally irreversible systems are characterized by a shift of the peak potential with the scan rate [84];

$$E_p = E^0 - (RT/\alpha n_a F)[0.78 - \ln(k^0/(D)^{1/2}) + \ln(\alpha n_a F\alpha/RT)^{1/2}] \quad \text{.....3.12}$$

Where α is the transfer coefficient and n_a is the number of electrons involved in the charge transfer step. Thus E_p occurs at potentials higher than E^0, with the over potential related to k^0 (standard rate constant) and α. Independent of the value k^0, such peak displacement can be compensated by an appropriate change of the scan rate. The peak potential and the half-peak potential (at 25^0 C) will differ by 48/ αn mV. Hence, the voltammogram becomes more drawn-out as αn decreases.

The peak current, given by

$$i_p = (2.99\times10^5)n(\alpha n_a)^{1/2}ACD^{1/2}v^{1/2} \quad \text{.....3.13}$$

is still proportional to the bulk concentration , but will be lower in height (depending upon the value of α) . Assuming α = 0.5, the ratio of the reversible–to–irreversible current peaks is 1.27 (i.e. the peak current for the irreversible process is about 80% of the peak for a reversible one). For quasi-reversible systems (with $10^{-1} > k^0 > 10^{-5}$ cm/s) the current is controlled by both the charge transfer and mass transport. The shape of the cyclic voltammogram is a function of the ratio k^0 $(\pi vnFD/RT)^{1/2}$. As the ratio increases, the process approaches the reversible case. For small values of it, the system exhibits an irreversible behavior. Overall, the voltammograms of a quasi-reversible system are more drawn out and exhibit a larger separation in peak potential compared to a reversible system.

Unlike the reversible process in which the current is purely mass transport controlled, currents due to quasi-reversible process are controlled by a mixture of mass transport and charge transfer kinetics [85, 86]. The process occurs when the relative rate of electron transfer with respect to that of mass transport is insufficient to maintain Nernst equilibrium at the electrode surface.

3.5 Pulse methods

The basis of all pulse techniques is the difference in the rate of decay of the charging and the faradaic currents following a potential step (or pulse). The charging current decays considerably faster than the faradaic current. A step in the applied potential or current represents an instantaneous alteration of the electrochemical system. Analysis of the evolution of the system after perturbation permits deductions about electrode reactions and their rates to be made. The potential step is the base of pulse voltammetry. After applying a pulse of potential, the capacitive current dies away faster than the faradic one and the current is measured at the end of the pulse. This type of sampling has the advantage of increased sensitivity and better characteristics for analytical applications. At solid electrodes there is an additional advantage of discrimination against blocking of the electrode reaction by adsorption [87]. Three of these pulse techniques are widely used.

- Normal Pulse Voltammetry (NPV)
- Differential Pulse Voltammetry (DPV)
- Square Wave Voltammetry (SWV)

In this research work differential pulse voltammetry was used for the quantitative determination of VB_6, VC and UA.

3.6 Differential Pulse Voltammetry (DPV)

Differential pulse voltammetry (DPV) is a technique in which potential is applied after certain period of time and measures the resulting faradic current as a function of applied potential either in oxidation or reduction. It is designed to minimize background charging currents. The waveform in DPV is a sequence of pulses, where a baseline potential is held for a specified period of time prior to the application of a potential pulse. Current is sampled just prior to the application of the potential pulse. The potential is then stepped by a small amount (typically < 100 mV) and current is sampled again at the end of the pulse. The potential of the working electrode is then stepped back by a lesser value than during the forward pulse such that baseline potential of each pulse is incremented throughout the sequence.

By contrast, in normal pulse voltammetry the current resulting from a series of ever larger potential pulse is compared with the current at a constant 'baseline' voltage. Another type of pulse voltammetry is square wave voltammetry, which can be considered a special type of differential pulse voltammetry in which equal time is spent at the potential of the ramped baseline and potential of the superimposed pulse. The potential wave form consists of small pulses (of constant amplitude) superimposed upon a staircase wave form [88]. Unlike NPV, the current is sampled twice in each pulse Period (once before the pulse, and at the end of the pulse), and the difference between these two current values is recorded and displayed.

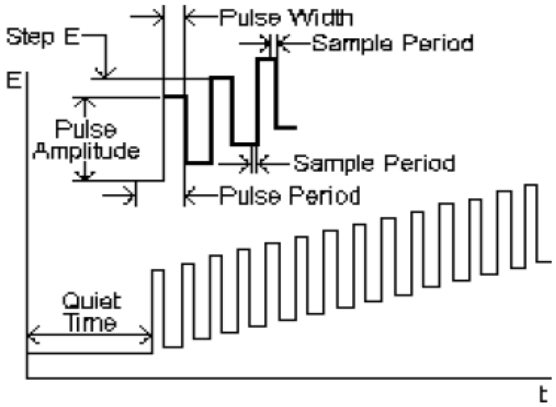

Figure 3.2: Scheme of application of potential

3.7 Important features of DPV

Differential pulse voltammetry has following important features in this work:

i) Current is sampled just prior to the application of the potential pulse.

ii) DPV help to improve the sensitivity of the detection and the resolution of the voltammogram.

3.8 Computer Controlled Potentiostats (for CV and DPV experiment)

Potentiostats/ Galvanostats (µStat 400, DropSens, Spain) is the main instrument for voltammetry, which has been applied to the desired potential to the electrochemical cell (i.e. between a working electrode and a reference electrode), and a current-to-voltage converter, which measures the resulting current, and the data acquisition system produces the resulting voltammogram.

3.9 Electrochemical Cell

An electrochemical cell is a device capable of either generating electrical energy from chemical reactions or facilitating chemical reactions through the introduction of electrical energy [89]. A typical electrochemical cell consists of the sample dissolved in a solvent, an ionic electrolyte, and three (or sometimes two) electrodes (Figure 3.3). These are reference electrode (RE), working electrode (WE), and counter electrode (CE) (also called the secondary or auxiliary electrode). The applied potential is measured against the RE, while the CE closes the electrical circuit for the current to flow. The experiments are performed by a potentiostat that effectively controls the voltage between the RE and WE, while measuring the current through the CE (the WE is connected to the ground). Cells (sample holders) come in a variety of sizes, shapes, and materials. The type used depends on the amount and type of sample, the technique, and the analytical data to be obtained. The material of the cell (glass, Teflon, polyethylene) is selected to minimize reaction with the sample. In this investigation three electrodes electrochemical cell has been used. It has advantages over two electrodes cell because of using 3rd electrode. It reduces the solvent resistance and ensures that no electron transfer through the reference electrode.

Figure 3.3: The three electrode system consisting of a working electrode, a reference electrode and a counter electrode.

3.10 Electrodes

Three types of electrodes are used in this research:

i) Working electrodes are Glassy carbon (GC) electrode with 3.0 mm diameter disc, Gold (Au) & Platinum (Pt) electrode with 1.6 mm diameter disc.

ii) Ag/AgCl (standard NaCl) electrode used as reference electrode from BASi, USA

iii) Counter electrode is a Pt wire

The working electrode is an electrode on which the reaction of interest is occurring. The reference electrode is a half-cell having a known electrode potential and it keeps the potential between itself and the working electrode. The counter electrode is employed to allow for accurate measurements to be made between the working and reference electrodes.

3.11 Supporting electrolyte

The supporting electrolyte is an inert soluble ionic salt added to the solvent; generally in 10-fold or 100-fold excess over the concentration of the species being studied. The inertness meant here is the ability to avoid oxidation or reduction at the indicating or reference electrode during the course of the electrochemical measurements.

There are three functions of the supporting electrolyte. First, it carries most of the ionic current of the cell since its concentration is much larger than that of the other species in solution. Thus it serves to complete the circuit of the electrochemical cell and keep the cell resistance at a low value. Second, it maintains a constant ionic strength. This is necessary because the structure of the inter phase region should not change significantly if a reaction occurs there. A stable structure is created on the electrolyte side by adding a high concentration of an inert salt. Third, migration current observed is reduced by the presence of large excess of ions that are not electrochemically active at the potentials in use, because they can carry an ionic current without permitting its conversion into electronic, and hence net or measured, current at the electrodes.

3.12 Preparation of buffer solutions

Preparation of different kinds of buffer solution is discussed below:

Acetate Buffer Solution: To prepare acetate buffer (pH 3.0-5.0) solution definite amount of sodium acetate was dissolved in 0.5M acetic acid in a volumetric flask and the pH was measured. The pH of the buffer solution was adjusted by further addition of acetic acid and / or sodium acetate.

Phosphate Buffer Solution: Phosphate buffer solution (pH 6.0-8.0) was prepared by mixing a solution of 0.5M sodium dihydrogen ortho-phosphate ($NaH_2PO_4.2H_2O$) with a solution of 0.5M disodium hydrogen ortho-phosphate ($Na_2HPO_4.2H_2O$). The pH of the prepared solution was measured with pH meter.

Bicarbonate Buffer Solution: To prepare hydroxide buffer (pH 9.0-11.0) solution definite amount of sodium hydroxide was dissolved in 0.5M sodium bicarbonate in a volumetric flask. The pH of the prepared solution was measured with pH meter.

3.13 Electrode polishing

Materials may be adsorbed to the surface of a working electrode after each experiment. Then the current response will degrade and the electrode surface needs to clean. In this case, the cleaning required is light polishing with 0.05µm alumina powder. A few drops of polish are placed on a polishing pad and the electrode is held vertically and the polish rubbed on in a figure-eight pattern for a period of 30 seconds to a few minutes depending upon the condition of the electrode surface. After polishing the electrode surface is rinsed thoroughly with deionized water.

3.14 Preparation of modified electrodes

In this study, Glassy carbon (GC), Gold (Au) and Platinum (Pt) electrodes purchase from the BASi, USA are used as working electrode. Electrode preparation includes polishing and conditioning of the electrode. The electrode was polished with 0.05µm alumina

powder on a wet polishing cloth. For doing so a part of the cloth was made wet with deionized water and alumina powder was sprinkled over it. Then the electrode was polished by softly pressing the electrode against the polishing surface at least 10 minutes before modify. The electrode surface would look like a shiny mirror after thoroughly washed with deionized water. Sulfolane was weighted and kept in phosphate buffer solution (pH 7). Then it was placed on a magnetic stirrer and stirred for 30 minutes at room temperature. The freshly cleaned bare electrode was modified with Sulfolane by using CV technique. The potential was cycled for 15 scans at a range of -1.0 V to 2.0 V at 100 mV s^{-1}. Then the modified electrode was activated in PBS (pH 7) by applying continuous potential cycled for 5 scans at a range of -0.5 V to 1.2 V. Then the modified electrode was dried by nitrogen gas for 10 minutes. Then a thin layer of Sulfolane was appeared on the surface of the electrode.

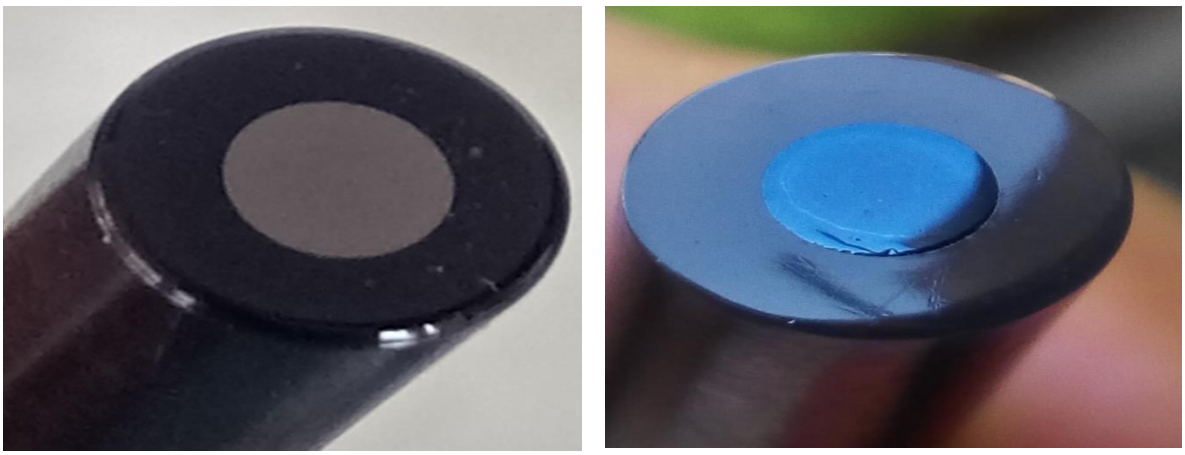

Bare GC electrode Sulfolane modified GC electrode

Figure 3.4: Bare and Sulfolane modified GC electrode

3.15 Preparation of Solutions

All standard solution of VB_6, VC and UA was prepared in 50ml 0.5M PBS (pH 7). Tablet samples are dissolved in 50ml 0.5M PBS (pH 7) with continues stirring by magnetic stirrer.

3.16 Removing Dissolved Oxygen from Solution

Dissolved oxygen can interfere with observed current response so it is needed to remove it. Experimental solution was indolent by purging for at least 5-10 minutes with 99.99% pure and dry nitrogen gas (BOC, Bangladesh). By this way, traces of dissolved oxygen were removed from the solution.

3.17 Experimental procedure

The electrochemical cell filled with solution 50mL of the experimental solution and the Teflon cap was placed on the cell. The working electrode together with reference electrode and counter electrode was inserted through the holes. The electrodes were sufficiently immersed. The solution system is deoxygenated by purging the nitrogen gas for about 10 minutes. The solution has been kept quiet for 10 seconds. After determination the potential window the voltammogram was taken at various scan rates, pH and concentrations from the Drop View Software.

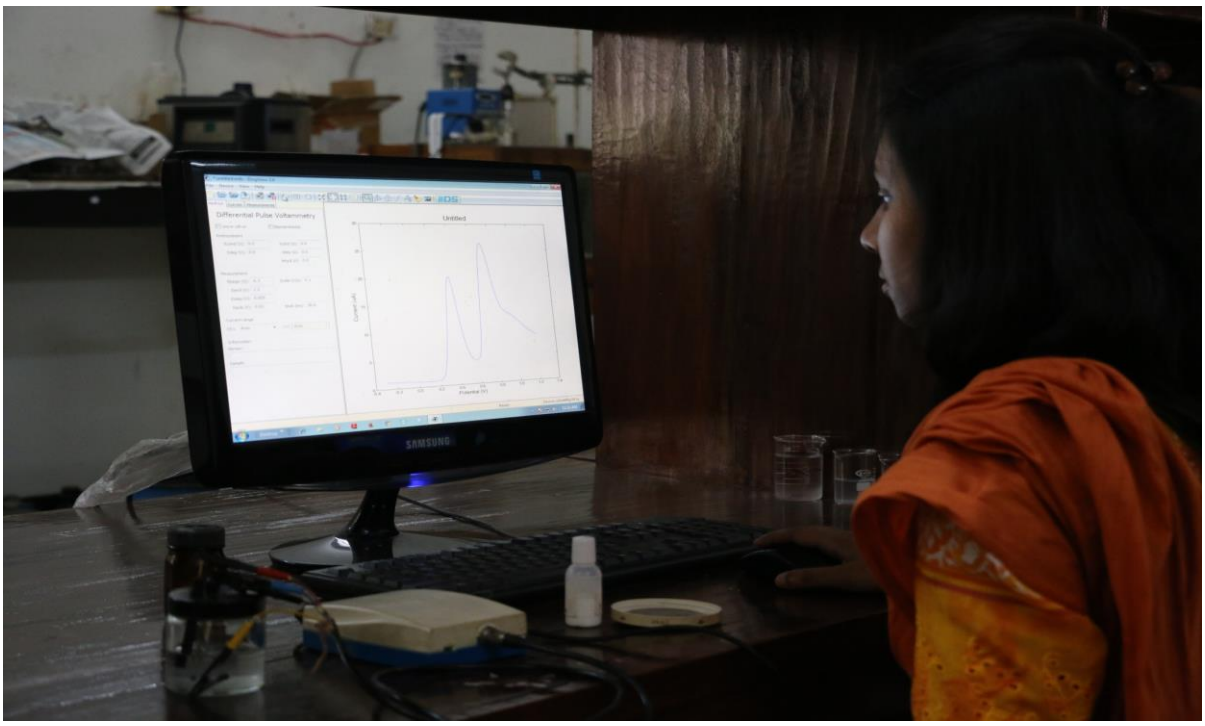

Figure 3.5: Experimental setup (Software controlled Potentiostats (μstat 400))

3.18 UV-Visible Spectrophotometry

In spectrometric analysis a source of radiation is used that extends into the ultraviolet region of the spectrum. The instrument employed for this purpose is a spectrophotometer. An optical spectrometer is an instrument possessing an optical system which can produce dispersion of incident electromagnetic radiation, and with which measurements can be made of the quantity of transmitted radiation at selected wavelength of the spectral range. A photometer is a device for measuring the intensity of transmitted radiation. When combined in the spectrophotometer the spectrometer and photometer are employed conjointly to produce a signal corresponding to the difference between the transmitted radiation of a reference material and that of a sample of selected wavelengths.

The essential parts of spectrophotometer are:

1. A source of radiant energy
2. A monochromator
3. Glass or silica cells for holding the solvent and for the solution under test
4. A device to receive of measure the beam or beam of radiant energy passing through the solvent or solution.

Lambert law states that when monochromatic light passes through a transparent medium, the rate of decrease in intensity with the thickness of the medium is proportional to the intensity of light [90]. This is equivalent to stating that the intensity of the emitted light decrease exponentially as the thickness of the absorbing medium increase arithmetically, or that any layer of given thickness of the medium absorbs the same fraction of the light incident upon it.

Beer studied the effect of concentration of the colored constituent in solution upon the light transmission. He found the same relation between transmission and concentration as Lambert had discovered between transmission and thickness of the layer. By combining both of the theories the final expression can be written as,

$$A = \log \frac{I_0}{I_t} = acl$$

Here, Io=intensity of the incident light; It=intensity of the transmitted light; A=Absorbance of the medium and l are dimensions of the cell.

Figure 3.6: UV-visible spectrophotometer

A computer controlled spectrophotometer (Thermo Scientific, USA) was used for UV-Vis experiment in a pair of quartz cells.

3.19 Standard deviation

In probability and statistics, the standard deviation of a probability distribution, random variable, or population or multiset of values is a measure of the spread of its values. It is usually denoted with the letter σ (lower case sigma). It is defined as the square root of the variance.

To understand standard deviation, keep in mind that variance is the average of the squared differences between data points and the mean. Variance is tabulated in units squared. Standard deviation, being the square root of that quantity, therefore measures the spread of data about the mean, measured in the same units as the data.

Said more formally, the standard deviation is the root mean square (RMS) deviation of values from their arithmetic mean. For example, in the population {4, 8}, the mean is 6

and the deviations from mean are {-2, 2}. Those deviations squared are {4, 4} the average of which (the variance) is 4. Therefore, the standard deviation is 2. In this case 100% of the values in the population are at one standard deviation of the mean.

The standard deviation is the most common measure of statistical dispersion, measuring how widely spread the values in a data set are. If the data points are close to the mean, then the standard deviation is small. As well, if many data points are far from the mean, then the standard deviation is large. If all the data values are equal, then the standard deviation is zero. [91].

3.20 Recovery percentage

Recovery percentage is an indication of a measurement that indicates the accuracy of a measurement or quantitative determination. The percentage of the recovered amount with response to amount taken is termed as recovery percentage as below-

$$\%\ of\ Recovery = \frac{amount\ found}{total\ amount\ taken} \times 100$$

CHAPTER IV

Results and Discussion

Cyclic voltammetry (CV) and differential pulse voltammetry (DPV) techniques were used to investigate the electrochemical behavior of Vitamin-B_6 (VB_6), Vitamin-C (VC) and Uric Acid (UA) in presence of buffer solution by using bare and modified Glassy carbon (GC), Gold (Au) and Platinum (Pt) electrodes. In concordance with the experiment we have abstracted precious information considering electrochemical oxidations of VB_6, VC and UA which has been disputed elaborately in following section. DPV and UV-Vis spectroscopy were used to all quantitative estimation of VB_6, VC and UA in this work.

4.1 Electrochemical behavior of VB_6, VC and UA at bare electrodes

4.1.1 Electrochemical behavior of VB_6, VC and UA at bare GC electrode

Figure 4.1 shows the cyclic voltammogram (CV) of the ternary solution of VB_6, VC and UA at bare GC electrode in Phosphate buffer solution (PBS) (pH 7). It shows two anodic peaks at 0.40 V and 0.80 V. It indicates that the bare GC electrode is unable to separate the individual oxidation peaks of VB_6, VC and UA by using CV technique.

Figure 4.2 shows the differential pulse voltammogram (DPV) of the ternary solution of VB_6, VC and UA at bare GC electrode in PBS (pH 7). It shows two peaks at 0.32 V and 0.71V where three electroactive compounds present in the solution. It also indicates that the bare GC electrode is unable to separate the individual oxidation peaks of VB_6, VC and UA by using DPV technique.

4.1.2 Electrochemical behavior of VB_6, VC and UA at bare Au electrode

Figure 4.3 shows the cyclic voltammogram (CV) of the ternary solution of VB_6, VC and UA at bare Au electrode in PBS (pH 7). It shows only one anodic peak at 0.61 V. It

indicates that the bare Au electrode is unable to separate the individual oxidation peaks of VB_6, VC and UA by using CV technique.

Figure 4.4 shows the differential pulse voltammogram (DPV) of the ternary solution of VB_6, VC and UA at bare Au electrode in PBS (pH 7). It shows two peaks at 0.55 V and 0.96 V where three electroactive compounds present in the solution. It also indicates that the bare Au electrode is unable to separate the individual oxidation peaks of VB_6, VC and UA by using DPV technique.

4.1.3 Electrochemical behavior of VB_6, VC and UA at bare Pt electrode

Figure 4.5 shows the cyclic voltammogram (CV) of the ternary solution of VB_6, VC and UA at bare Pt electrode in PBS (pH 7). It shows only one anodic peak at 0.59 V. It indicates that the bare Pt electrode is unable to separate the individual oxidation peaks of VB_6, VC and UA by using CV technique.

Figure 4.6 shows the differential pulse voltammogram (DPV) of the ternary solution of VB_6, VC and UA at bare Pt electrode in PBS (pH 7). It shows two peaks at 0.53 V and 0.96 V where three electroactive compounds present in the solution. It also indicates that the bare Pt electrode is unable to separate the individual oxidation peaks of VB_6, VC and UA by using DPV technique.

From the observations of the electrochemical behavior of VB_6, VC and UA in ternary solution it is clear that the bare electrodes (GC, Au and Pt) are unable to separate the individual oxidation peaks of VB_6, VC and UA. So, simultaneous determination of these three compounds in ternary mixture is not possible at bare electrodes by using the CV or DPV techniques.

4.2 Modfication of GC electrode with Sulfolane (SFL):

In order to get response from VB_6, VC and UA in a mixture and to improve the selectivity of GC electrode, it was modified with SFL solution. The SFL solution was prepared in PBS (pH 7).

Figure 4.7 shows the continuous CVs of SFL thin film formation onto a bare GC electrode in SFL solution over the potential range of –1.0 V to +2.0 V for 15 cycles at 0.2 V/s scan rate. As can be seen, the anodic peak current increase and the cathodic peak current is also increase, indicating the formation and growth of an electro active layer on the GC electrode surface. After twelve cycles, the increase of these peaks current tended to be stable. It is assumed that a uniform and thin film was present on the surface of GC electrode.

4.3 Electrochemical behavior of VB_6, VC and UA at SFL modified electrodes

4.3.1 Electrochemical behavior of VB_6, VC and UA at SFL modified GC electrode

Figure 4.8 shows the CV of the ternary solution of VB_6, VC and UA at SFL modified GC electrode in PBS (pH 7). It can be seen that it shows three different anodic peaks at 0.18 V for VC, 0.34 V for UA and 0.79 V for VB_6. It indicates that the SFL modified GC electrode is enable to separate the individual oxidation peaks of VB_6, VC and UA by using CV technique. An electrochemically modified electrode is less prone to surface fouling compared to a bare electrode. It also reduces the overvoltage and overcomes the slow kinetics of many electrode processes, thus facilitating the redox process of the compounds, which generally results in increased selectivity and sensitivity of determinations [92]. In this point of view, SFL enhance the selectivity of GC electrode and gives three separated peaks of VB_6, VC and UA with great sensitivity compared to the bare electrode.

Figure 4.9 shows the DPV of the ternary solution of VB_6, VC and UA at SFL modified GC electrode in PBS (pH 7). It can be seen that it shows three different peaks at 0.09 V for VC, 0.32 V for UA and 0.73 V for VB_6. It indicates that the SFL modified GC electrode is enable to separate the individual oxidation peaks of VB_6, VC and UA by using DPV technique.

4.3.2 Electrochemical behavior of VB_6, VC and UA at SFL modified Au electrode

Figure 4.10 shows the CV of the ternary solution of VB_6, VC and UA at SFL modified Au electrode in PBS (pH 7) and at scan rate 0.1V/s. It can be seen that it shows only one

anodic peak at 0.59 V. It indicates that the SFL modified Au electrode is unable to separate the individual oxidation peaks of VB_6, VC and UA by using CV technique. As the oxidation peaks of the compounds are not separated after modifying the electrode, it can be said that the SFL may not deposited on the surface of Au electrode and the oxidation peaks are overlapped at same potential like the bare electrode.

Figure 4.11 shows the DPV of the ternary solution of VB_6, VC and UA at SFL modified Au electrode in PBS (pH 7). It can be seen that it shows two different anodic peaks at 0.50V and 1.05 V as the bare electrode shows. It indicates that the SFL modified Au electrode is unable to separate the individual oxidation peaks of VB_6, VC and UA by using DPV technique. This means that the deposition of SFL at the surface of Au electrode is not so good or the oxidation of VB_6, VC and UA at the surface of Au electrode is not so good.

4.3.3 Electrochemical behavior of VB_6, VC and UA at SFL modified Pt electrode

Figure 4.12 shows the CV of the ternary solution of VB_6, VC and UA at SFL modified Pt electrode in PBS (pH 7). It can be seen that it shows only one anodic peak at 0.56 V. It indicates that the SFL modified Pt electrode is unable to separate the individual oxidation peaks of VB_6, VC and UA by using CV technique.

Figure 4.13 shows the DPV of the ternary solution of VB_6, VC and UA at SFL modified Pt electrode in PBS (pH 7). It can be seen that it shows two different anodic peaks at 0.50 V and 0.94 V as the bare electrode shows. It indicates that the SFL modified Pt electrode is unable to separate the individual oxidation peaks of VB_6, VC and UA by using DPV technique.

4.4 Electrode selection

After analyzing the CVs and DPVs for the electrochemical behavior of VB_6, VC and UA at SFL modified GC, Au and Pt electrodes (Figure 4.14 and Figure 4.15), it is clear that the separation of the oxidation peaks as well as peak intensity of VB_6, VC and UA at SFL modified GC electrode is clear than that of Au and Pt electrodes. For this concern, SFL

modified GC electrode was selected to analysis the electrochemical behavior and quantitative determination of VB_6, VC and UA.

4.5 pH study

Figure 4.16 shows the cyclic voltammograms of the ternary mixture of VB_6, VC and UA in different buffer solution (pH 3, 5, 7 and 9). Figure 4.17 shows the plots of peak currents vs pH. Table 4.1 shows that UA have the maximum peak current in PBS (pH 7) and VB_6 and VC have the maximum peak current in acidic medium (pH 5). But UA was not dissolved at pH 5 and the peak current is very low. The peak current of VB_6 and VC at pH 7 is nearly close to pH 5. So, for the best consideration about the solubility and peak currents pH 7 was selected for the determination of VB_6, VC and UA in ternary mixture.

4.6 Electrochemical Study

4.6.1 Cyclic voltammetric behavior of Vitamin-B_6 (VB_6) at bare GC electrode

Figure 4.18 shows the cyclic voltammogram of 2.5 mM VB_6 in 0.5M PBS (pH 7) and only 0.5M PBS (pH 7) at scan rate 0.1V/s. The voltammogram of only 0.5M PBS (black line) shows no oxidation peak at bare GC electrode. 2.5 mM VB_6 (green line) shows one oxidation peak at 0.74 V and peak current is 35µA. CV of VB_6 in PBS does not show any cathodic peak at bare GC electrode.

4.6.2 Cyclic voltammetric behavior of Vitamin-C (VC) at bare GC electrode

Figure 4.19 shows the cyclic voltammogram of 2.5 mM VC in 0.5M PBS (pH 7) and only 0.5M PBS (pH 7) at scan rate 0.1V/s. The voltammogram of only 0.5M PBS (black line) shows no oxidation peak at bare GC electrode. 2.5 mM VC (blue line) shows one oxidation peak at 0.34 V and peak current is 49 µA. CV of VC in PBS does not show any cathodic peak at bare GC electrode.

4.6.3 Cyclic voltammetric behavior of Uric Acid (UA) at bare GC electrode

Figure 4.20 shows the cyclic voltammogram of 2.5 mM UA in 0.5M PBS (pH 7) and only 0.5M PBS (pH 7) at scan rate 0.1V/s. The voltammogram of only 0.5M PBS (black line) shows no oxidation peak at bare GC electrode. 2.5 mM UA (red line) shows one oxidation peak at 0.35 V and peak current is 74 µA. CV of UA in PBS does not show any cathodic peak at bare GC electrode.

4.6.4 Determination of VB_6 and VC at bare GC electrode using cyclic voltammetric technique

CV of 2.5 mM VB_6 and 2.5 mM VC was taken for the simultaneous detection at bare GC electrode. CV shows two anodic peaks at 0.78V and 0.40V. This indicates that the oxidation of VB_6 and VC have a significant potential difference (Figure 4.21). The peak at 0.78 V is for VB_6 and at 0.40 V is for VC. Peak current of VB_6 and VC at bare GC electrode is 29µA and 3µA respectively. Determination of VB_6 and VC at bare GC electrode is possible but at SFL modified GC electrode they show a significant increase of current that is very important to determine the amount of VB_6 and VC in a low concentration sample.

4.6.5 Determination of VC and UA at bare GC electrode using cyclic voltammetric technique

CV of 2.5 mM VC and 2.5 mM UA was taken for the simultaneous detection at bare GC electrode. The peaks of 2.5 mM VC and 2.5 mM UA was overlapped in the binary solution containing VC and UA (Figure 4.22).

VC in PBS gives one anodic peak at 0.34 V. On the other hand UA gives an anodic peak at 0.35 V. The binary mixture of VC and UA shows a single anodic peak was found at 0.50 V which is at high potential than the peaks for individual VC and UA. No cathodic peak observed for the binary mixture of VC and UA at bare GC electrode. The anodic peak in the binary mixture is the combined peak of both of the species which is due to the fouling effect. As VC and UA are oxidized at a close potential range, it causes an overlapping

oxidation peak at bare electrode. As they do not give individual response when both are present in the mixture, their simultaneous detection at bare GC electrode is impossible.

4.6.6 Determination of UA and VB_6 at bare GC electrode using cyclic voltammetric technique

CV of 2.5 mM UA and 2.5 mM VB_6 was taken for the simultaneous detection at bare GC electrode. CV shows two anodic peaks at 0.35 V and 0.74 V. This indicates that the oxidation of UA and VB_6 have a significant potential difference (Figure 4.23). The peak at 0.35 V is for UA and at 0.74 V is for VB_6. Peak current of VB_6 and VC at bare GC electrode is 29µA and 3µA respectively. Determination of UA and VB_6 at bare GC electrode is possible but at SFL modified GC electrode they show a significant increase of current that is very important to determine the amount of UA and VB_6 in a low concentration sample.

4.6.7 Determination of VB_6, VC and UA at bare GC electrode using cyclic voltammetric technique

VB_6 in PBS gives one anodic peak at 0.74 V, VC in PBS gives one anodic peak at 0.34 V and UA in PBS gives one anodic peak at 0.35 V. For the ternary mixture of VB_6, VC and UA in PBS, two anodic peaks were found at 0.41 V and 0.80 V which is at high potential than the oxidation potential of VB_6, VC and UA. No cathodic peak was observed for the ternary mixture of VB_6, VC and UA at bare GC electrode (Figure 4.24). The anodic peak at 0.35 V in the ternary mixture is the combined peak of VC and UA. VB_6 gives an individual peak for the difference of oxidation potential compared to VC and UA. VC and UA are oxidized at a close potential, so their combined solution gives response as if a solution of double concentration. Bare GC electrode does not give separate peaks for simultaneous detection of VB_6, VC and UA in their ternary solution.

4.7 Cyclic voltammetric behavior of SFL at Modified GC electrode

Figure 4.25 shows the cyclic voltammogram of SFL solution at modified GC electrode. SFL in PBS solution shows no anodic or cathodic peak in the measurement potential of

VB_6, VC and UA within -0.3 V to +1.2 V. It indicates that the deposited SFL film on GC electrode surface just enhance the signals of analytes without interfering with their oxidation potential and sensitivity.

4.8 Cyclic voltammetric behavior of VB_6 at SFL modified GC electrode

Figure 4.26 shows the cyclic voltammogram of 2.5 mM VB_6 in PBS (pH 7) and only PBS at SFL modified GC electrode. There is no peak for PBS but a sharp and well defined peak is observed for VB_6 at 0.72 V.

4.8.1 Comparison of the CV of VB_6 at Bare and SFL modified GC electrode

Fig. 4.27 shows the comparison between the behaviors of VB_6 at bare and SFL modified GC electrode. At bare GC electrode VB_6 gives an anodic peak at 0.74 V having peak current 35 µA. But, at SFL modified GC electrode VB_6 gives an anodic peak at 0.72 V having peak current 49 µA. It is clear that the anodic peak intensity of VB_6 at SFL modified GC electrode is sharp and well defined than that of bare GC electrode. The position of the anodic peak of VB_6 at SFL modified GC electrode is shifted significantly and current is prominent than that of bare GC electrode.

4.8.2 Scan rate effect of VB_6 at SFL modified GC electrode

Figure 4.28 shows the CVs of 2.5 mM VB_6 at different scan rates. The CVs were taken at SFL modified GC electrode in PBS (pH 7).The current potential data, peak potential separation, peak currents are represented in Table 4.1.

From table 4.1, it is clear that the peak current of VB_6 is gradually increased with the increase of scan rate. The peak current of VB_6 increased with the increase of square root of scan rate ($v^{1/2}$) (Figure 4.29), the corresponding trend line is a straight line which passes through the origin indicates that the oxidation process of VB_6 is a diffusion controlled process [93].

4.8.3 Cyclic voltammetric behavior of VC at SFL modified GC electrode

Figure 4.30 shows the cyclic voltammogram of 2.5 mM VC in PBS (pH 7) and only PBS at SFL modified GC electrode. There is no peak for PBS but a sharp and well defined anodic peak is observed for VC at 0.15 V.

4.8.4 Comparison of the CV of VC at bare and SFL modified GC electrode

Figure 4.31 shows the comparison between the behaviors of VC at bare and SFL modified GC electrode. At bare GC electrode VC gives an anodic peak at 0.34 V having peak current 49µA. But, at SFL modified GC electrode VC gives an anodic peak at 0.15 V having peak current 60 µA. It is clear that the peak intensity of VC at SFL modified GC electrode is sharp and well defined than that of bare GC electrode. The position of the anodic peak of VC at SFL modified GC electrode is shifted significantly and current is prominent than that of bare GC electrode.

4.8.5 Scan rate effect of VC at SFL modified GC electrode

Figure 4.32 shows the CVs of 2.5 mM VC at different scan rates. The CVs were taken at SFL modified GC electrode in PBS (pH 7).The current potential data, peak potential separation, peak currents are represented in Table 4.2.

From table 4.2, it is clear that the peak current of VC is gradually increased with the increase in scan rate. The anodic peak current of VC increased with the increase of square root of scan rate ($v^{1/2}$) (Figure 4.33), the corresponding trend line is straight line which passes through the origin indicates that the oxidation process of VC is a diffusion controlled process [93].

4.8.6 Cyclic voltammetric behavior of UA at SFL modified GC electrode

Figure 4.34 shows the cyclic voltammogram of 2.5 mM UA in PBS (pH 7) and only PBS at SFL modified GC electrode. There is no peak for PBS but a sharp and well defined anodic peak is observed for UA at 0.33 V.

4.8.7 Comparison of the CV of UA at bare and SFL modified GC electrode

Fig. 4.35 shows the comparison between the behaviors of UA at bare and SFL modified GC electrode. At bare GC electrode UA gives an anodic peak at 0.35 V having peak current 74 µA. But, at SFL modified GC electrode UA gives an anodic peak at 0.33 V having peak current 77 µA. It is clear that the peak intensity of UA at SFL modified GC electrode is sharp and well defined than that of bare GC electrode. The position of the anodic peak of UA at SFL modified GC electrode is shifted significantly and current is prominent than that of bare GC electrode.

4.8.8 Scan rate effect of UA at SFL modified GC electrode

The CVs of 2.5 mM UA at different scan rates are shown in Figure 4.36. The CVs were taken at SFL modified GC electrode in PBS (pH 7). The current potential data, peak potential separation, peak currents are represented in Table 4.3.

From table 4.3, it is clear that the peak current of UA is gradually increased with the increase of scan rate. The anodic peak current of UA increased with the increase of square root of scan rate ($v^{1/2}s^{-1/2}$) (Figure 4.37), the corresponding trend line is a straight line which is not passed through the origin indicates that the oxidation process of UA is an impurely diffusion controlled process [93].

4.9 Determination of VB_6, VC and UA in binary and ternary mixture at SFL modified GC electrode

4.9.1 Determination of VB_6 and VC at SFL modified GC electrode using CV

Figure 4.38 shows the CV of a binary mixture (2.5 mM) of VB_6 and VC at bare GC and SFL modified GC electrode. The CVs of VB_6, VC and the binary mixture (2.5 mM) of VB_6 and VC at SFL modified GC electrode are shown in Fig. 4.39. At SFL modified GC electrode, the binary mixture of VB_6 and VC shows two anodic peaks at 0.73 V and 0.07V respectively. The peak currents of VB_6 and VC are 50 µA and 8 µA respectively. The

binary mixture of VB_6 and VC shows two oxidation peaks at 0.78 V and 0.40 V for their difference of oxidention potential. The peak currents of VB_6 and VC were 29 µA and 3 µA respectively. From the positions and currents of the peaks it can be explained that the peaks of both VB_6 and VC are sharp and well defined at SFL modified GC electrode and having higher peak current than that of bare GC electrode. So, the SFL modified GC electrode can determine the amount of VB_6 and VC accurately compared to bare GC electrode.

4.9.2 Determination of VC and UA at SFL modified GC electrode using CV

CV of a binary mixture (2.5 mM) of VC and UA at bare and SFL modified GC electrode shows in Fig. 4.40. The CVs of VC, UA and the binary mixture (2.5 mM) of VC and UA in PBS at SFL modified GC electrode are shown in Fig. 4.41. For the mixture of VC and UA there only one peak was observed at 0.5 V at bare GC electrode. At SFL modified GC electrode, VC and UA gives two anodic peaks at 0.19 V and 0.35V respectively. From the positions of the anodic peak it can be explained that the peaks of both VC and UA are separated at SFL modified GC electrode. The SFL modified GC electrode can separate the anodic peaks of VC and UA when they are present in a binary mixture.

4.9.3 Determination of UA and VB_6 at SFL modified GC electrode using CV

CV of a binary mixture (2.5 mM) of UA and VB_6 at bare GC and SFL modified GC electrode shows in Fig. 4.42. The CVs of UA, VB_6 and the binary mixture (2.5 mM) of UA and VB_6 at SFL modified GC electrode are shown in Fig. 4.43. At SFL modified GC electrode, UA and VB_6 shows two anodic peaks at 0.33 V and 0.78 V respectively. The peak currents of UA and VB_6 are 92 µA and 33 µA respectively. Binary mixture of UA and VB_6 shows two peaks at 0.35 V and 0.74 V for their difference of oxidation potential. The peak currents of UA and VB_6 were 36 µA and 19 µA at bare GC electrode. From the positions and currents of the peaks it can be explained that the peaks of both UA and VB_6 are sharp and well defined at SFL modified GC electrode having peak current prominent than that of bare GC electrode. So SFL modified GC electrode can determine the amount of UA and VB_6 accurately compared to bare GC electrode.

4.9.4 Determination VB_6, VC and UA at SFL modified GC electrode using CV

CV of a ternary mixture (2.5 mM) of VB_6, VC and UA at bare GC and SFL modified GC electrode shows in Fig. 4.44. The CVs of VB_6, VC and UA and their ternary mixture (2.5 mM) at SFL modified GC electrode are shown in Fig. 4.45. At SFL modified GC electrode VB_6, VC and UA shows three anodic peaks at 0.79 V, 0.18 V and 0.34 V respectively. The peak currents of VB_6, VC and UA are 34 µA, 9 µA and 90 µA respectively. For the mixture of VB_6, VC and UA, two peaks were observed at 0.5 V and 0.74V respectively at bare GC electrode. In fig. 4.45, the positions and currents of the peaks indicates that the SFL modified GC electrode can separate the peaks with good sensitivity compared to the bare GC electrode. So, SFL modified GC electrode can be used for the detection of VB_6, VC and UA in a ternary mixture

4.10 Determination of VB_6, VC and UA at SFL modified GC electrode using differential pulse voltammetric (DPV) technique

All the DPV experiments were taken at Epulse = 0.02 V and tpulse = 20 ms.

4.10.1 Determination of VB_6 and VC at SFL modified GC electrode using DPV

DPV of a binary mixture (2.5 mM) of VB_6 and VC at bare GC and SFL modified GC electrode shows in Fig. 4.46. The DPVs of VB_6, VC and their binary mixture (2.5 mM) at SFL modified GC electrode is shown in Fig. 4.47. At SFL modified GC electrode binary mixture of VB_6 and VC shows two anodic peaks at 0.69 V and 0.12 V respectively. The peak currents of VB_6 and VC are 24µA and 16µA at SFL modified GC electrode. From the positions and currents of the peaks it can be explained that the peaks of both VB_6 and VC are sharp and well defined at SFL modified GC electrode having higher peak current prominent than that of bare GC electrode. So, the SFL modified GC electrode can determine the amount of VB_6 and VC accurately compared to bare GC electrode using DPV technique.

4.10.2 Determination of VC and UA at SFL modified GC electrode using DPV

DPV of a binary mixture (2.5 mM) of VC and UA at bare GC and SFL modified GC electrode shows in Fig. 4.48. The DPVs of VC, UA and the binary mixture (2.5 mM) at SFL modified GC electrode are shown in Fig. 4.49. Binary mixture of VC and UA shows two oxidation peaks at 0.13 V and 0.33V respectively. For the mixture of VC and UA, there only one peak was observed at 0.50 V that was the overlapped peak of both VC and UA at bare GC electrode. In Fig. 4.49, the positions of the oxidation peaks indicate that the peaks of both VC and UA are separated at SFL modified GC electrode. The SFL modified GC electrode can separate the peaks of VC and UA when they are present in a binary mixture by using DPV technique.

4.10.3 Determination of UA and VB_6 at SFL modified GC electrode using DPV

DPV of a binary mixture (2.5 mM) of UA and VB_6 at bare GC and SFL modified GC electrode shows in Fig. 4.50. The DPVs of UA, VB_6 and the binary mixture (2.5 mM) at SFL modified GC electrode are shown in Fig. 4.51. At SFL modified GC electrode, binary mixture of UA and VB_6 shows two oxidation peaks at 0.31 V and 0.71V respectively. The peak currents of UA and VB_6 are 66 µA and 17 µA respectively. From the positions and currents of the peaks it can be explained that the peaks of both UA and VB_6 are sharp and well defined at SFL modified GC electrode having higher peak current prominent than that of bare GC electrode. So, the SFL modified GC electrode can determine the amount of UA and VB_6 accurately compared to bare GC electrode using DPV technique.

4.10.4 Determination VB_6, VC and UA at SFL modified GC electrode using DPV

DPV of a ternary mixture (2.5 mM) of VB_6, VC and UA at bare GC and SFL modified GC electrode shows in Fig. 4.52. The DPVs of VB_6, VC and UA and their ternary mixture (2.5 mM) at SFL modified GC electrode are shown in Fig. 4.53. At SFL modified GC electrode ternary mixture of VB_6, VC and UA gives three oxidation peaks at 0.73 V, 0.09 V and 0.32 V respectively. The peak currents of VB_6, VC and UA are 21 µA, 9 µA and 63 µA respectively.

For the mixture of VB_6, VC and UA, two peaks were observed at 0.32 V and 0.71 V respectively at bare GC electrode. In fig. 4.53, the positions and currents of the peaks indicates that the SFL modified GC electrode can separate the peaks with high sensitivity compared to the bare GC electrode. So, the SFL modified GC electrode can be used for the determination (qualitative & quantitative) of VB_6, VC and UA in a ternary mixture using DPV technique.

4.11 Quantitative estimation of VB_6, VC and UA at SFL modified GC electrode in binary and ternary mixture:

For the calculation of sensitivity and detection limit of the analytes we need the surface area of SFL modified GC electrode. The surface area experiment is given below,

4.11.1 Electrode surface area calculation:

Fig. 4.54 shows the CVs of potassium ferrocyanide in KCl solution and table 4.5 shows the peak current of potassium ferrocyanide at different scan rate at SFL modified GC electrode.

Electrode surface area was calculated by Randles–Sevcik equation using ferrocyanide at different scan rates in 1M KCL solution.

In general, the peak current of diffusion controlled reversible or quasi-reversible electro - chemical reaction follows Randles–Sevcik equation [97].

$$Ip = 0.4463nF\sqrt{\frac{nFD}{RT}}AC\sqrt{v} \quad \text{----------} \quad (1)$$

Where Ip: the peak current, n: the number of electrons, F: Faraday constant, T: the temperature in Kelvin, R: the gas constant, A: the surface area of the working electrode, D: the diffusion coefficient of the electroactive species, C: the bulk concentration of the electroactive species and *v*: the scan rate of voltammograms.

From Equation (1) we get,

$$\text{Slope} = 0.4463nF\sqrt{\frac{nFD}{RT}}AC$$

$$A = \frac{Slope}{0.4463nF\sqrt{\frac{nFD}{RT}}C}$$

From the curve (Fig 4.55) the value of slope is ~6.4×10^{-5} and the standard value of diffusion coefficient for ferrocyanide on GCE is 1.52×10^{-6} cm^2/s. where concentration C = 2×10^{-6} mol/cm^3 so we get,

$$A = \frac{6.4\times10^{-5}}{0.4463\times1\times96500\sqrt{\frac{1\times96500\times 1.52\times10^{-6}}{8.314\times 298}}\times2\times10^{-6}}$$

A = 0.097 cm^2

Bare GC electrode (diameter = 3mm) has the surface area 0.071 cm^2. Surface area of SFL modified GC electrode is 0.097 cm^2 indicates that the surface area of GC electrode increased after modify.

4.11.2 Simultaneous quantitative determination of VB_6 and VC at SFL modified GC electrode

DPVs of simultaneous change of VB_6 and VC (0.5-2.5 mM) are shown in Fig. 4.56. Peak currents of VB_6 and VC were increased linearly with the increase of their concentrations. The linear regression equation for VB_6 and VC is Ip (VB_6) =8.368_{VB6}+4.936 (R^2= 0.996) and Ip (VC) =6.208_{VC}-0.786 (R^2= 0.992) respectively (Fig. 4.57). The average current increase for VB_6 and VC is 4.3µA and 3.1µA respectively. The sensitivity was calculated for the binary mixture of VB_6 and VC. The sensitivity of VB_6 and VC are 43.74µA/mM/cm^2 and 31.80µA/mM/cm^2 respectively. Limit of detection (LoD) was calculated by signal to noise ratio (S/N=3). The LoD of VB_6 and VC are 1.74μML^{-1} and 1.26$\mu ML^{-1.}$

4.11.3 Simultaneous quantitative determination of VC and UA at SFL modified GC electrode

DPVs of simultaneous change of VC and UA (0.5-2.5 mM) are shown in Fig. 4.58. All solutions were freshly prepared in PBS (pH 7). Peak currents of VC and UA are increased linearly with the increase of their concentrations. The linear regression equation for VC and UA is Ip (VC) $=4.168_{VC}+0.77$ ($R^2= 0.997$) and Ip (UA) $= 11.53_{UA}+36.80$ ($R^2= 0.994$) respectively (Fig. 4.59). The average current increase for VC and UA is 2.1µA and 5.8µA respectively. The sensitivity was calculated for the binary mixture of VC and UA. The sensitivity of VC and UA are 21.38µA/mM/cm^2 and 60.27µA/mM/cm^2 respectively. Limit of detection (LoD) was calculated by signal to noise ratio (S/N=3). The LoD of VC and UA are 1.96µML^{-1} and 0.70µML^{-1} respectively.

4.11.4 Simultaneous quantitative determination of UA and VB_6 at SFL modified GC electrode

DPVs of simultaneous change of UA and VB_6 (0.5-2.5 mM) are shown in Fig. 4.60. Peak currents of UA and VB_6 are increased linearly with the increase of concentrations. The linear regression equation for UA and VB_6 is Ip (UA) $=14.04_{UA}+36.63$ ($R^2= 0.997$) and Ip (VB_6) $=5.274_{VB6}+4.163$ ($R^2= 0.996$) respectively (Fig. 4.61). The average current increase for UA and VB_6 is 7.1µA and 2.7µA respectively. The sensitivity was calculated for the binary mixture of UA and VB_6. The sensitivity of UA and VB_6 are 73.55µA/mM/cm^2 and 27.54µA/mM/cm^2 respectively. Limit of detection (LoD) was calculated by signal to noise ratio (S/N=3). The LoD of UA and VB_6 are 0.68µML^{-1} and 1.87µML^{-1} respectively.

4.12 Quantitative determination of VB_6, VC and UA in ternary mixture at SFL modified GC electrode

4.12.1 Quantitative determination of VB_6 at constant concentration of VC and UA at SFL modified GC electrode

DPV of the ternary mixture of VB_6, VC and UA at SFL modified GC electrode is shown in Fig. 4.62, where the concentration of VC and UA were kept constant and the concentration

of VB_6 was varied successively. Fig. 4.63 shows the calibration curve for different concentrations of VB_6. This calibration curve can be used to determine VB_6 in presence of VC and UA in a ternary mixture. In case of VB_6 the peak current increases with the linear regression equation, Ip (VB_6) = 4.268_{VB6}+0.076 (R^2= 0.997).

4.12.2 Quantitative determination of VC at constant concentration of UA and VB_6 at SFL modified GC electrode

DPV of the ternary mixture of VB_6, VC and UA at SFL modified GC electrode is shown in Fig. 4.64, where the concentration of UA and VB_6 were kept constant and the concentration of VC was varied successively. Fig. 4.65 shows the calibration curve for different concentrations of VC. This calibration curve can be used to determine VC in presence of UA and VB_6 in a ternary mixture. In case of VC the peak current increases with the linear regression equation, Ip (VC) = 4.32_{VC}-0.18 (R^2=0.997).

4.12.3 Quantitative determination of UA at constant concentration of VC and VB_6 at SFL modified GC electrode

DPV of the ternary mixture of VB_6, VC and UA at SFL modified GC electrode is shown in Fig. 4.66, where the concentration of VC and VB_6 were kept constant and the concentration of UA was varied successively. Fig. 4.67 shows the calibration curve for different concentrations of UA. This calibration curve can be used to determine UA in presence of VC and VB_6 in a ternary mixture. In case of UA the peak current increases with the linear regression equation, Ip (UA) = 19.39_{UA}+24.02 (R^2= 0.994).

4.12.4 Quantitative determination of VB_6 and VC at constant concentration of UA at SFL modified GC electrode

DPV of the ternary mixture of VB_6, VC and UA at SFL modified GC electrode is shown in Fig. 4.68, where the concentration of UA was kept constant and the concentrations of VB_6 and VC were varied successively. Fig. 4.69 shows the calibration curve for different concentrations of VB_6 and VC. This calibration curve can be used to determine VB_6 and VC in presence of UA in a ternary mixture. In case of VB_6 and VC the peak current

increases with the linear regression equations, Ip (VB_6) = 6.442_{VB6}+1.683 (R^2= 0.997) and Ip (VC) = 4.61_{VC}-1.269 (R^2= 0.995) respectively.

4.12.5 Quantitative determination of VC and UA at constant concentration of VB_6 at SFL modified GC electrode

DPV of the ternary mixture of VB_6, VC and UA at SFL modified GC electrode is shown in Fig. 4.70, where the concentration of VB_6 was kept constant and the concentrations of VC and UA were varied successively. Fig. 4.71 shows the calibration curve for different concentrations of VC and UA. This calibration curve can be used to determine VC and UA in presence of VB_6 in a ternary mixture. In case of VC and UA the peak current increases with the linear regression equations, Ip (VC) = 4.462_{VC}-0.199 (R^2= 0.998) and Ip (UA) = 11.72_{UA}+24.57 (R^2= 0.993) respectively.

4.12.6 Quantitative determination of UA and VB_6 at constant concentration of VC at SFL modified GC electrode

DPV of the ternary mixture of VB_6, VC and UA at SFL modified GC electrode is shown in Fig. 4.72, where the concentration of VC was kept constant and the concentrations of UA and VB_6 were varied successively. Fig. 4.73 shows the calibration curve for different concentrations of UA and VB_6. This calibration curve can be used to determine UA and VB_6 in presence of VC in a ternary mixture. In case of UA and VB_6 the peak current increases with the linear regression equations, Ip (UA) = 14.36_{UA}+28.14 (R^2= 0.994) and Ip (VB_6) = 3.486_{VB6}+9.401 (R^2= 0.998) respectively.

4.12.7 Simultaneous quantitative determination of VB_6, VC and UA at SFL modified GC electrode in a ternary mixture

DPV of the ternary mixture of the different concentrations of VB_6, VC and UA at SFL modified GC electrode are shown in Fig. 4.74. Fig. 4.75 shows the calibration curve for different concentrations of VB_6, VC and UA. These calibration curve can be used to determine VB_6, VC and UA quantitatively in a ternary mixture. The peak currents of VB_6, VC and UA increased linearly with the increase of their concentrations over the range of

0.5-2.5 mM. The linear regression equations of VB_6, VC and UA are Ipa (VB_6) = 5.61_{VB6}+3.945 (R^2 = 0.999), Ipa (VC) = 4.446_{VC}-0.289 (R^2=0.999) and Ipa (UA) = 19.02_{UA}+23.42 (R^2 = 0.996), respectively. The sensitivity of VB_6, VC and UA are 41.8, 31.1 and 138.1 µA/mM/cm^2 and detection limits are 0.8, 1.0 and 0.2 µM respectively.

The linear regression equations of the calibration curves for single concentration change, binary concentration change and ternary concentration changes are nearly equal which indicates that they do not interfere in the determination of each other. So, this modified electrode sensor can be used to determine the target analytes (VB_6, VC and UA) individually, in a binary mixture and in a ternary mixture.

4.13 Interference study

Figure 4.76 shows the DPV of the ternary solution of VB_6, VC and UA in the presence of paracetamol, thiamine (vitamin B_1), nicotinamide (vitamin B_3), histidine, aspargine, lysine, proline, phenylalanine and glucose as interfering agents. From the voltammogram it is clear that the peak position of VB_6 (0.77V), VC (0.19 V) and UA (0.35 V) are not influenced by the interfering substances. The peak positions are remaining unchanged like they appeared when no interfering substances present (Fig. 4.8). An oxidation peak appeared for paracetamol at 0.46 V without interfering the peak positions of VB_6, VC and UA. So, the SFL modified GC electrode does not show any interference in the peak potential range of VB_6, VC and UA by the mentioned interfering substances.

4.14 Quantitative Analysis of real and tablet samples

Quantitative analysis in real (tablet and blood serum) samples was done by using this method. For each analyte recovery percentage (R %) and standard deviation (SD) was calculated to evaluate the consistency of the modified electrode sensor. The quantitative determination of each tablet samples was valided by UV-Vis method and the quantitative determination of UA in blood serum was valided by pathological report.

4.14.1 Quantitative analysis of VB_6 in standard and tablet samples

4.14.1.1 Quantitative analysis of standard VB_6

DPV of different amount of standard VB_6 in 50mL PBS (pH 7) under optimum condition are shown in Fig. 4.77. Table 4.6 shows the peak current for different amount of VB_6. Fig. 4.78 shows the calibration curve of VB_6 with response to different amount. The regression equation for the calibration curve of VB_6 is Ip = 0.926x+5.612 (R^2=0.992). This equation was used to determine the unknown amount in the real and tablet samples where, "Ip" is the peak current of the sample and "x" is the amount of the sample.

Table 4.7 shows the recovery percentage data of standard VB_6 using the regression equation of the calibration curve. The recovery percentage is found 98-103% indicates that the modified electrode sensor has the ability to determine the amount of VB_6 with high accuracy.

Table 4.8 shows the data of the determination of known 25mg standard VB_6 sample (5 times) for the standard deviation calculation. The standard deviation was found ±0.2mg. It is clear that the sensor can determine the amount with high consistency.

4.14.1.2 Determination of VB_6 in tablet samples using SFL modified GC electrode sensor

For each determination 1/2 parts of the tablet was dissolved in 50mL of PBS (pH 7).

Calculation of the amount

Fig. 4.79 shows the DPVs of the tablet samples in PBS (pH 7) at scan rate 0.1V/s and table 4.9 shows the current data of tablet samples.

VB_6 in Acliz Plus tablet

The linear regression equation of VB_6 (Fig. 4.78) is Ip = 0.926x+5.612 where, "Ip" is the peak current of the VB_6 in Acliz Plus and "x" is the amount.

For Acliz Plus, the current found 28.62µA.

So, X= (28.62-5.612)/0.926

X= 24.8 mg in 1/2 parts of the tablet. [For each determination 1/2 parts of the tablet was dissolved in 50mL of PBS (pH 7)].

So, total amount of VB_6 in Acliz Plus tablet is 24.8×2= 49.6 mg.

Same calculation was considered for every tablet sample. The amount of VB_6 in each tablet found by using this method is shown in table 4.10.

4.14.1.3 Determination of VB_6 in tablet samples using UV-Visible method

For each determination 1/3 parts of the tablet was dissolved in 1000mL of water.

Fig. 4.80 shows the UV-Vis spectra of different concentrations (80-240ppm) of VB_6 using water as solvent. Table 4.11 shows the absorbance for different concentrations of VB_6. Fig. 4.81 shows the calibration curve of VB_6 with response to different concentrations. The regression equation for the calibration curve of VB_6 is $A = 0.0072x+0.5336$ ($R^2=0.9999$). This equation is used to determine the unknown amount in the tablet samples where, "A" is the absorbance of the sample and "x" is the amount of the sample.

Table 4.11 shows the quantitative determination of VB_6 in different commercial tablets of different pharmaceuticals using UV-Visible technique with standard deviations. Each replicates were repeated by 4 times. Table 4.13 shows the comparison of the determination of VB_6 using UV-Visible technique with the determination of VB_6 using SFL modified GC electrode.

4.14.2 Quantitative analysis of VC in standard and tablet samples

4.14.2.1 Quantitative analysis of standard VC

DPV of different amount of standard VC in 50mL PBS (pH 7) under optimum condition are shown in Fig. 4.82. Table 4.14 shows the peak current for different amount of VC. Fig. 4.83 shows the calibration curve of VC with response to different amount. The regression equation for the calibration curve of VC is $Ip = 0.634x+10.17$ ($R^2=0.984$). This equation is used to determine the unknown amount in the real and tablet samples where, "Ip" is the peak current of the sample and "x" is the amount of the sample.

Table 4.15 shows the recovery percentage data of standard VC using the regression equation of the calibration curve. The recovery percentage is found 100-103% indicates that the modified electrode sensor has the ability to determine the amount of VC with high accuracy.

Table 4.16 shows the data of the determination of known 35mg standard VC sample (5 times) for the standard deviation calculation. The standard deviation was found ±0.6mg. It is clear that the sensor can determine the amount with high consistency.

4.14.2.2 Determination of VC in tablet samples using SFL modified GC electrode sensor

For each determination 1/12 parts of the tablet was dissolved in 50mL of PBS (pH 7).

Calculation of the amount

Fig. 4.84 shows the DPVs of the tablet samples in PBS (pH 7) at scan rate 0.1V/s and table 4.17 shows the current data of tablet samples.

VC in Cevit tablet

The linear regression equation of VC (Fig. 4.83) is Ip = 0.634x+10.17 where, "Ip" is the peak current of the VC in Cevit and "x" is the amount.

For Cevit, the current found 23.33μA.

So, X= (23.33-10.17)/0.634

X= 20.8 mg in 1/12 parts of the tablet. [For each determination 1/12 parts of the tablet was dissolved in 50mL of PBS (pH 7)].

So, total amount of VC in Cevit tablet is 20.8×12= 249.6 mg.

Same calculation was considered for Cecon and Vasco. But for Nutrivit C and Ascobex 1/10 parts of the tablet was dissolved in 50mL of PBS (pH 7) for each determination. So, the amount of VC in Nutrivit C and Ascobex is found by multiplying the amount "x" with 10.

The amount of VC in each tablet found by using this method is shown in table 4.18.

4.14.2.3 Determination of VC in tablet samples using UV-Visible method

For each determination 1/3 parts of the tablet was dissolved in 1000mL of water.

Fig. 4.85 shows the UV-Vis spectra of different concentrations (80-240ppm) of VC using water as solvent. Table 4.19 shows the absorbance for different concentrations of VC. Fig. 4.86 shows the calibration curve of VC with response to different concentrations. The regression equation for the calibration curve of VC is A = 0.0035x+0.2016 (R^2=0.9902). This equation is used to determine the unknown amount in the real and tablet samples where, "A" is the absorbance of the sample and "x" is the amount of the sample.

Table 4.20 shows the quantitative determination of VC in different commercial tablets of different pharmaceuticals using UV-Visible technique with standard deviations. Each replicates were repeated by 4 times for the standard deviation calculation. Table 4.21 shows the comparison of the determination of VC using UV-Visible technique with the determination of VC using SFL modified GC electrode.

4.14.3 Quantitative analysis of UA in standard and blood sample

4.14.3.1 Quantitative analysis of standard UA

DPV of different amount of standard UA in 50mL PBS (pH 7) under optimum condition are shown in Fig. 4.87. Table 4.22 shows the peak current for different amount of UA. Fig. 4.88 shows the calibration curve of UA with response to different amount. The regression equation for the calibration curve of UA is Ip = 16.26x-0.063 (R^2=0.996). This equation is used to determine the unknown amount in the real samples where, "Ip" is the peak current of the sample and "x" is the amount of the sample.

Table 4.23 shows the recovery percentage data of standard UA using the regression equation of the calibration curve. The recovery percentage is found 96-110% indicates that the modified electrode sensor has the ability to determine the amount of UA with high accuracy.

Table 4.24 shows the data of the determination of known 10mg standard UA sample (5 times) for the standard deviation calculation. The standard deviation was found ±0.5mg. It is clear that the sensor can determine the amount with high consistency.

4.14.3.2 Determination of UA in blood sample using SFL modified GC electrode sensor

For the determination of UA in blood sample 2.5mL blood sample was dissolved in 22.5mL PBS (pH 7) and the solution was diluted for 10 times. Fig. 4.89 shows the DPV of the blood sample in PBS (pH 7) at scan rate 0.1V/s.

Calculation of the amount of UA in Blood sample

The linear regression equation of UA (Fig. 4.87) is Ip = 16.26x-0.063 where, "Ip" is the peak current of the UA in blood sample and "x" is the amount. The peak current found for the blood sample was 2.75μA.

So, X= (2.75+0.063)/16.26

X= 0.173 [For the determination of UA 2.5mL blood serum was dissolved in 22.5mL PBS (pH 7)].

So, the amount of UA in 25mL solution is 0.173×10= 1.73 and the total amount of UA in 100mL or 1dl solution is 1.73×4= 6.9mg.

The amount of UA in the same blood sample was checked from a pathology. Table 4.25 shows the comparison between the amounts of UA determined by using SFL modified GC electrode and the amount of UA given by the pathological report in the same sample.

Table 4.1: Peak currents (Ip) of VB_6, VC and UA in different buffer solutions at Sulfolane modified GC electrode

Buffer solution (pH)	Peak current of VB_6 (Ip/µA)	Peak current of VC (Ip/µA)	Peak current of UA (Ip/µA)
3	44.79	33.74	10.65
5	56.38	43.80	13.96
7	51.72	38.78	89.52
9	36.00	27.90	51.93

Table 4.2: Peak current (Ip) of 2.5 mM VB_6 in PBS (pH 7) at Sulfolane modified GC electrode at different scan rates

Scan rate (v/Vs^{-1})	Sq. root of scan rate ($v^{1/2}$/$V^{1/2}s^{-1/2}$)	Peak current (Ip/µA)
0.05	0.22	41.68
0.10	0.32	60.02
0.20	0.45	74.89
0.30	0.55	109.49
0.40	0.63	118.10

Table 4.3: Peak current (Ip) of 2.5 mM VC in PBS (pH 7) at Sulfolane modified GC electrode at different scan rates

Scan rate (v/Vs^{-1})	Sq. root of scan rate ($v^{1/2}$/$V^{1/2}s^{-1/2}$)	Peak current (Ip/µA)
0.05	0.22	76.67
0.10	0.32	100.65
0.20	0.45	145.17
0.30	0.55	186.07
0.40	0.63	218.22

Table 4.4: Peak current (Ip) of 2.5 mM UA in PBS (pH 7) at Sulfolane modified GC electrode at different scan rates

Scan rate (v/Vs^{-1})	Sq. root of scan rate ($v^{1/2}$/$V^{1/2}s^{-1/2}$)	Peak current (Ip/µA)
0.05	0.22	67.78
0.10	0.32	83.33
0.20	0.45	137.69
0.30	0.55	171.07
0.40	0.63	209.02

Table 4.5: Peak current (Ipa and Ipc) of 2 mM potassium ferrocyanide in KCl at Sulfolane modified GC electrode at different scan rates

Scan rate (v/Vs^{-1})	Sq. root of scan rate ($v^{1/2}$/$V^{1/2}s^{-1/2}$)	Anodic peak current (Ipa/µA)	Cathodic peak current (Ipc/µA)
0.05	0.22	16.33	-17.80
0.10	0.32	21.27	-26.72
0.15	0.39	26.57	-32.80
0.20	0.45	31.18	-37.13
0.25	0.50	33.47	-38.73

Table 4.6: Amount (mg) and peak current (Ip) of VB_6 in PBS at Sulfolane modified GC electrode

Amount (mg)	Peak current (Ip/µA)
10	13.61
15	19.57
20	25.40
25	29.39
30	33.90
35	37.63
40	41.99

Table 4.7: Recovery percentage of the determination of standard VB_6 using Sulfolane modified GC electrode

Amount (mg)	Added (mg)	Total (mg)	Found (mg)	Recovery (%)
25	0	25	25.1	100.4
25	5	30	30.2	100.7
25	10	35	34.9	99.7
25	15	40	39.8	99.5

Table 4.8: Determination of the standard deviation of standard VB_6 using Sulfolane modified GC electrode

Standard VB_6 (mg)	Peak current (Ip/µA)	Found (mg)	Average (mg)	Standard deviation (±mg)
25.0	29.07	25.3	25.0	0.2
25.0	28.68	24.9		
25.0	28.63	24.9		
25.0	28.90	25.1		
25.0	28.70	24.9		

Table 4.9: Peak current (Ip) of VB_6 in different tablet samples

Tablet sample	Peak current (Ip/µA)
Acliz Plus	28.62
NVP	28.57
Vertina Plus	29.34
Eminil Plus	23.30
Sixvit	27.58

Table 4.10: Amount found (mg) of VB_6 in tablet samples of different pharmaceutical company using Sulfolane modified GC electrode sensor

Tablets	Pharmaceutical name	Amount found (mg)	Amount labeled (mg)
Acliz Plus	Aristopharma	49.6	50
NVP	ACME	49.6	50
Vertina Plus	Square	48.8	50
Eminil Plus	Incepta	51.2	50
Sixvit	Beacon	19.1	20

Table 4.11: Concentration (ppm) and absorbance (A) of standard VB_6 using UV-Vis method

Concentration (ppm)	Absorbance (A)
80	1.109
120	1.402
160	1.696
200	1.984
240	2.265

Table 4.12: Determination of VB_6 in different tablet samples using UV-Visible technique

Tablets	Pharmaceutical name	Observations No.	Absorbance (A)	Quantity (mg)	Average±SD (mg)	Labeled (mg)
Acliz Plus	Aristopharma	1	1.986	49.9	49.9±0.1	50
		2	1.984	50.1		
		3	1.981	49.8		
		4	1.986	50.1		
NVP	ACME	1	1.603	49.5	49.5±0.1	50
		2	1.601	49.4		
		3	1.598	49.3		
		4	1.605	49.6		
Vertina Plus	Square	1	1.606	49.6	49.4±0.2	50
		2	1.600	49.4		
		3	1.599	49.3		
		4	1.597	49.2		
Eminil Plus	Insepta	1	1.663	52.3	51.5±0.5	50
		2	1.637	51.1		
		3	1.641	51.3		
		4	1.646	51.5		
Sixvit	Beacon	1	1.720	20.6	19.8±0.2	20
		2	1.716	20.5		
		3	1.706	20.3		
		4	1.704	20.3		

Table 4.13: Comparison of the amount of VB_6 determined by Sulfolane modified GC electrode sensor with UV-visible method

Tablets	Pharmaceutical name	Amount found by Sulfolane modified GC electrode sensor (mg)	Amount found by UV-Visible method (mg)	Amount labeled (mg)
Acliz Plus	Aristopharma	49.6±0.2	49.9±0.1	50
NVP	ACME	49.6±0.2	49.5±0.1	50
Vertina Plus	Square	48.8±0.2	49.4±0.2	50
Eminil Plus	Incepta	51.2±0.2	51.5±0.5	50
Sixvit	Beacon	19.1±0.2	19.8±0.2	20

Table 4.14: Amount (mg) and peak current (Ip) of VC in PBS at Sulfolane modified GC electrode

Amount (mg)	Peak current (Ip/μA)
10	15.03
15	20.93
20	23.29
25	26.28
30	29.45
35	32.41
40	34.95

Table 4.15: Recovery percentage of the determination of standard VC using Sulfolane modified GC electrode

Amount (mg)	Added (mg)	Total (mg)	Found (mg)	Recovery (%)
15	0	15	15.2	101.3
15	5	20	20.4	101.9
15	10	25	25.4	101.6
15	15	30	30.0	100.0
15	20	35	35.3	100.9

Table 4.16: Determination of the standard deviation of standard VC using Sulfolane modified GC electrode

Standard VC (mg)	Peak current (Ip/μA)	Found (mg)	Average (mg)	Standard deviation (±mg)
35	32.57	35.3	34.8	0.6
35	32.41	35.1		
35	31.78	34.1		
35	31.93	34.3		
35	32.52	35.3		

Table 4.17: Peak current (Ip) of VC in different tablet samples

Tablet sample	Peak current (Ip/μA)
Cevit	23.33
Nutrivit C	25.77
Ascobex	26.87
Cecon	23.33
Vasco	22.18

Table 4.18: Amount found (mg) of VC in tablet samples of different pharmaceutical company using Sulfolane modified GC electrode sensor

Tablets	Pharmaceutical name	Amount found (mg)	Amount labeled (mg)
Cevit	Square	249.6	250
Nutrivit C	ACI	246.7	250
Ascobex	Beximco	261.0	250
Cecon	ACME	247.2	250
Vasco	Opsonin	230.5	250

Table 4.19: Concentration (ppm) and absorbance (A) of standard VC using UV-Vis method

Concentration (ppm)	Absorbance (A)
80	0.302
120	0.430
160	0.517
200	0.629
240	0.731

Table 4.20: Determination of VC in different tablet samples using UV-Visible technique

Tablets	Pharmaceutical name	Observations No.	Absorbance (A)	Quantity (mg)	Average±SD (mg)	Labeled (mg)
Cevit	Square	1	0.638	249.4	249.6±1.5	250
		2	0.635	247.7		
		2	0.641	251.0		
		4	0.640	250.5		
Nutrivit C	ACI	1	0.633	246.5	247.3±0.8	250
		2	0.634	247.0		
		3	0.635	247.7		
		4	0.636	248.2		
Ascobex	Beximco	1	0.652	257.4	259.4±1.4	250
		2	0.658	260.8		
		3	0.656	259.7		
		4	0.656	259.7		
Cecon	ACME	1	0.634	247.0	246.6±0.5	250
		2	0.632	245.9		
		3	0.634	247.0		
		4	0.633	246.5		
Vasco	Opsonin	1	0.608	232.2	231.0±0.8	250
		2	0.605	230.5		
		3	0.605	230.5		
		4	0.606	231.0		

Table 4.21: Comparison of the amount of VC determined by Sulfolane modified GC electrode sensor with UV-visible method

Tablets	Pharmaceutical name	Amount found by Sulfolane modified GC electrode sensor (mg)	Amount found by UV-Visible method (mg)	Amount labeled (mg)
Cevit	Square	249.6±0.6	249.6±1.5	250
Nutrivit C	ACI	246.7±0.6	247.3±0.8	250
Ascobex	Beximco	261.0±0.6	259.4±1.4	250
Cecon	ACME	247.2±0.6	246.6±0.5	250
Vasco	Opsonin	230.5±0.6	231.0±0.8	250

Table 4.22: Amount (mg) and peak current (Ip) of UA in PBS at Sulfolane modified GC electrode

Amount (mg)	Peak current (Ip/µA)
0.1	1.38
0.2	3.28
0.3	4.53
0.4	6.05
0.5	7.87

Table 4.23: Recovery percentage of the determination of standard UA using Sulfolane modified GC electrode

Amount (mg)	Added (mg)	Total (mg)	Found (mg)	Recovery (%)
5	0.0	5.0	4.9	98.0
5	2.5	7.5	7.4	98.7
5	5.0	10.0	10.1	101.0
5	7.5	12.5	12.4	99.2
5	10.0	15.0	14.9	99.0

Table 4.24: Determination of the standard deviation of standard UA using Sulfolane modified GC electrode

Standard UA (mg)	Peak current (Ip/µA)	Found (mg)	Average (mg)	Standard deviation (±mg)
10	76.82	10.5	10.0	0.5
10	76.56	10.4		
10	72.80	9.5		
10	71.83	9.3		
10	75.25	10.1		

Table 4.25: Comparison of the amount of UA determined by Sulfolane modified GC electrode sensor with Pathological report

Sample	Amount found by Sulfolane modified GC electrode sensor (mg/dl)	Pathological report (mg/dl)
Blood Serum	6.9	6.9

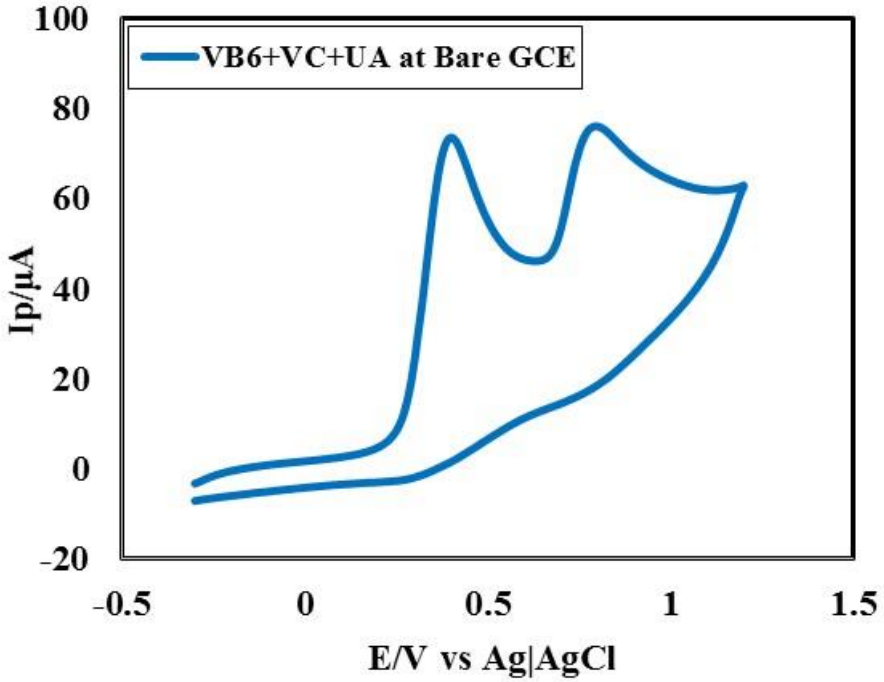

Figure 4.1: Cyclic voltammogram (CV) of 2.5 mM VB_6+ 2.5 mM VC+ 2.5 mM UA at bare GC electrode in phosphate buffer solution (PBS) (pH 7) and at scan rate 0.1 V/s.

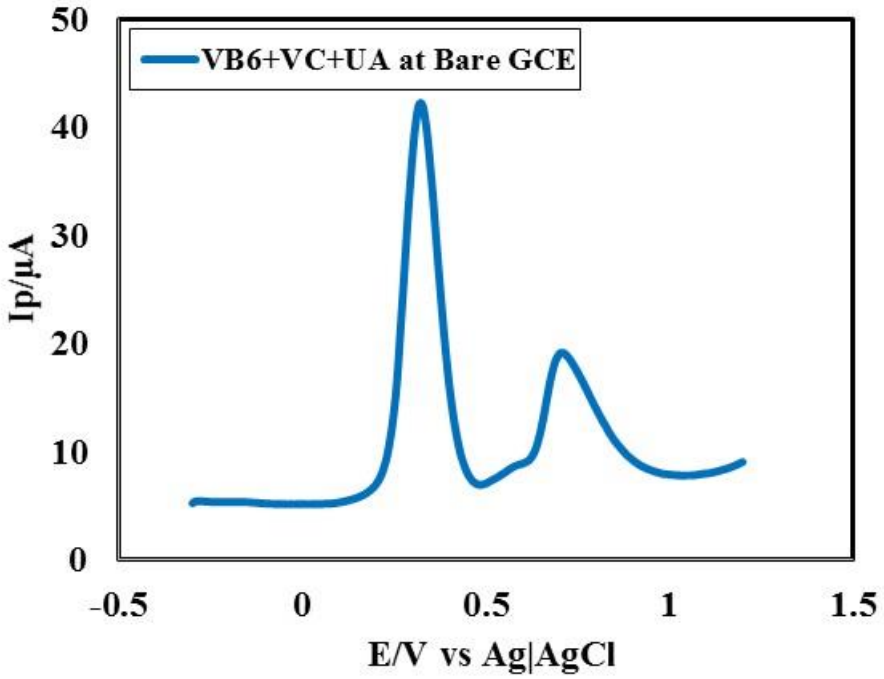

Figure 4.2: Differential pulse voltammogram (DPV) of 2.5 mM VB_6+ 2.5 mM VC+ 2.5 mM UA at bare GC electrode in PBS (pH 7) and at scan rate 0.1 V/s.

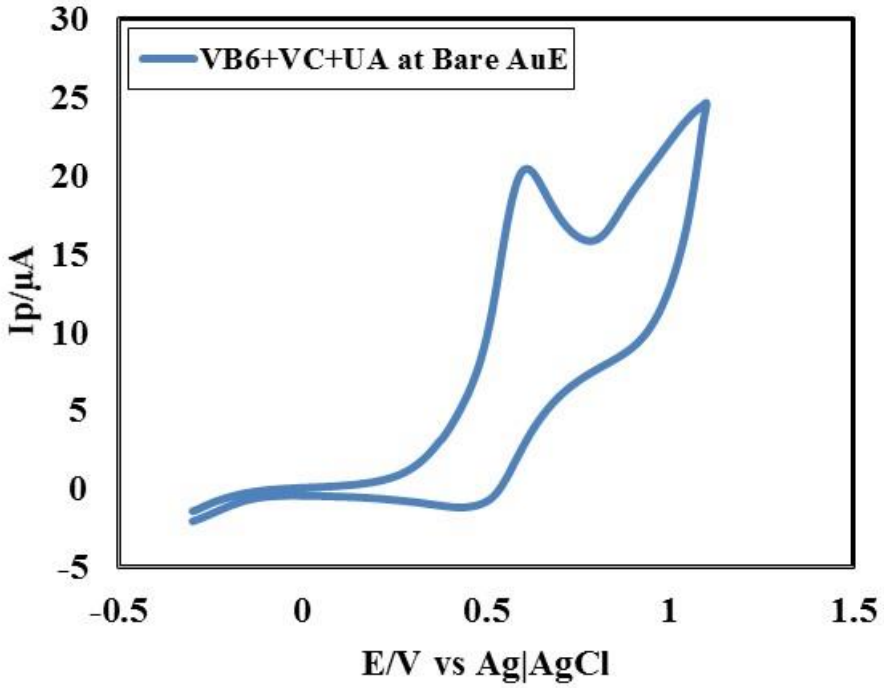

Figure 4.3: Cyclic voltammogram (CV) of 2.5 mM VB_6+ 2.5 mM VC+ 2.5 mM UA at bare Au electrode in PBS (pH 7) and at scan rate 0.1 V/s.

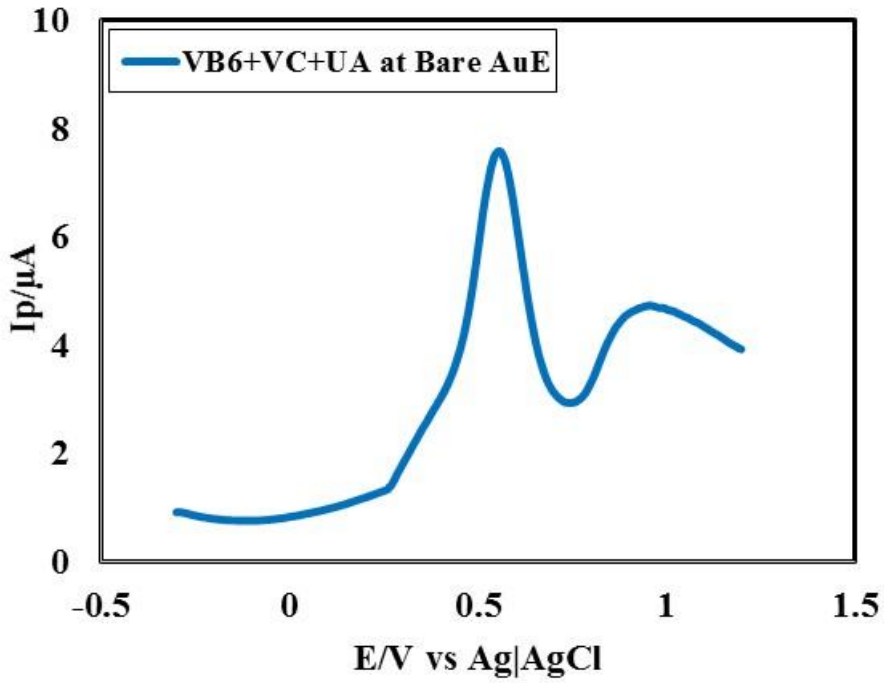

Figure 4.4: Differential pulse voltammogram (DPV) of 2.5 mM VB_6+ 2.5 mM VC+ 2.5 mM UA at bare Au electrode in PBS (pH 7) and at scan rate 0.1 V/s.

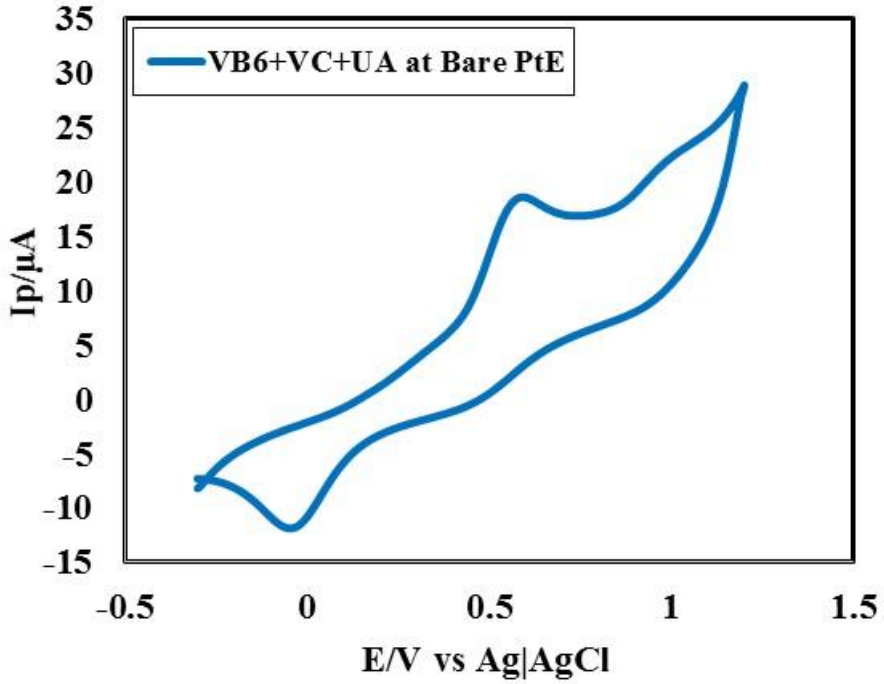

Figure 4.5: Cyclic voltammogram (CV) of 2.5 mM VB_6+ 2.5 mM VC+ 2.5 mM UA at bare Pt electrode in PBS (pH 7) and at scan rate 0.1 V/s.

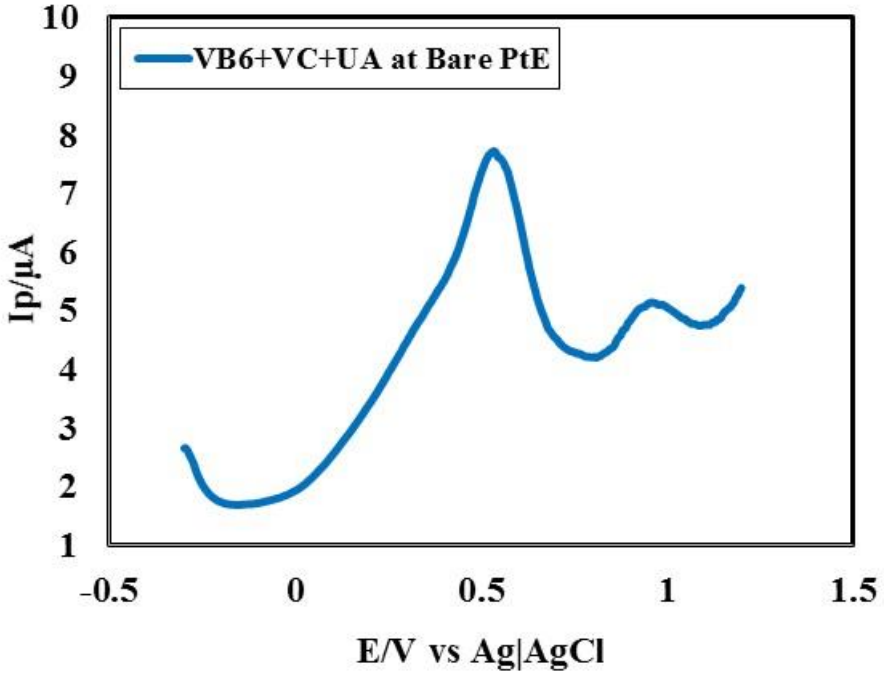

Figure 4.6: Differential pulse voltammogram (DPV) of 2.5 mM VB_6+ 2.5 mM VC+ 2.5 mM UA at bare Pt electrode in PBS (pH 7) and at scan rate 0.1 V/s.

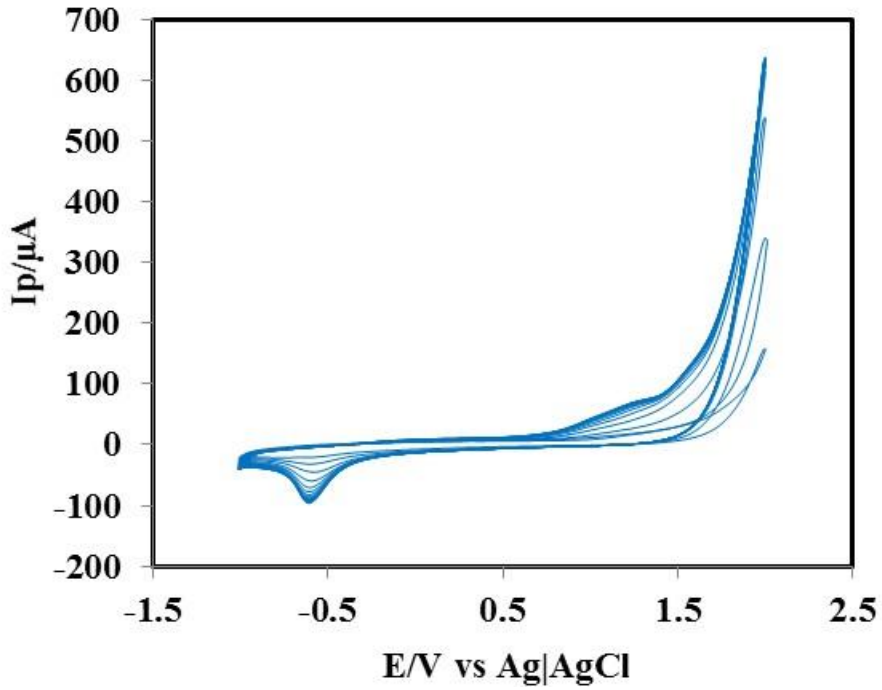

Figure 4.7: Cyclic voltammogram (CV) of Sulfolane (SFL) thin film growth on the surface of bare GC electrode at scan rate 0.2 V/s.

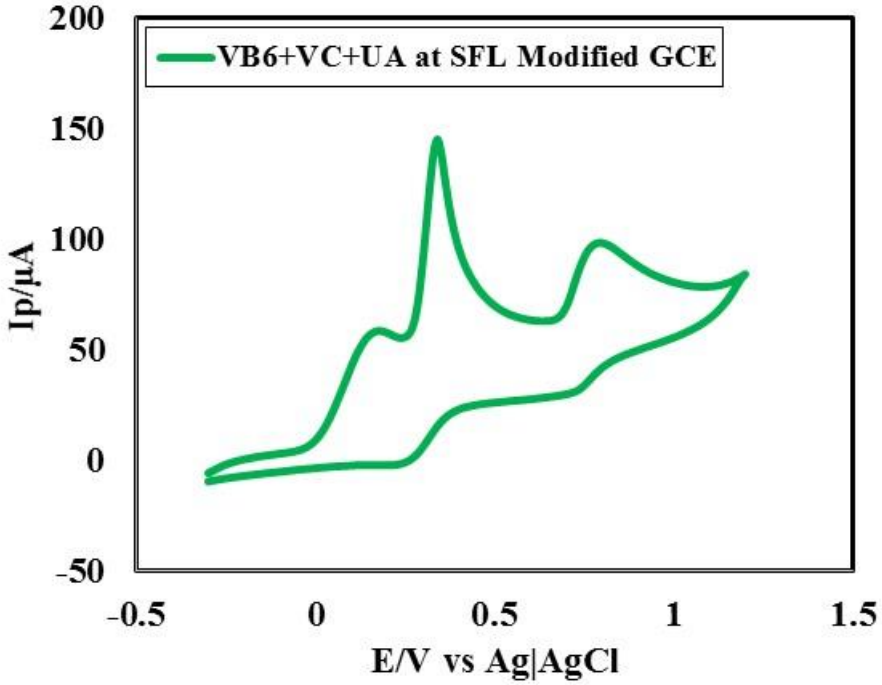

Figure 4.8: Cyclic voltammogram (CV) of 2.5 mM VB_6+ 2.5 mM VC+ 2.5 mM UA at SFL (SFL) modified GC electrode in PBS (pH 7) and at scan rate 0.1 V/s.

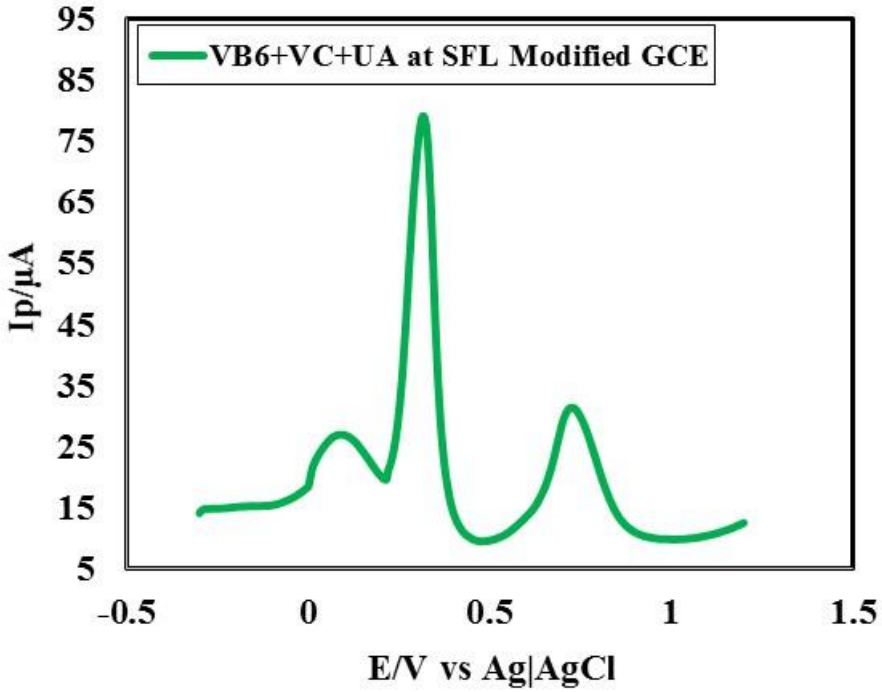

Figure 4.9: Differential pulse voltammogram (DPV) of 2.5 mM VB_6+ 2.5 mM VC+ 2.5 mM UA at SFL modified GC electrode in PBS (pH 7) and at scan rate 0.1 V/s.

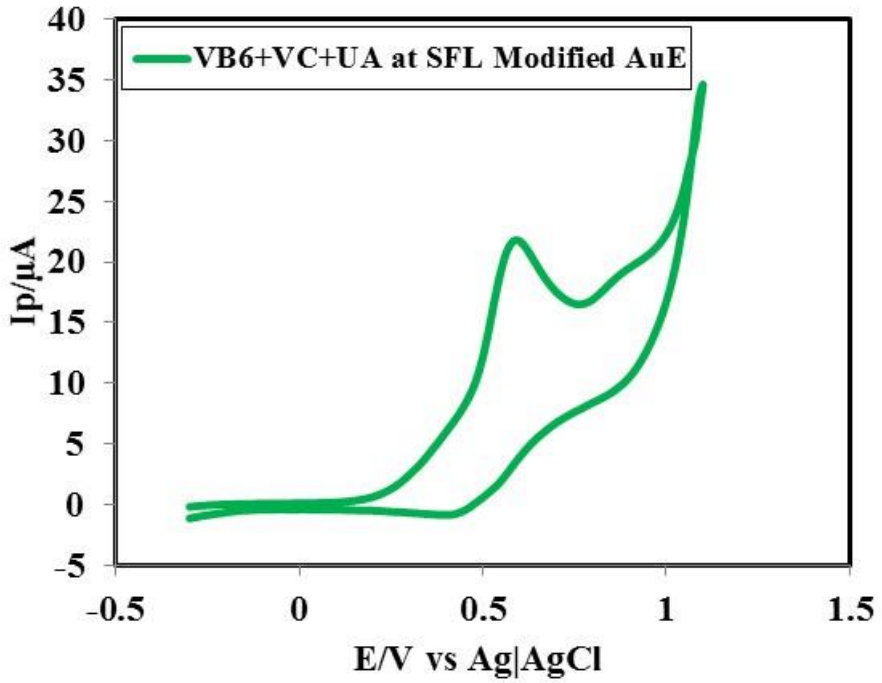

Figure 4.10: Cyclic voltammogram (CV) of 2.5 mM VB_6+ 2.5 mM VC+ 2.5 mM UA at SFL modified Au electrode in PBS (pH 7) and at scan rate 0.1 V/s.

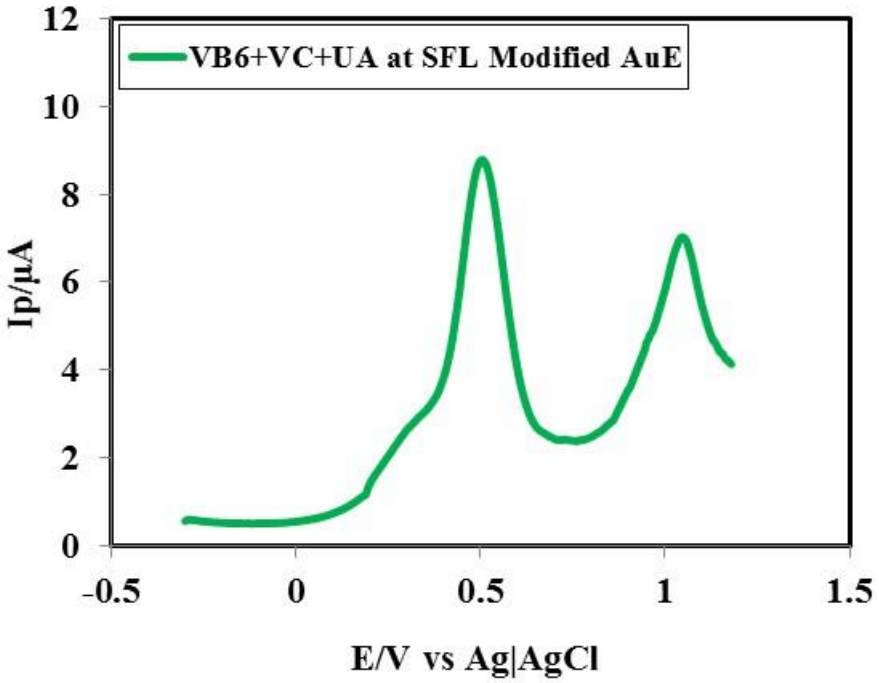

Figure 4.11: Differential pulse voltammogram (DPV) of 2.5 mM VB_6+ 2.5 mM VC+ 2.5 mM UA at SFL modified Au electrode in PBS (pH 7) and at scan rate 0.1 V/s.

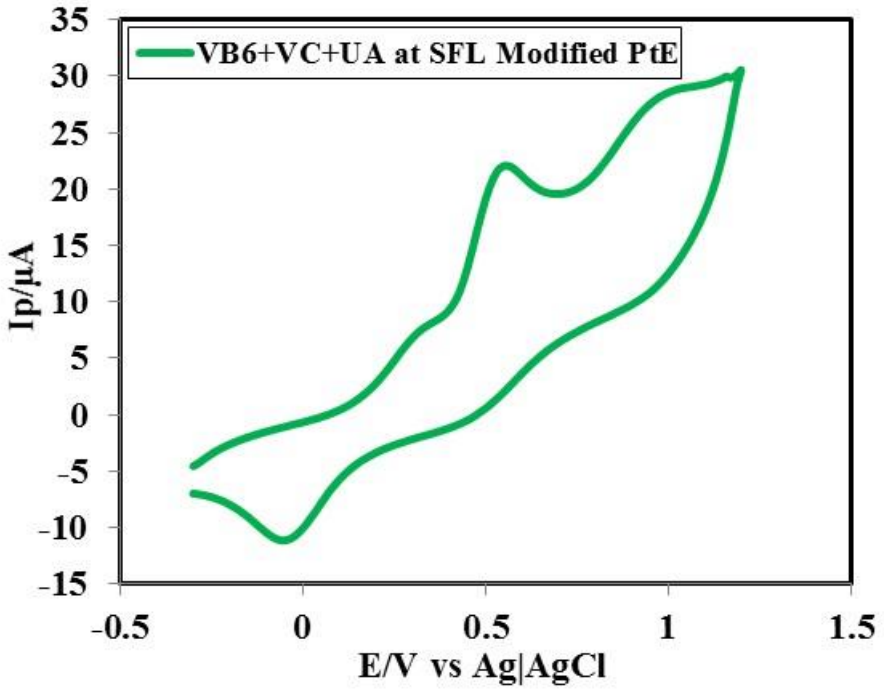

Figure 4.12: Cyclic voltammogram (CV) of 2.5 mM VB_6+ 2.5 mM VC+ 2.5 mM UA at SFL modified Pt electrode in PBS (pH 7) and at scan rate 0.1 V/s.

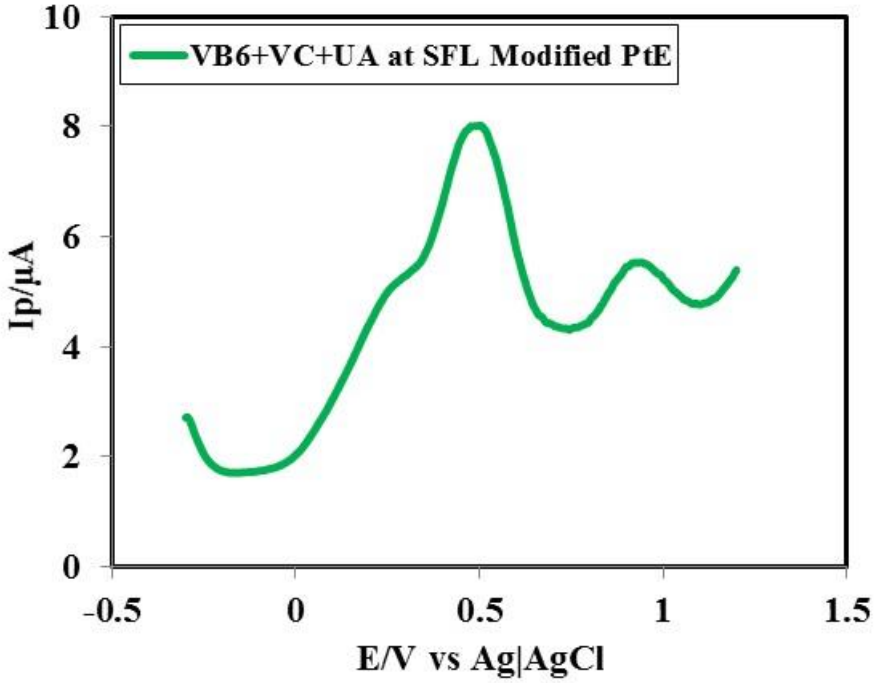

Figure 4.13: Differential pulse voltammogram (DPV) of 2.5 mM VB_6+ 2.5 mM VC+ 2.5 mM UA at SFL modified Pt electrode in PBS (pH 7) and at scan rate 0.1 V/s.

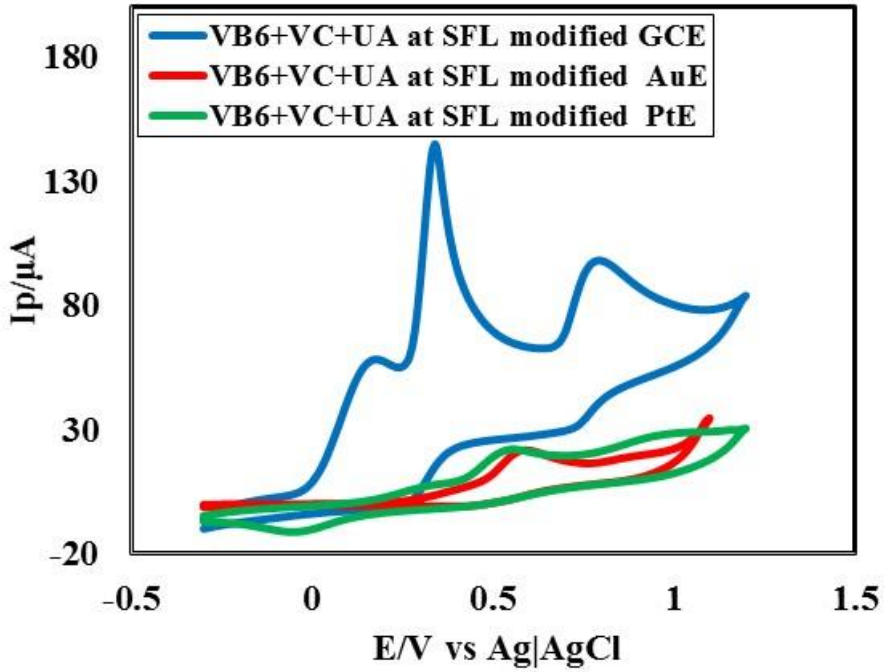

Figure 4.14: Cyclic voltammograms (CVs) of 2.5 mM VB_6+ 2.5 mM VC+ 2.5 mM UA in PBS (pH 7) at SFL modified GCE (blue line), SFL modified AuE (red line) and SFL modified PtE (green line) at scan rate 0.1 V/s.

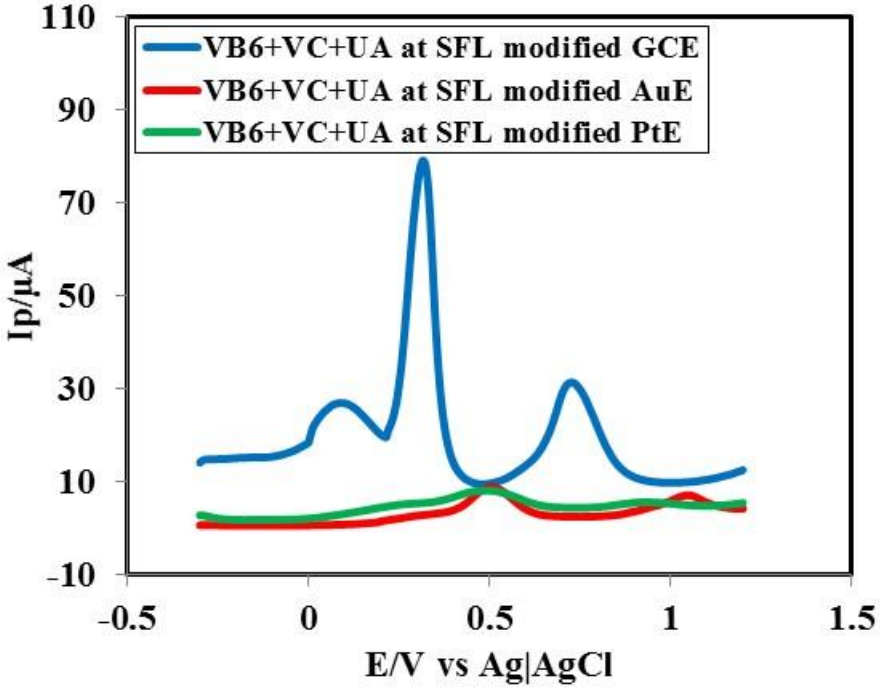

Figure 4.15: Differential pulse voltammograms (DPVs) of 2.5 mM VB_6+ 2.5 mM VC+ 2.5 mM UA in PBS (pH 7) at SFL modified GCE (blue line), SFL modified AuE (red line) and SFL modified PtE (green line) at scan rate 0.1 V/s.

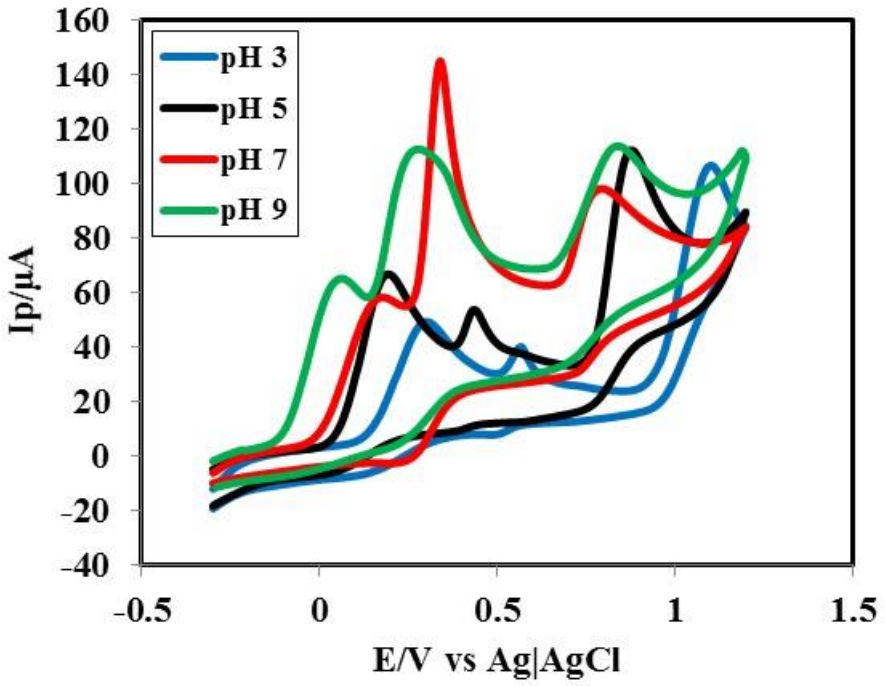

Figure 4.16: Cyclic voltammograms (CVs) of 2.5 mM VB_6+ 2.5 mM VC+ 2.5 mM UA in different buffer solution (pH 3, 5, 7 and 9) at SFL modified GC electrode.

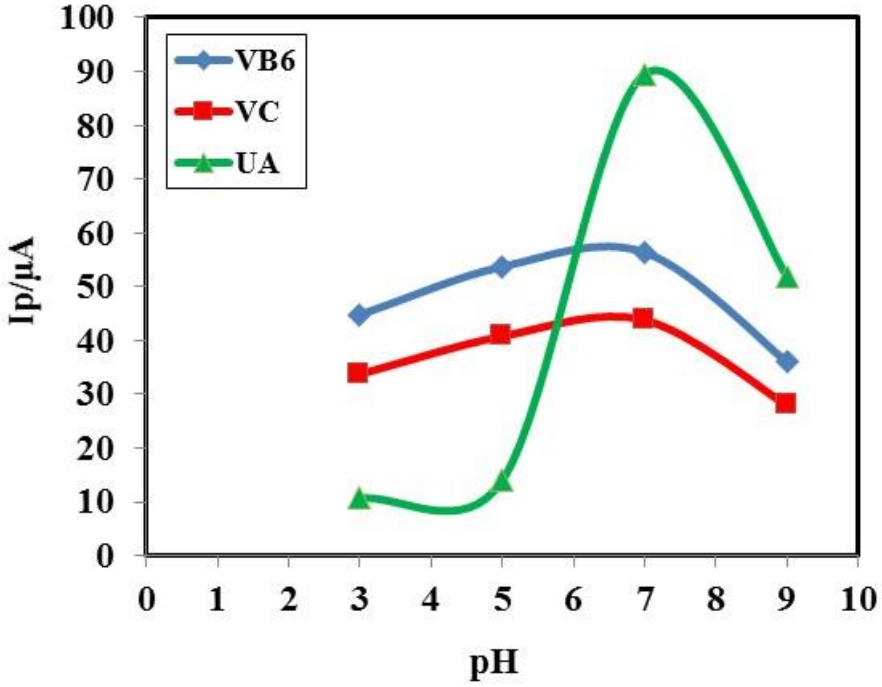

Figure 4.17: Plots of peak current (I_p) vs pH (3, 5, 7 and 9) of VB_6 (blue line), VC (red line) and UA (green line).

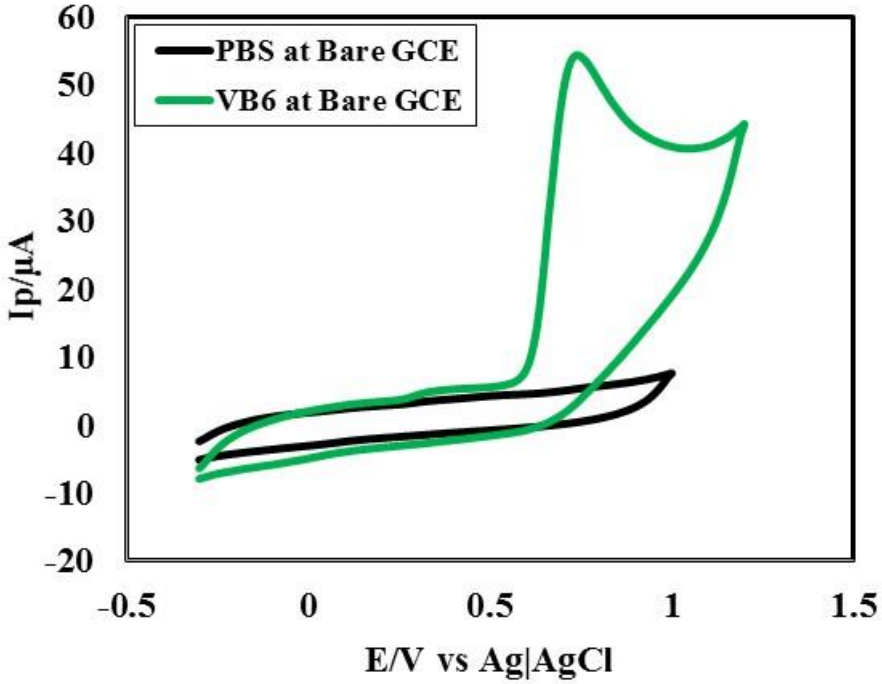

Figure 4.18: Cyclic voltammogrm (CV) of 2.5 mM VB_6 in 0.5M PBS (pH 7) (green line) and only 0.5M PBS (pH 7) (black line) at bare GC electrode at scan rate 0.1 V/s.

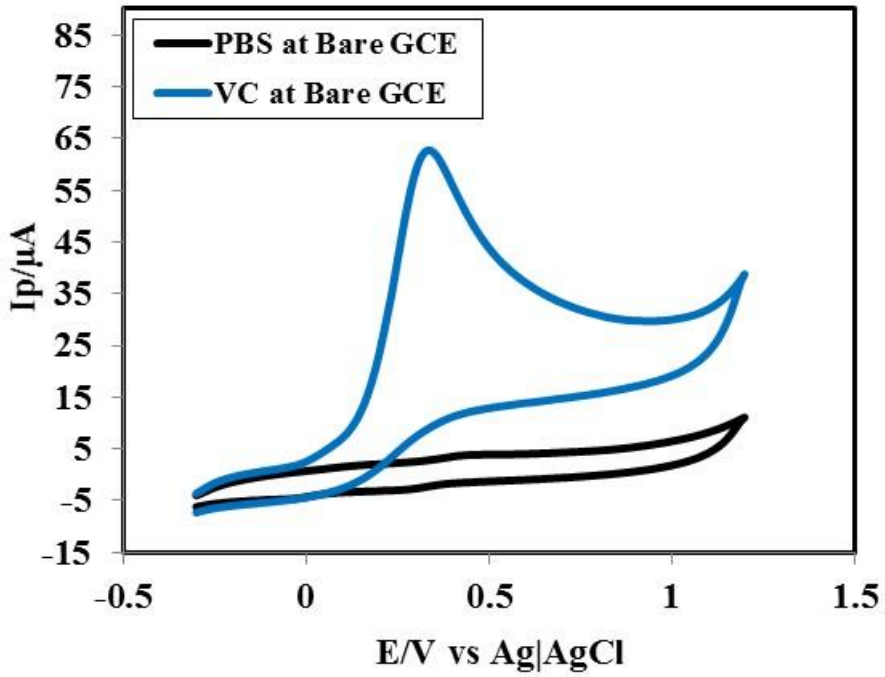

Figure 4.19: Cyclic voltammogrm (CV) of 2.5 mM VC in 0.5M PBS (pH 7) (blue line) and only 0.5M PBS (pH 7) (black line) at bare GC electrode at scan rate 0.1 V/s.

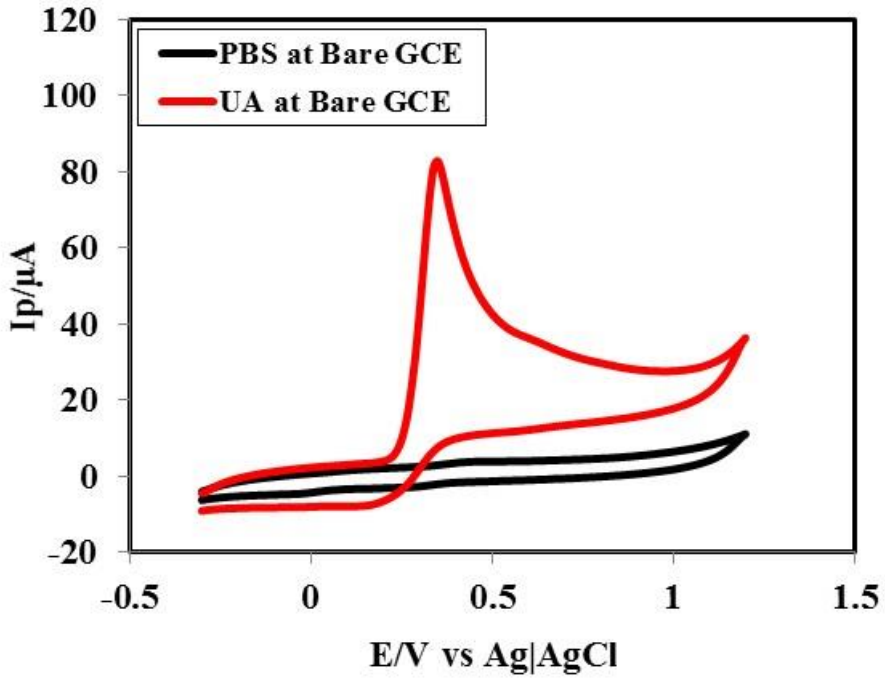

Figure 4.20: Cyclic voltammogrm (CV) of 2.5 mM UA in 0.5M PBS (pH 7) (red line) and only 0.5M PBS (pH 7) (black line) at bare GC electrode at scan rate 0.1 V/s.

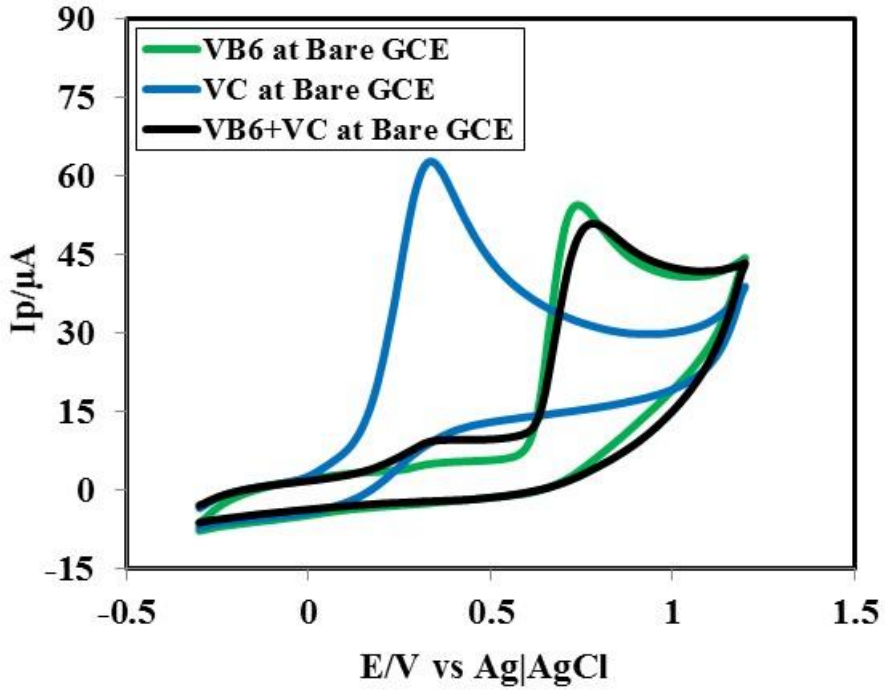

Figure 4.21: Cyclic voltammogram (CV) of 2.5 mM VB_6 (green line), 2.5 mM VC (blue line) and 2.5 mM VB_6+2.5 mM VC (black line) at bare GC electrode in PBS (pH 7) at scan rate 0.1 V/s.

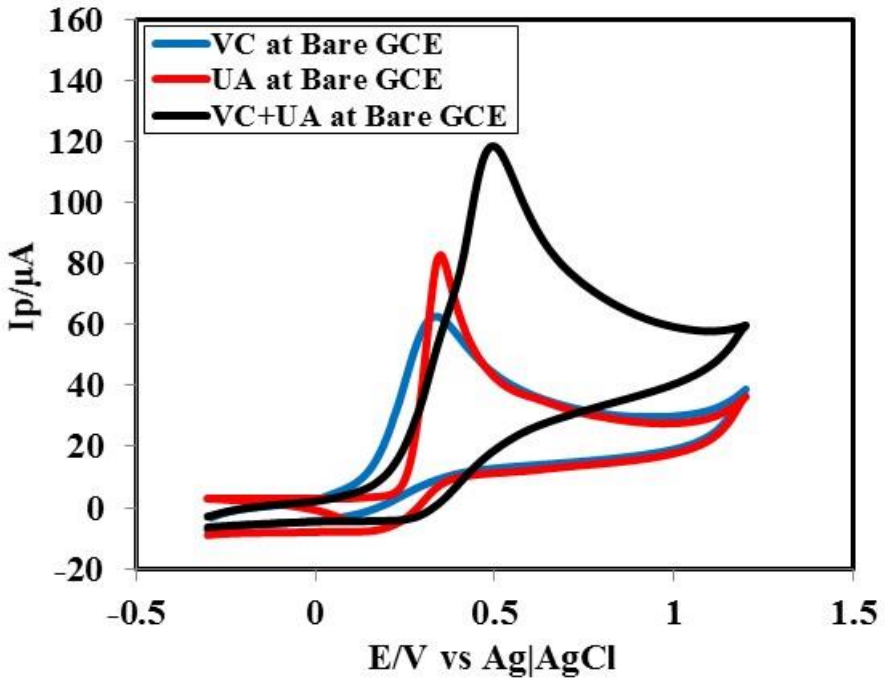

Figure 4.22: Cyclic voltammogram (CV) of 2.5 mM VC (blue line), 2.5 mM UA (red line) and 2.5 mM VC+2.5 mM UA (black line) at bare GC electrode in PBS (pH 7) at scan rate 0.1 V/s.

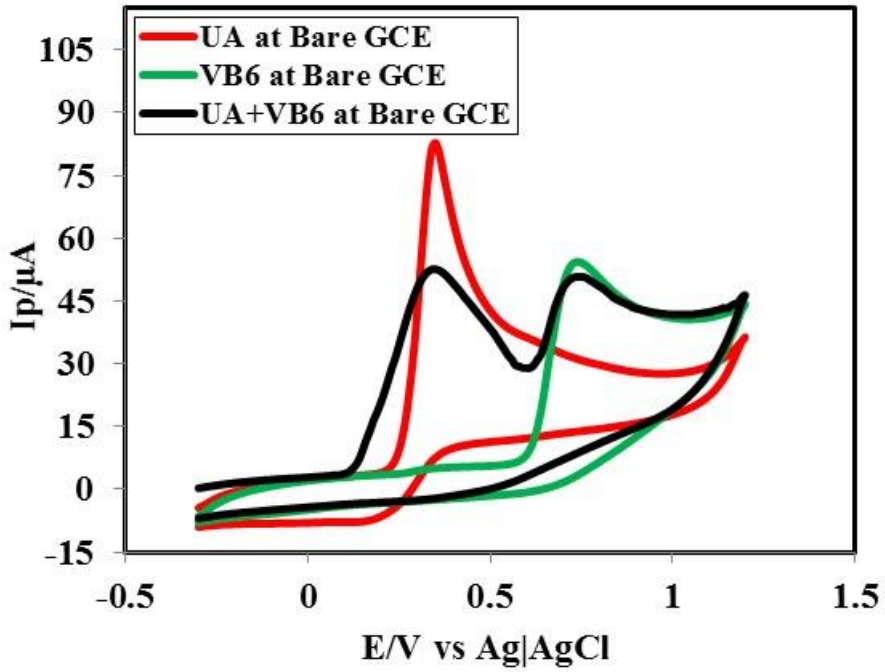

Figure 4.23: Cyclic voltammogram (CV) of 2.5 mM UA (red line), 2.5 mM VB_6 (green line) and 2.5 mM UA+2.5 mM VB_6 (black line) at bare GC electrode in PBS (pH 7) at scan rate 0.1 V/s.

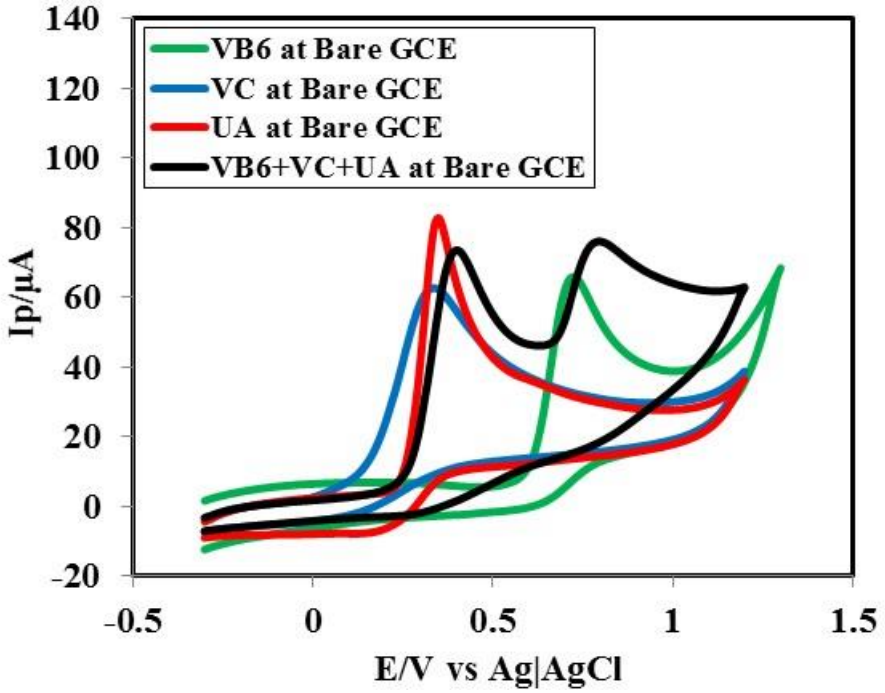

Figure 4.24: Cyclic voltammogram (CV) of 2.5 mM VB_6 (green line), 2.5 mM VC (blue line) and 2.5 mM UA (red line) and 2.5 mM VB_6+ 2.5 mM VC+ 2.5 mM UA (black line) at bare GC electrode in PBS (pH 7) at scan rate 0.1 V/s.

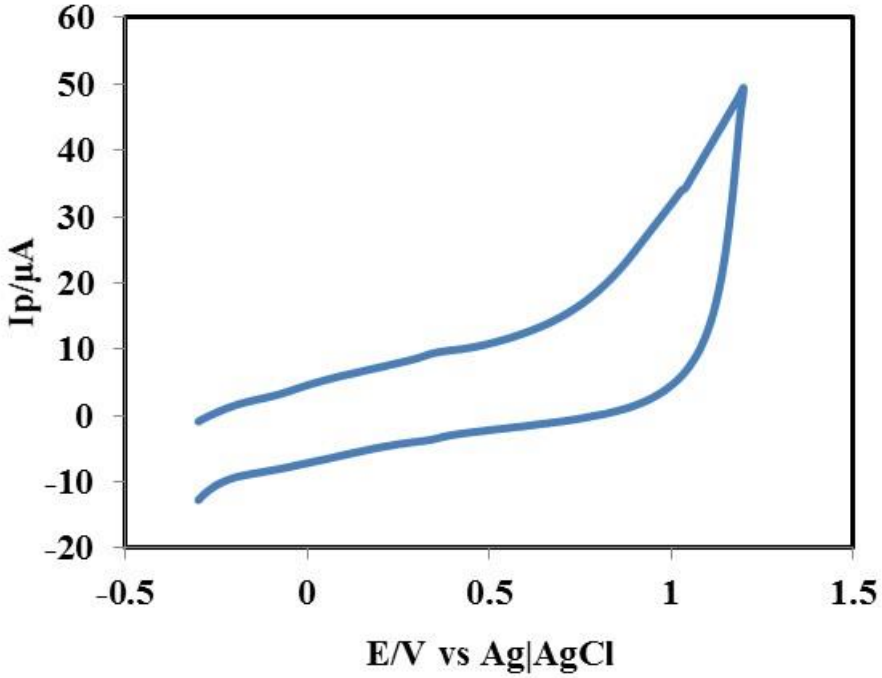

Figure 4.25: Cyclic voltammogram (CV) of SFL in PBS (pH 7) at Modified GC electrode at scan rate 0.1 V/s.

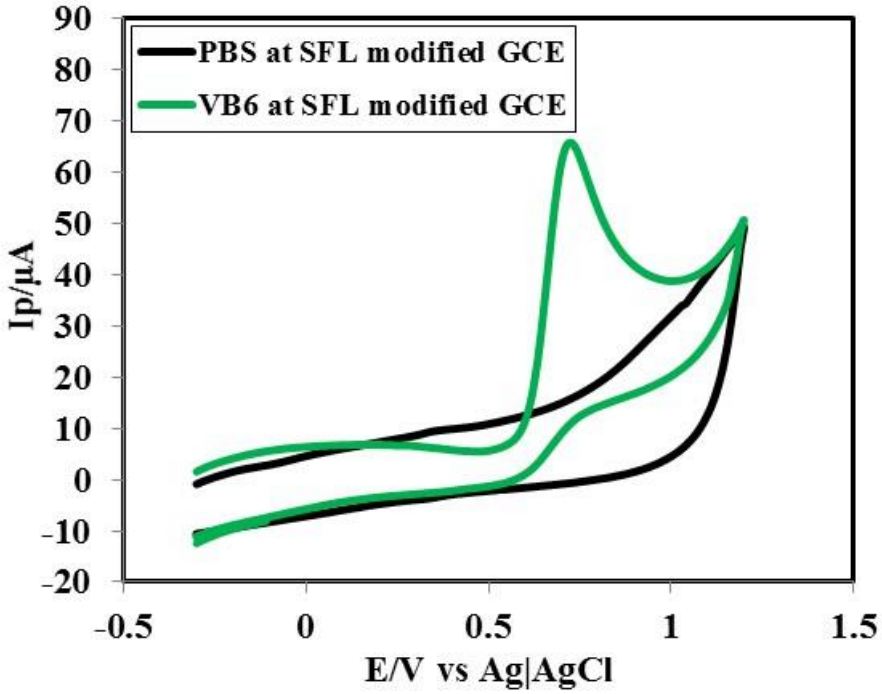

Figure 4.26: Cyclic voltammogram (CV) of 2.5 mM VB_6 in 0.5M PBS (pH 7) (green line) and only 0.5M PBS (pH 7) (black line) at SFL modified GC electrode at scan rate 0.1 V/s.

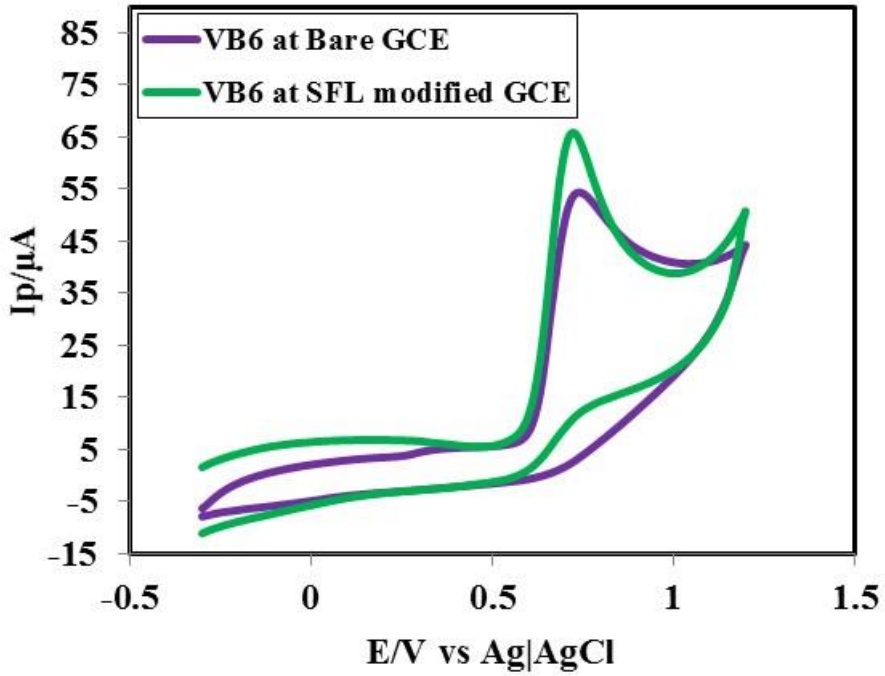

Figure 4.27: Cyclic voltammogram (CV) of 2.5 mM VB_6 in 0.5M PBS (pH 7) at bare (purple line) and SFL modified (green line) GC electrode at scan rate 0.1 V/s.

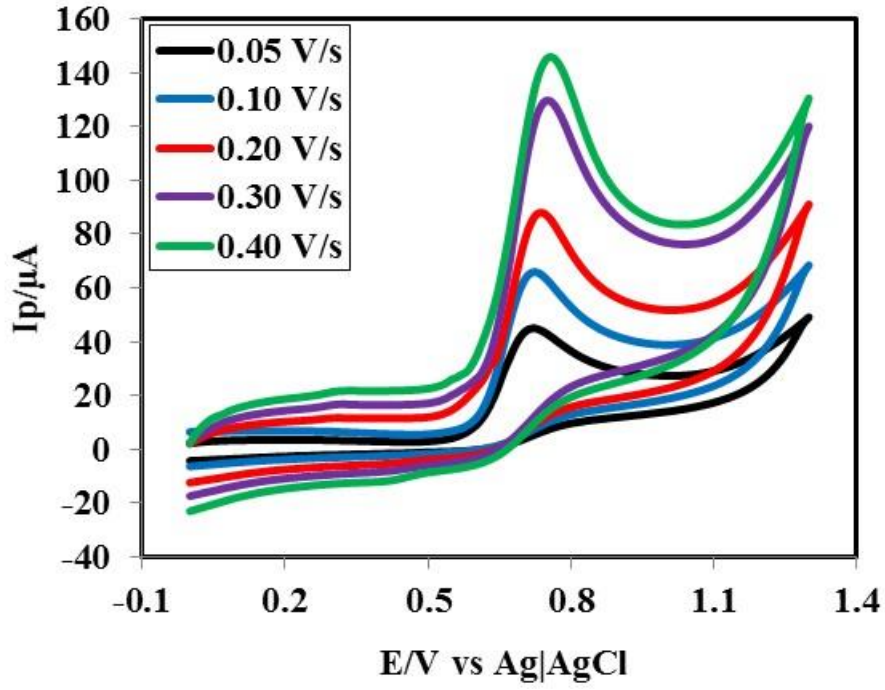

Figure 4.28: Cyclic voltammograms (CVs) of 2.5 mM VB_6 at SFL modified GC electrode in PBS (pH 7) at different scan rate 0.05 V/s, 0.10 V/s, 0.20 V/s, 0.30 V/s and 0.40 V/s.

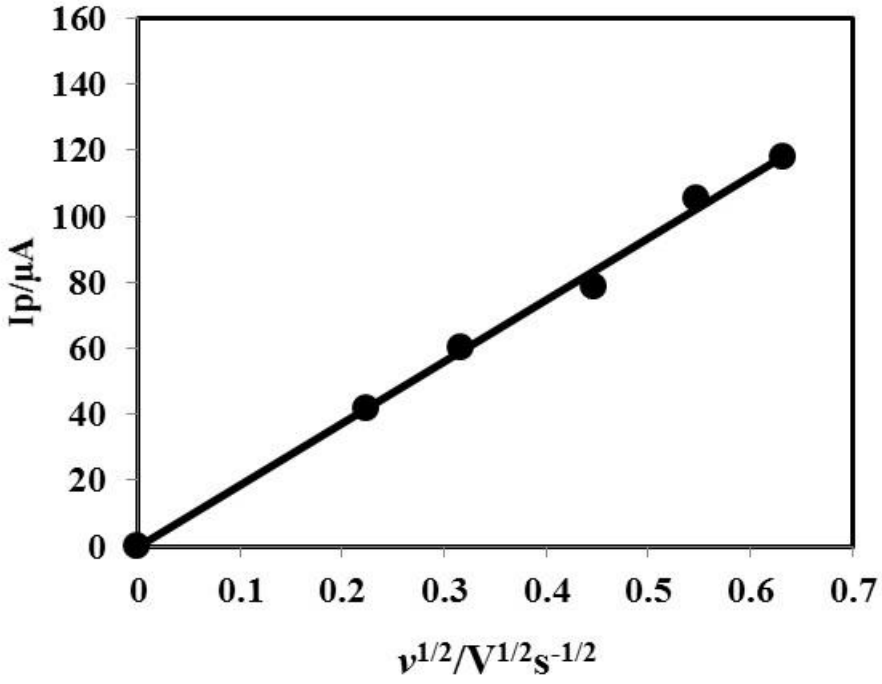

Figure 4.29: Plots of peak current (I_p) vs square root of scan rate ($\nu^{1/2}$) of 2.5 mM VB_6 at SFL modified GC electrode in PBS (pH 7).

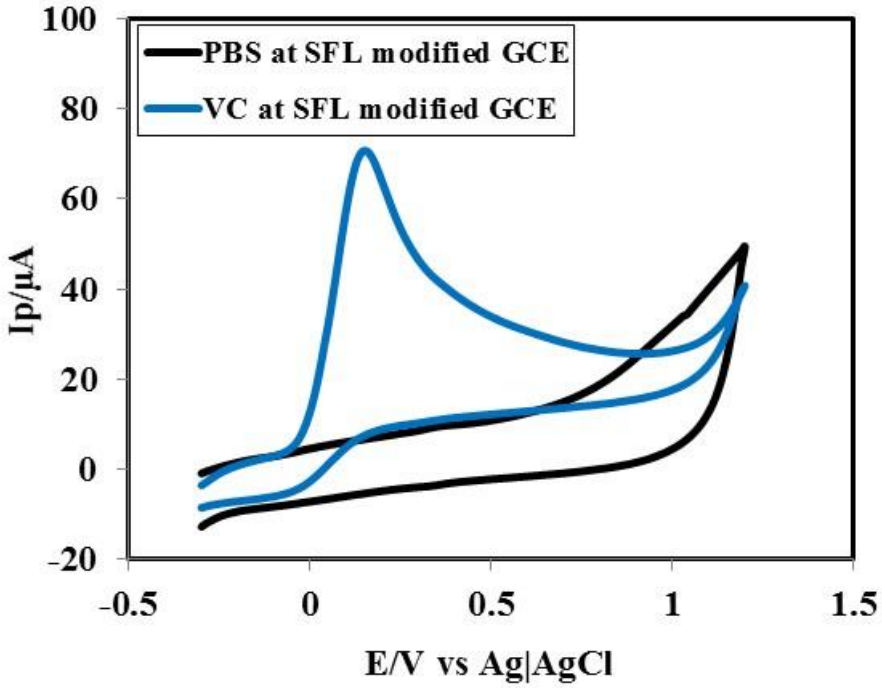

Figure 4.30: Cyclic voltammogram (CV) of 2.5 mM VC in 0.5M PBS (pH 7) (blue line) and only 0.5M PBS (pH 7) (black line) at SFL modified GC electrode at scan rate 0.1 V/s.

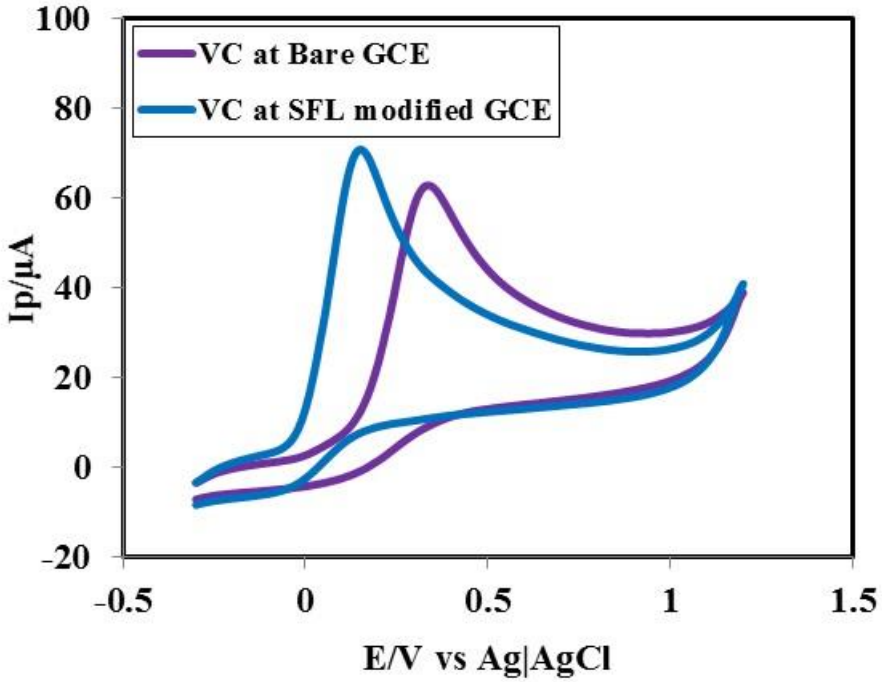

Figure 4.31: Cyclic voltammogram (CV) of 2.5 mM VC in 0.5M PBS (pH 7) at bare (purple line) and SFL modified (blue line) GC electrode at scan rate 0.1 V/s.

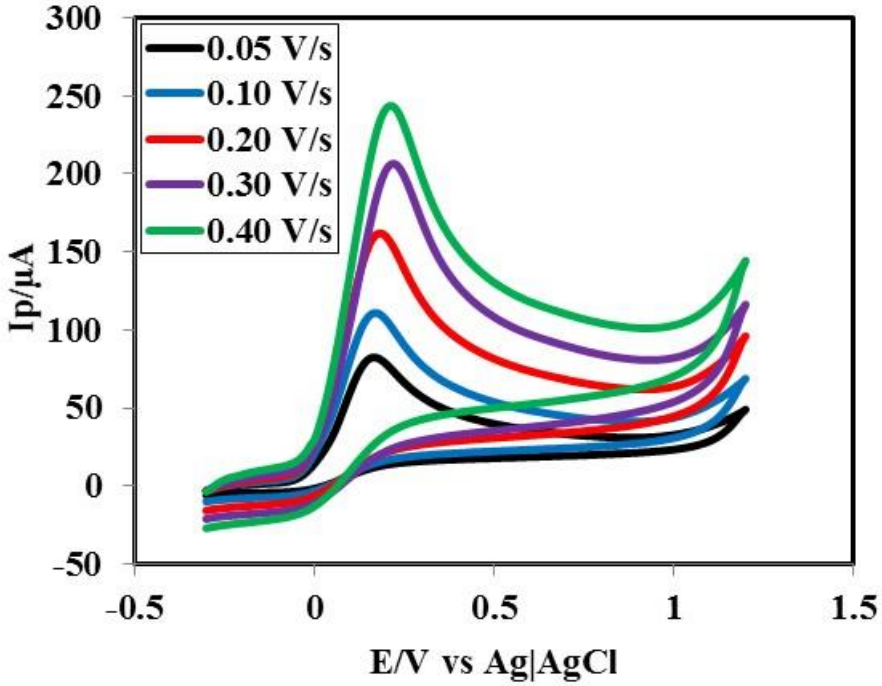

Figure 4.32: Cyclic voltammograms (CVs) of 2.5 mM VC at SFL modified GC electrode in PBS (pH 7) at different scan rate 0.05 V/s, 0.10 V/s, 0.20 V/s, 0.30 V/s and 0.40 V/s.

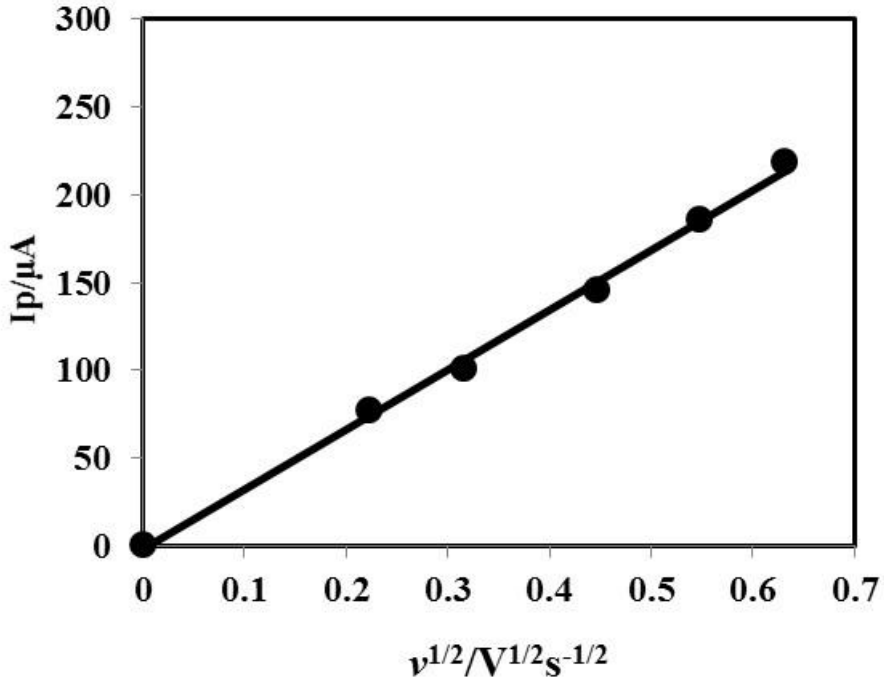

Figure 4.33: Plots of peak current (I_p) vs square root of scan rate ($v^{1/2}$) of 2.5 mM VC at SFL modified GC electrode in PBS (pH 7).

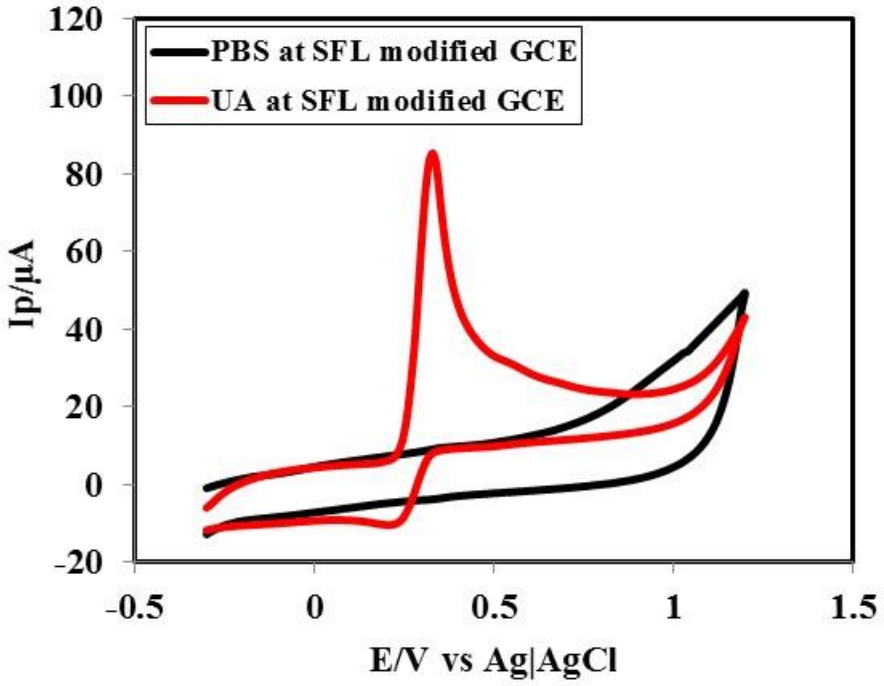

Figure 4.34: Cyclic voltammogram (CV) of 2.5 mM UA in 0.5M PBS (pH 7) (red line) and only 0.5M PBS (pH 7) (black line) at SFL modified GC electrode at scan rate 0.1 V/s.

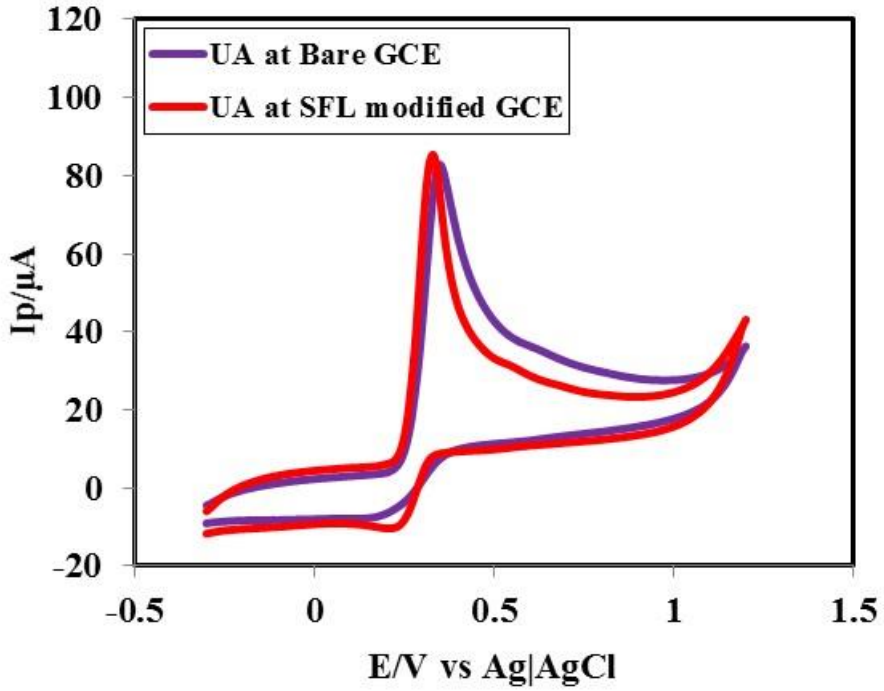

Figure 4.35: Cyclic voltammogram (CV) of 2.5 mM UA in PBS (pH 7) at bare (purple line) and SFL modified (red line) GC electrode at scan rate 0.1 V/s.

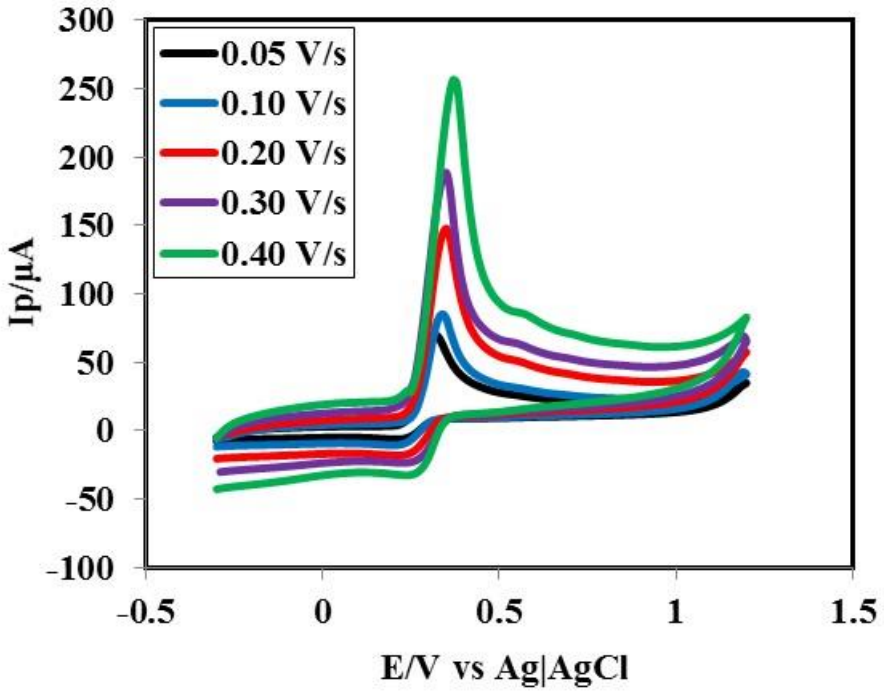

Figure 4.36: Cyclic voltammograms (CVs) of 2.5 mM UA at SFL modified GC electrode in PBS (pH 7) at different scan rate 0.05 V/s, 0.10 V/s, 0.20 V/s, 0.30 V/s and 0.40 V/s.

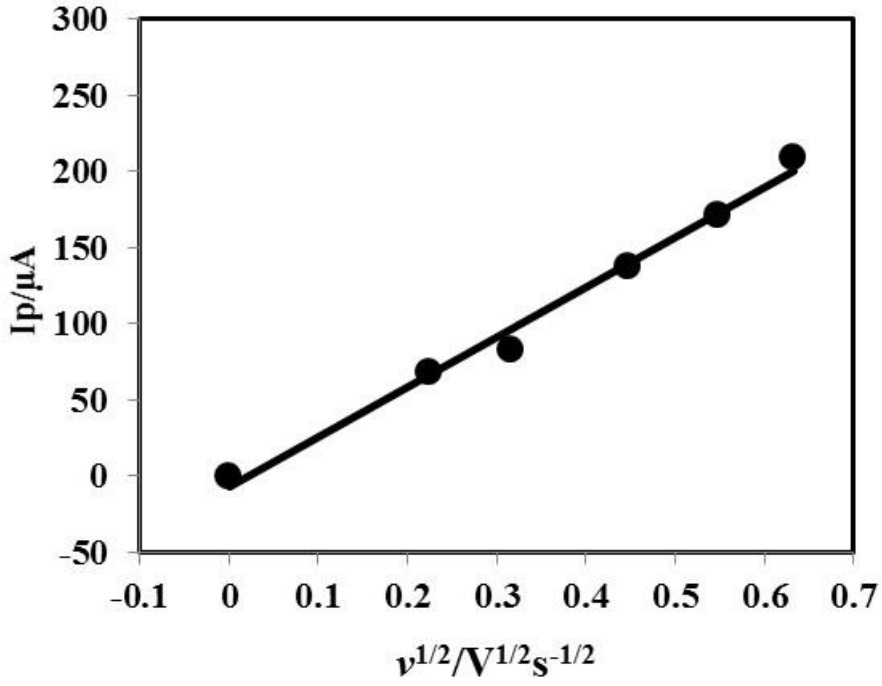

Figure 4.37: Plots of peak current (I_p) vs square root of scan rate ($v^{1/2}$) of 2.5 mM UA at SFL modified GC electrode in PBS (pH 7).

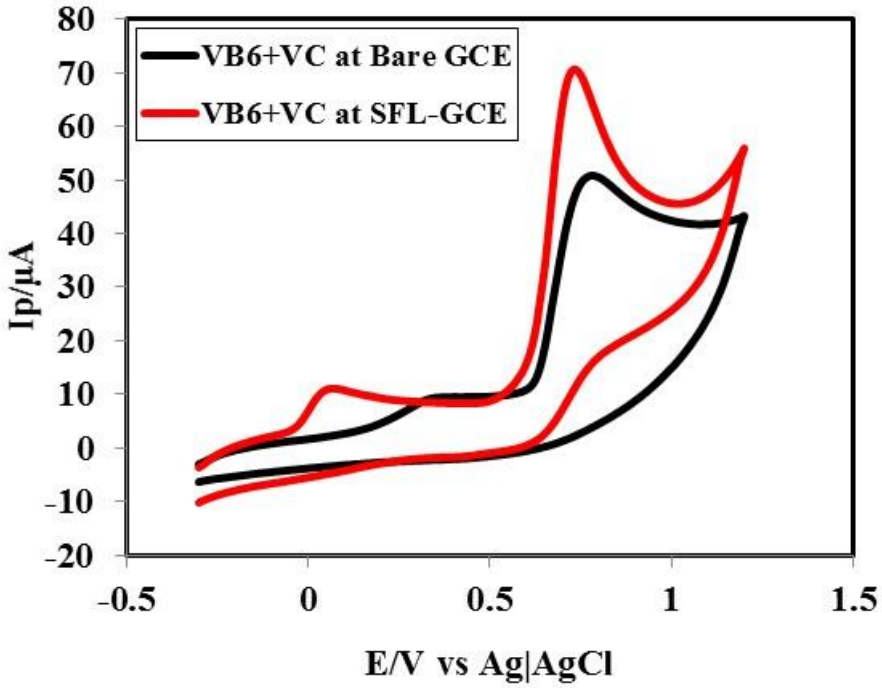

Figure 4.38: CV comparison of 2.5 mM VB_6+ 2.5 mM VC at bare (black line) and SFL modified GC electrode (red line) in PBS (pH 7) at scan rate 0.1 V/s.

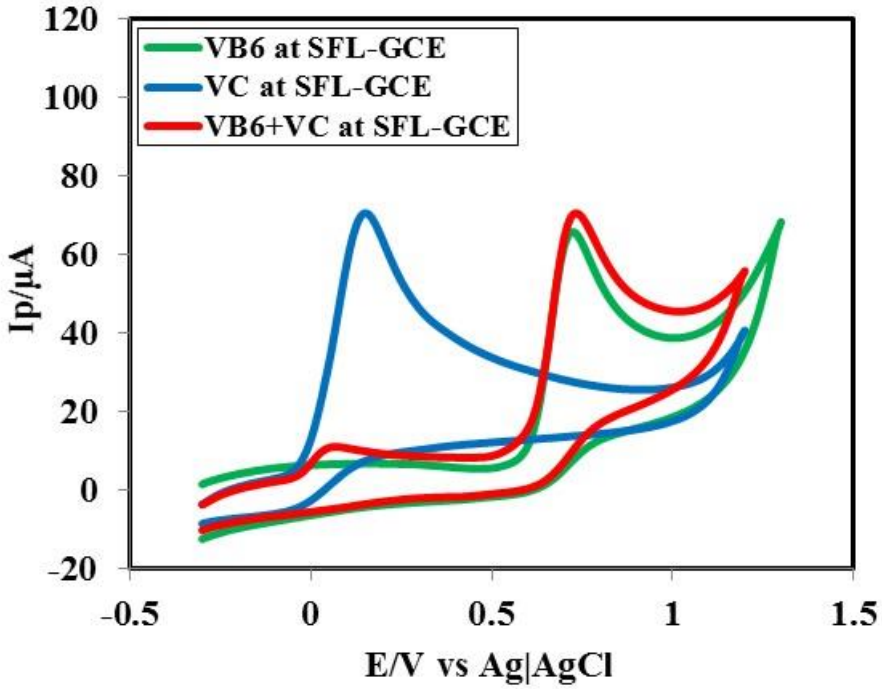

Figure 4.39: Cyclic voltammogram (CV) of 2.5 mM VB_6 (green line), 2.5 mM VC (blue line) and 2.5 mM VB_6+2.5 mM VC (red line) at SFL modified GC electrode in PBS (pH 7) at scan rate 0.1 V/s.

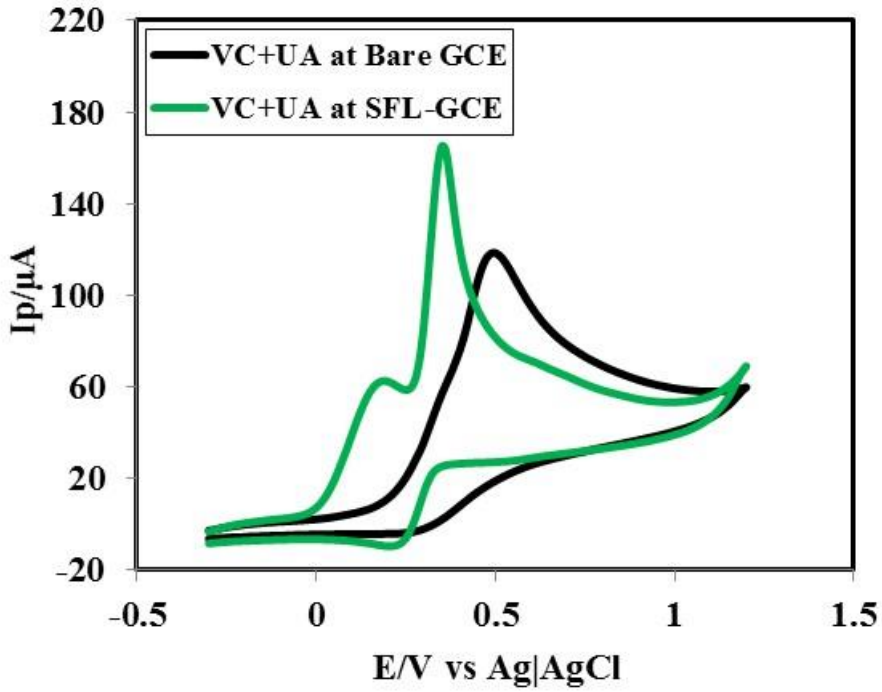

Figure 4.40: CV comparison of 2.5 mM VC+ 2.5 mM UA at bare (black line) and SFL modified GC electrode (green line) in PBS (pH 7) at scan rate 0.1 V/s.

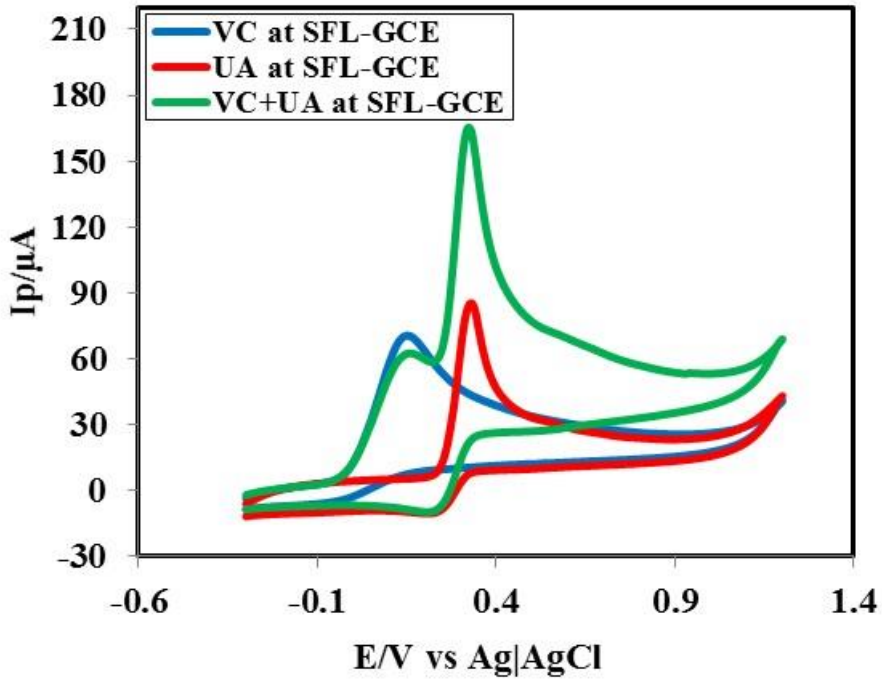

Figure 4.41: Cyclic voltammogram (CV) of 2.5 mM VC (blue line), 2.5 mM UA (red line) and 2.5 mM VC+ 2.5 mM UA (green line) at SFL modified GC electrode in PBS (pH 7) at scan rate 0.1 V/s.

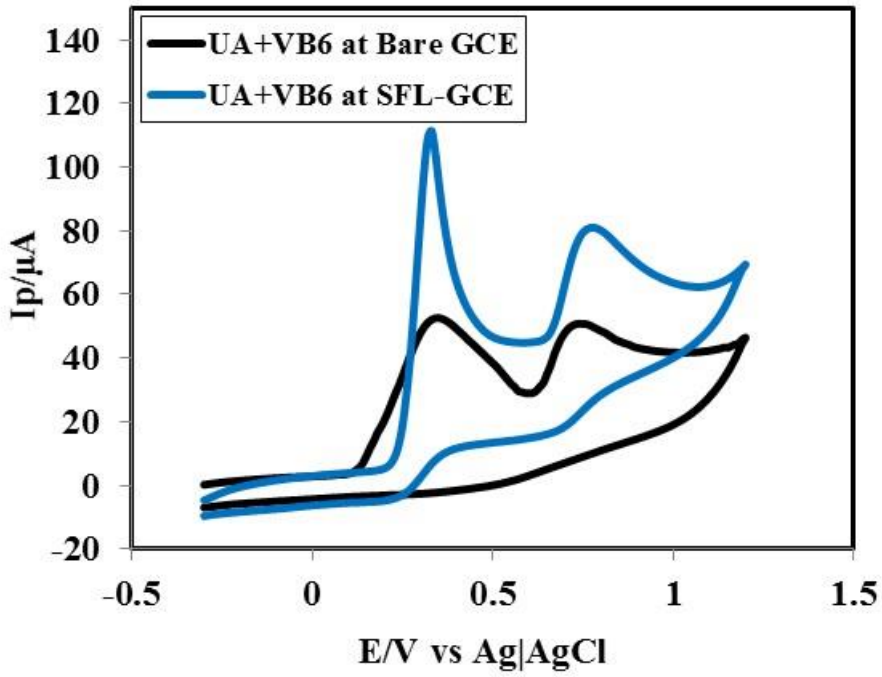

Figure 4.42: CV comparison of 2.5 mM UA+ 2.5 mM VB_6 at bare (black line) and SFL modified GC electrode (blue line) in PBS (pH 7) at scan rate 0.1 V/s.

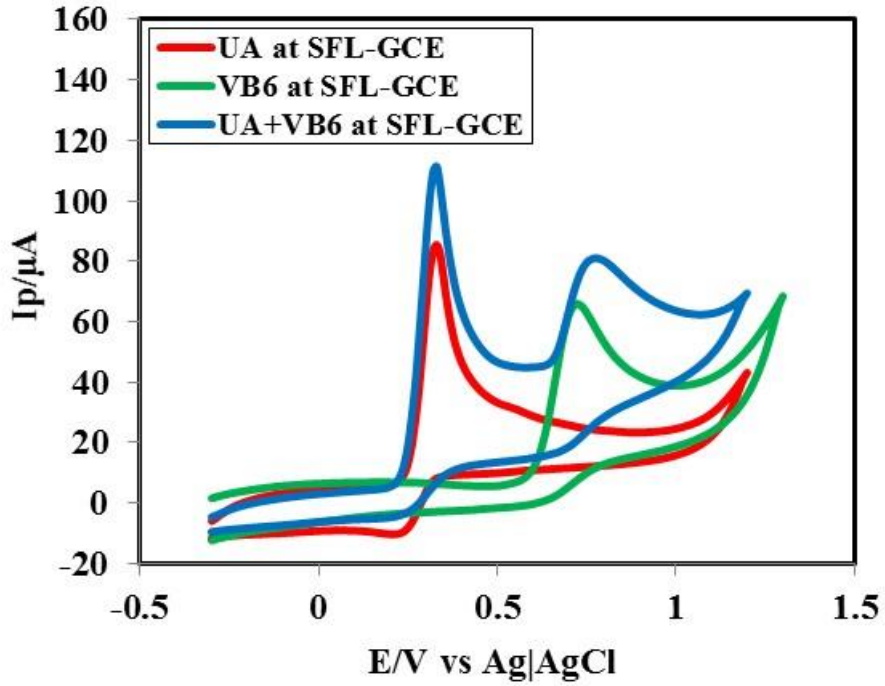

Figure 4.43: Cyclic voltammogram (CV) of 2.5 mM UA (red line), 2.5 mM VB_6 (green line) and 2.5 mM UA+ 2.5 mM VB_6 (blue line) at SFL modified GC electrode in PBS (pH 7) at scan rate 0.1 V/s.

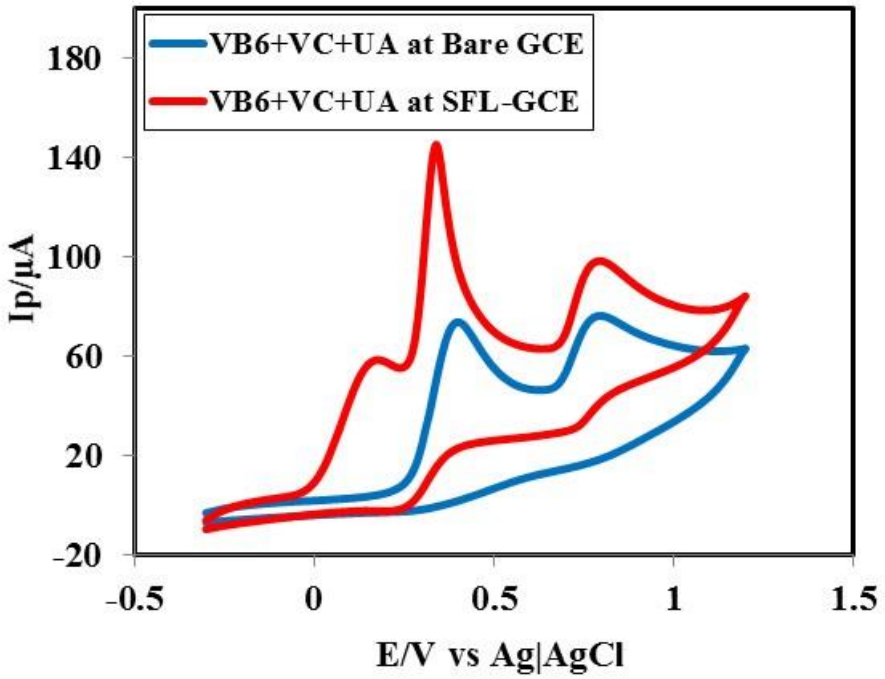

Figure 4.44: CV comparison of 2.5 mM VB_6+ 2.5 mM VC+ 2.5 mM UA at bare (blue line) and SFL modified GC electrode (red line) in PBS (pH 7) at scan rate 0.1 V/s.

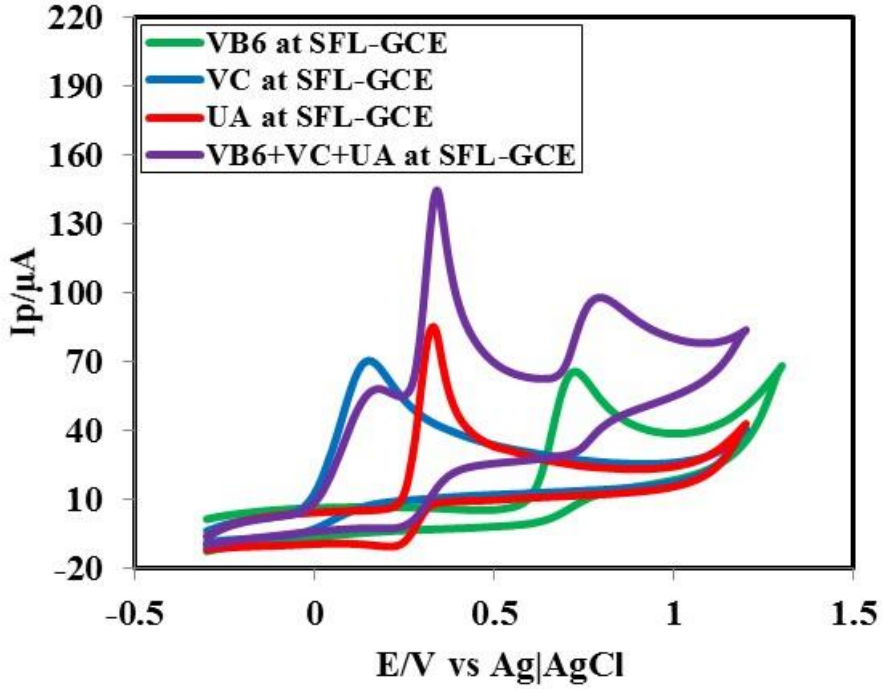

Figure 4.45: Cyclic voltammogram (CV) of 2.5 mM VB_6 (green line), 2.5 mM VC (blue line), 2.5 mM UA (red line) and 2.5 mM VB_6+ 2.5 mM VC+ 2.5 mM UA (purple line) at SFL modified GC electrode in PBS (pH 7) at scan rate 0.1 V/s.

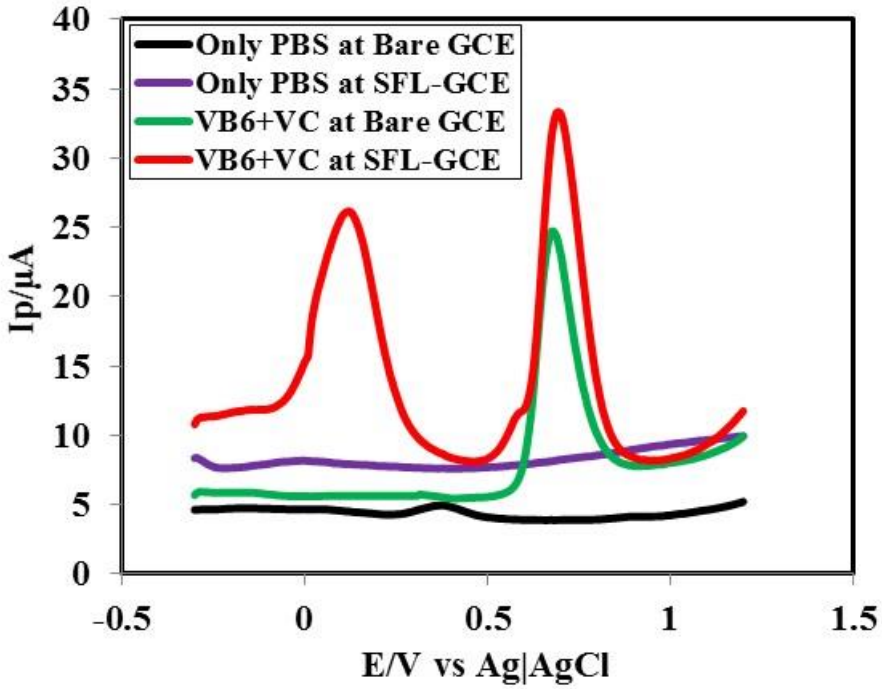

Figure 4.46: Differential pulse voltammogram (DPV) of only PBS (pH 7) at bare (black line) and SFL modified GC electrode (purple line) and 2.5 mM VB_6+ 2.5 mM VC at bare (green line) and SFL modified GC electrode (red line) at scan rate 0.1 V/s.

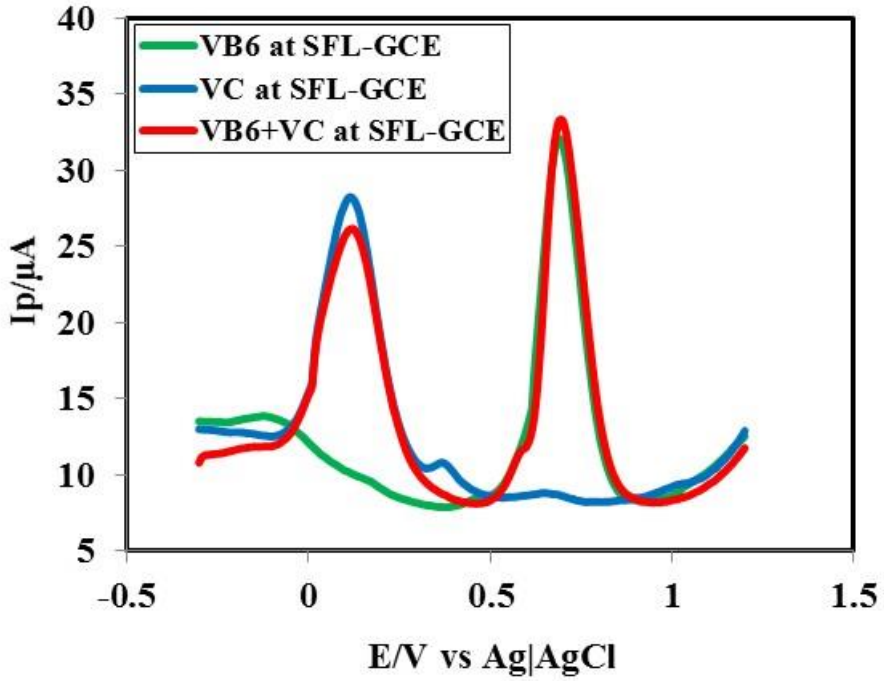

Figure 4.47: Differential pulse voltammogram (DPV) of 2.5 mM VB_6 (green line), 2.5 mM VC (blue line) and 2.5 mM VB_6+ 2.5 mM VC (red line) in PBS (pH 7) at SFL modified GC electrode at scan rate 0.1 V/s.

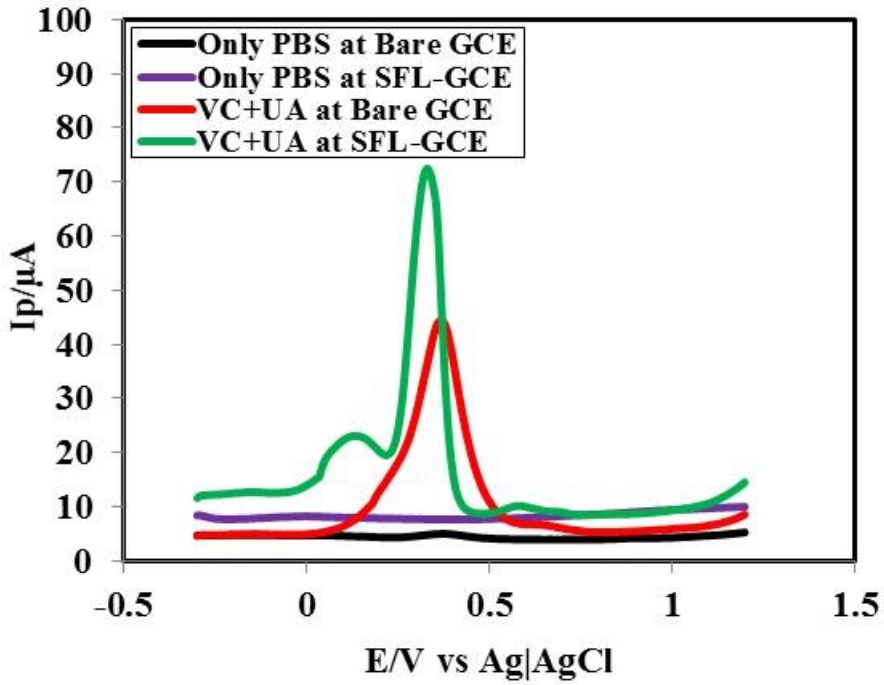

Figure 4.48: Differential pulse voltammogram (DPV) of only PBS (pH 7) at bare (black line) and SFL modified GC electrode (purple line) and 2.5 mM VC+ 2.5 mM UA at bare (red line) and SFL modified GC electrode (green line) at scan rate 0.1 V/s.

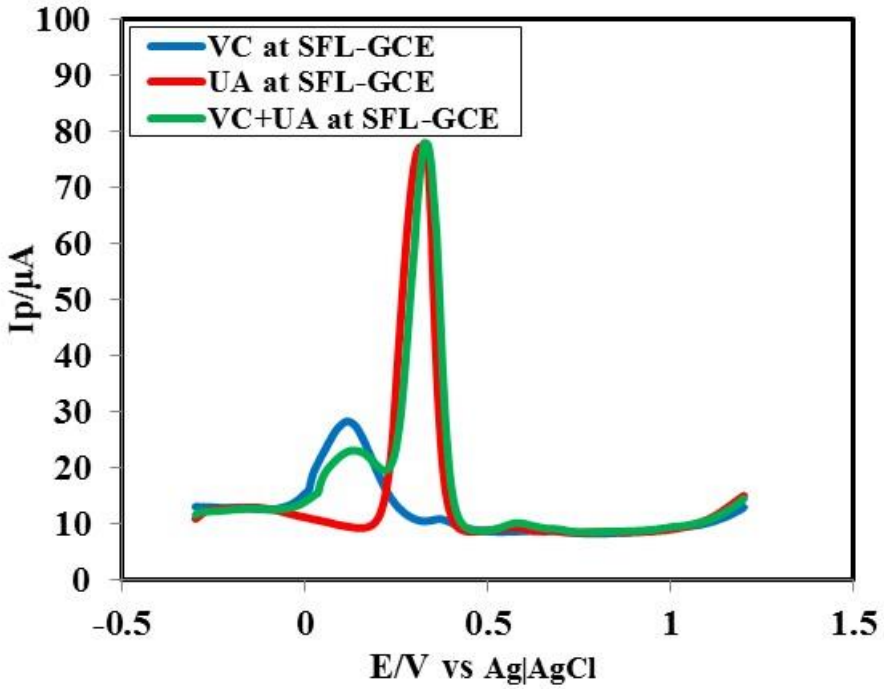

Figure 4.49: Differential pulse voltammogram (DPV) of 2.5 mM VC (blue line), 2.5 mM UA (red line) and 2.5 mM VC+ 2.5 mM UA (green line) in PBS (pH 7) at SFL modified GC electrode at scan rate 0.1 V/s.

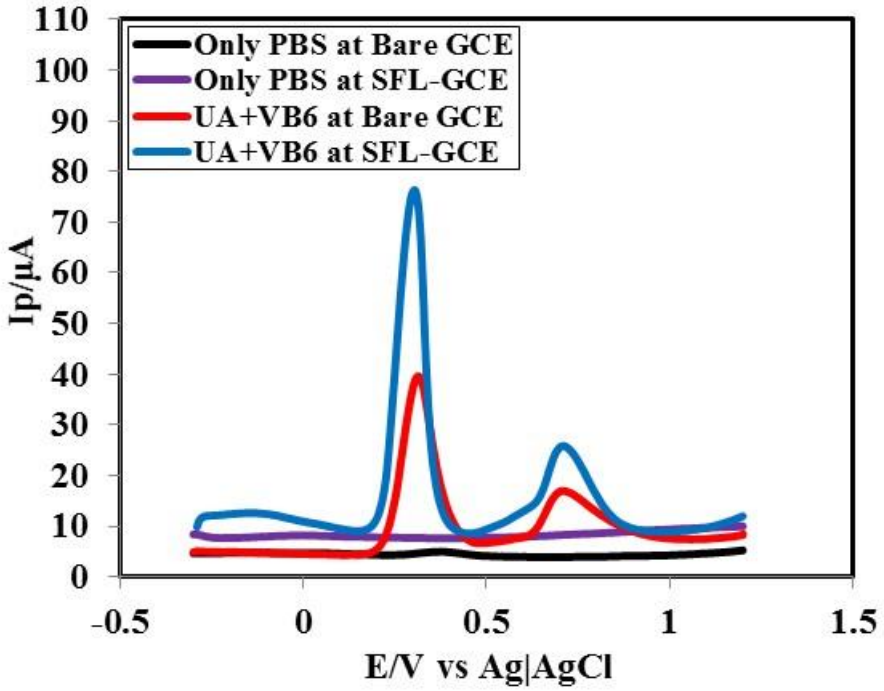

Figure 4.50: Differential pulse voltammogram (DPV) of only PBS (pH 7) at bare (black line) and SFL modified GC electrode (purple line) and 2.5 mM UA+ 2.5 mM VB_6 at bare (red line) and SFL modified GC electrode (blue line) at scan rate 0.1 V/s.

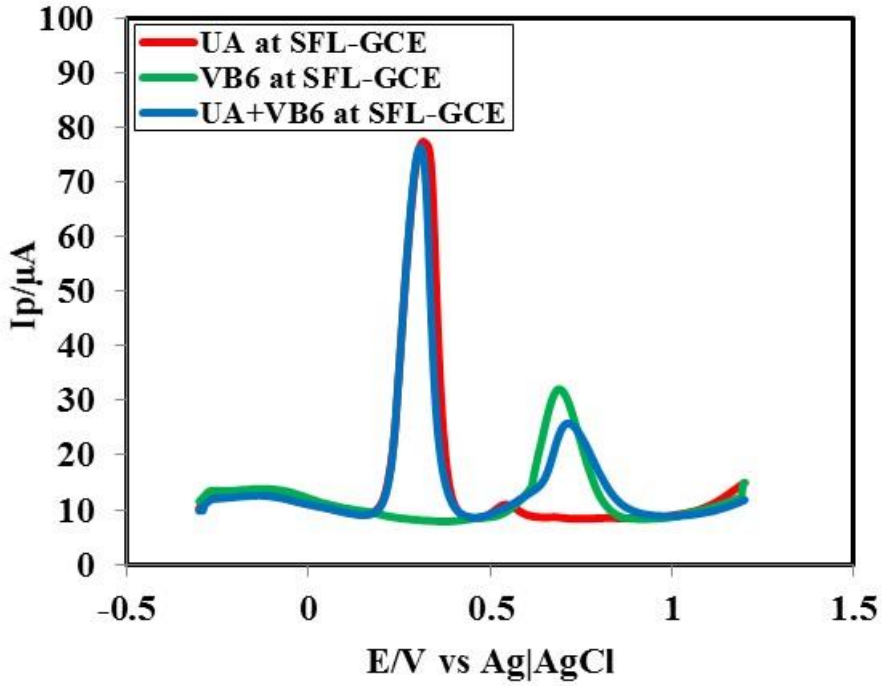

Figure 4.51: Differential pulse voltammogram (DPV) of 2.5 mM UA (red line), 2.5 mM VB_6 (green line) and 2.5 mM UA+ 2.5 mM VB_6 (blue line) in PBS (pH 7) at SFL modified GC electrode at scan rate 0.1 V/s.

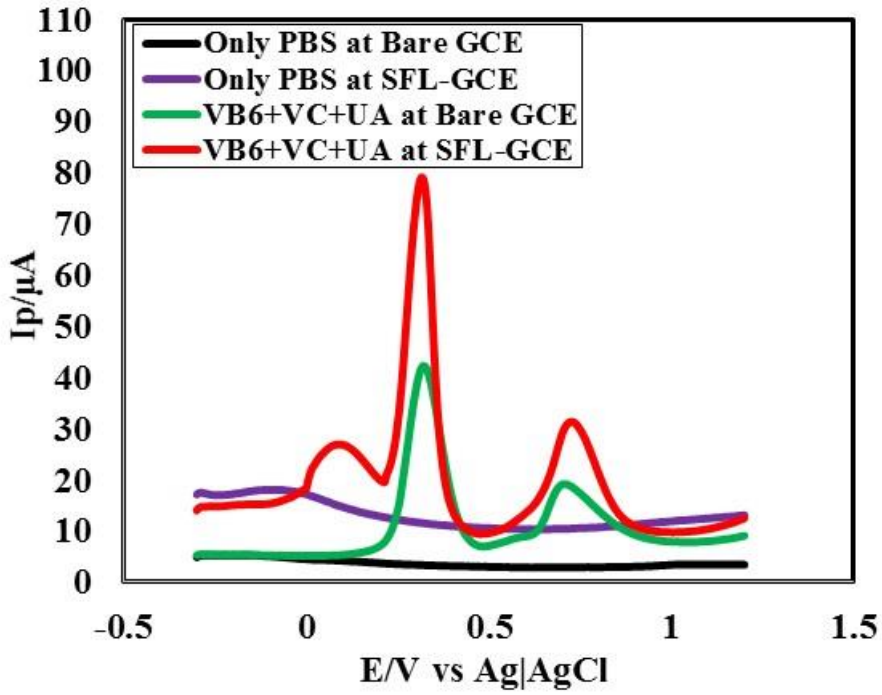

Figure 4.52: Differential pulse voltammogram (DPV) of only PBS (pH 7) at bare (black line) and SFL modified GC electrode (purple line) and 2.5 mM VB_6+ 2.5 mM VC+ 2.5 mM UA at bare (green line) and SFL modified GC electrode (red line) at scan rate 0.1 V/s.

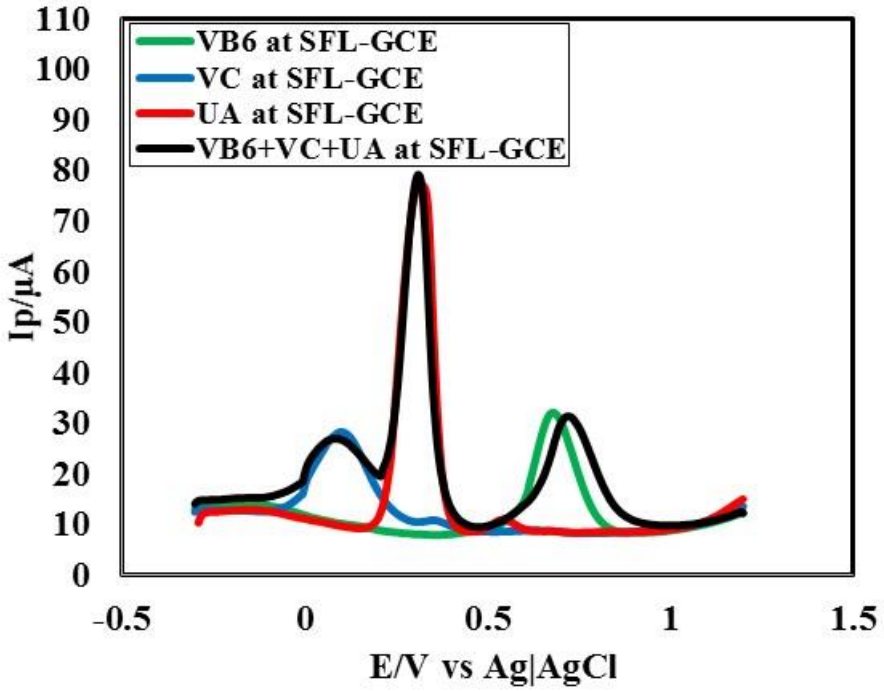

Figure 4.53: Differential pulse voltammogram (DPV) of 2.5 mM VB_6 (green line), 2.5 mM VC (blue line), 2.5 mM UA (red line) and 2.5 mM VB_6+ 2.5 mM VC+ 2.5 mM UA (black line) in PBS (pH 7) at SFL modified GC electrode at scan rate 0.1 V/s.

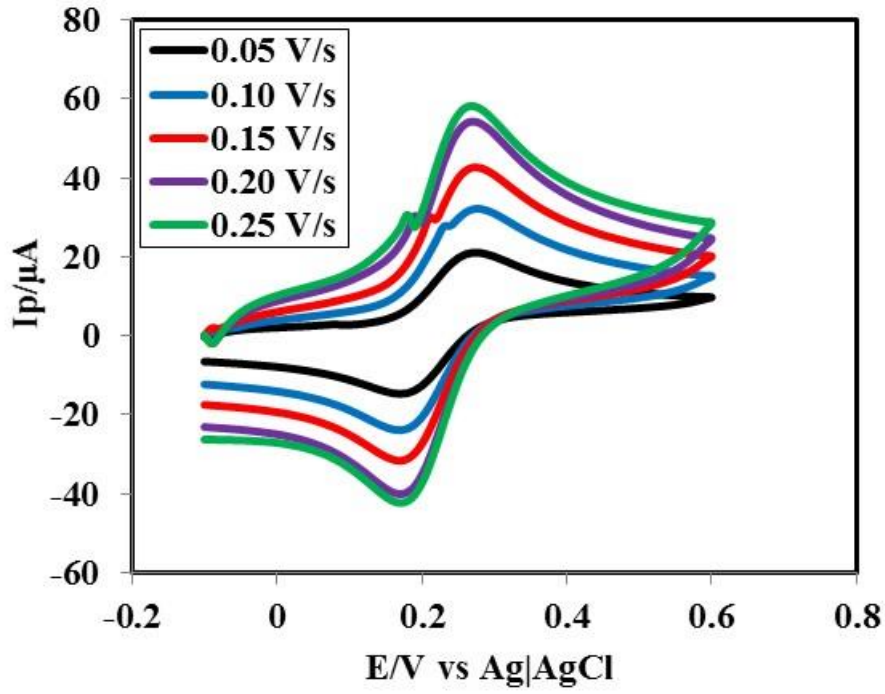

Figure 4.54: Cyclic voltammograms (CVs) of 2 mM potassium ferrocyanide on SFL modified GCE at different scan rate of 0.05 V/s, 0.10 V/s, 0.15 V/s, 0.20 V/s and 0.25 V/s in 1 M KCl as supporting electrolyte.

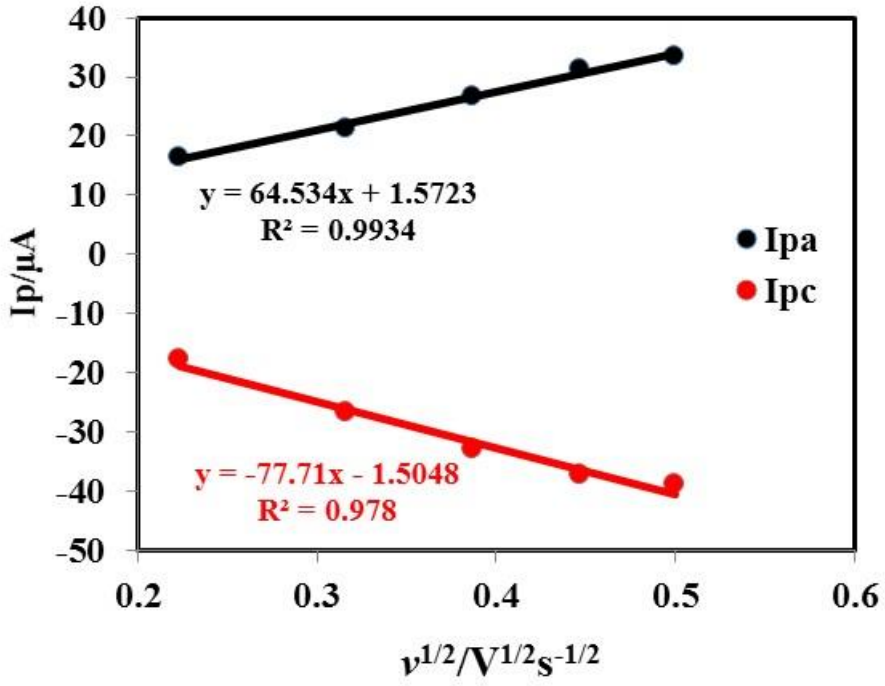

Figure 4.55: The anodic and the cathodic peak current of potassium ferrocyanide vs square root of the scan rates.

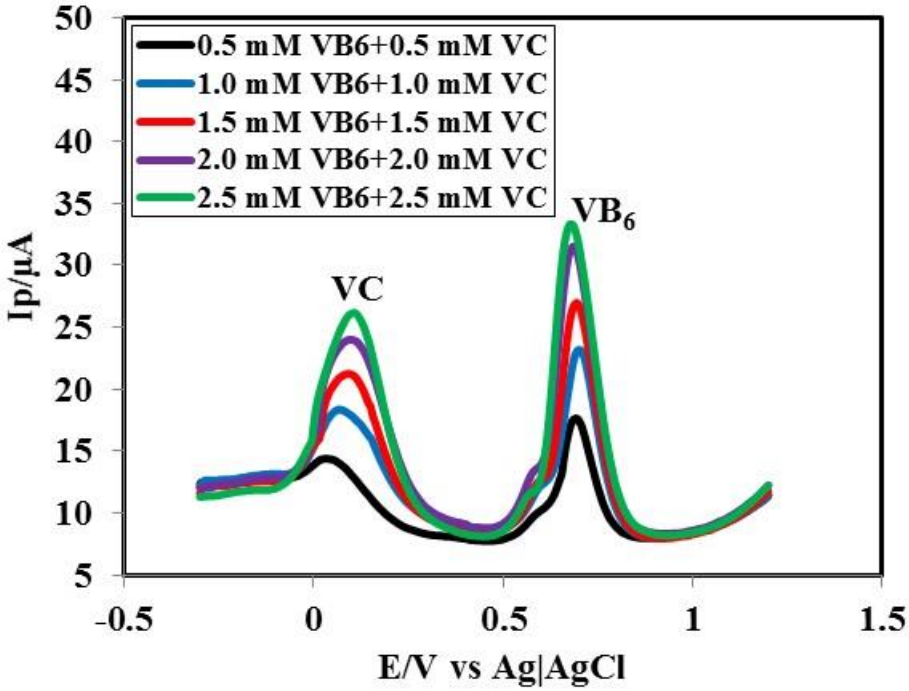

Figure 4.56: Differential pulse voltammogram (DPV) of simultaneous concentration change for VB_6 and VC (0.5-2.5 mM) at SFL modified GC electrode in PBS (pH 7) at scan rate 0.1 V/s.

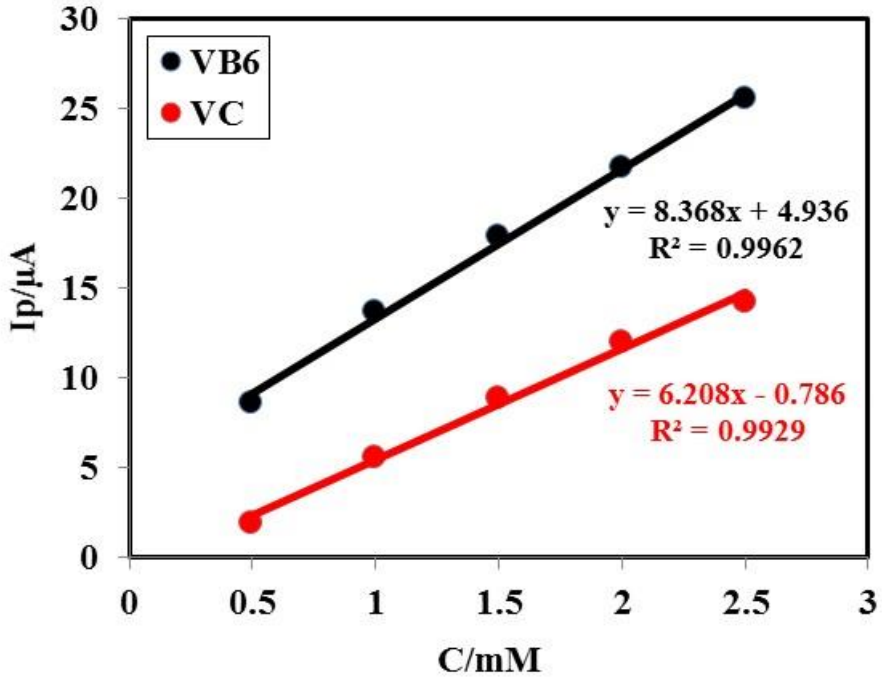

Figure 4.57: Plots of peak current (I_p) vs concentration (C) of VB_6 (black line) and VC (red line) in a binary mixture at SFL modified GC electrode.

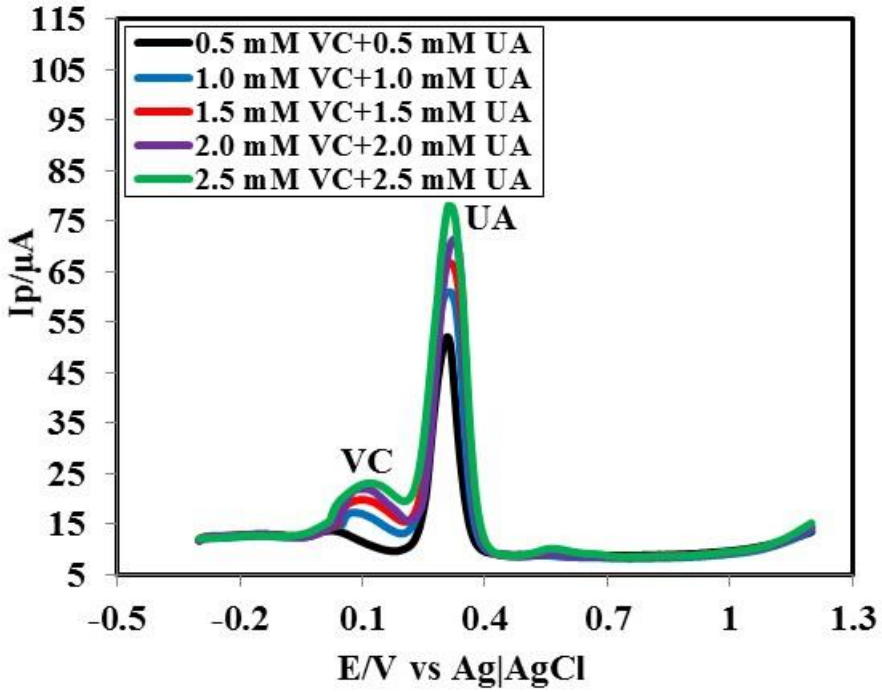

Figure 4.58: Differential pulse voltammogram (DPV) of simultaneous concentration change for VC and UA (0.5-2.5 mM) at SFL modified GC electrode in PBS (pH 7) at scan rate 0.1 V/s.

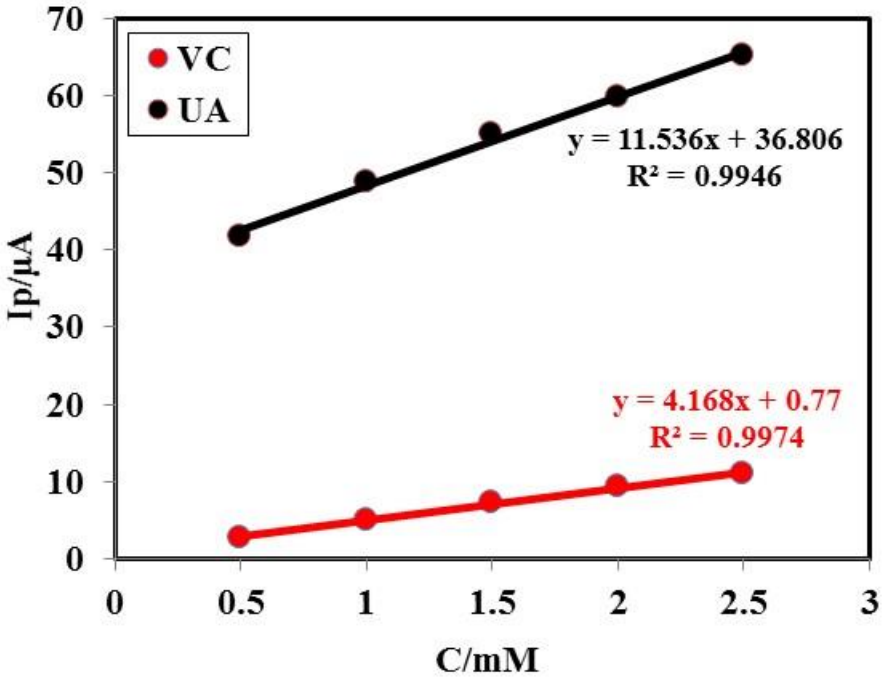

Figure 4.59: Plots of peak current (I_p) versus concentration (C) of VC (red line) and UA (black line) in a binary mixture at SFL modified GC electrode.

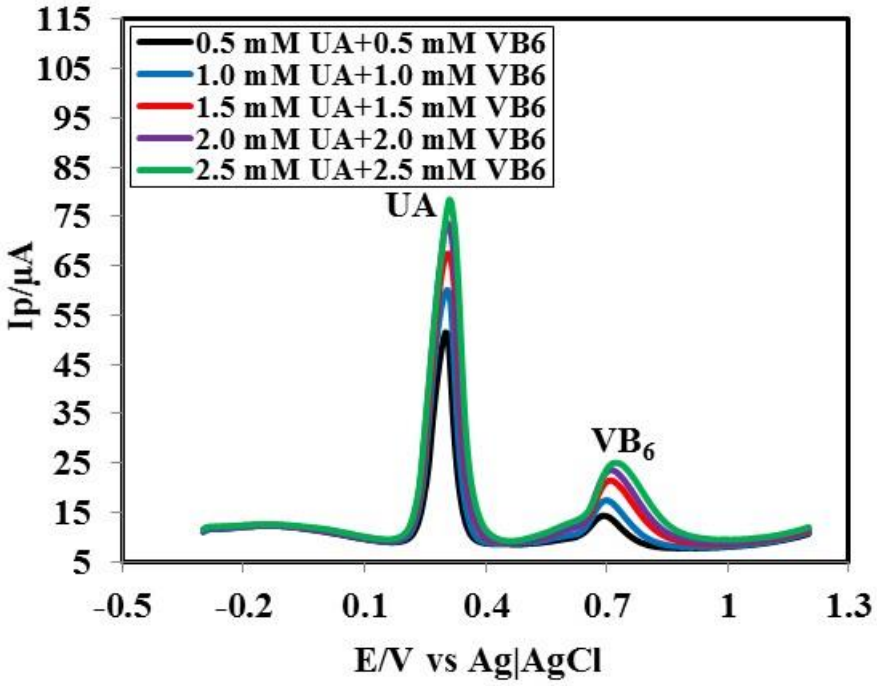

Figure 4.60: Differential pulse voltammogram (DPV) of simultaneous concentration change for UA and VB_6 (0.5-2.5 mM) at SFL modified GC electrode in PBS (pH 7) at scan rate 0.1 V/s.

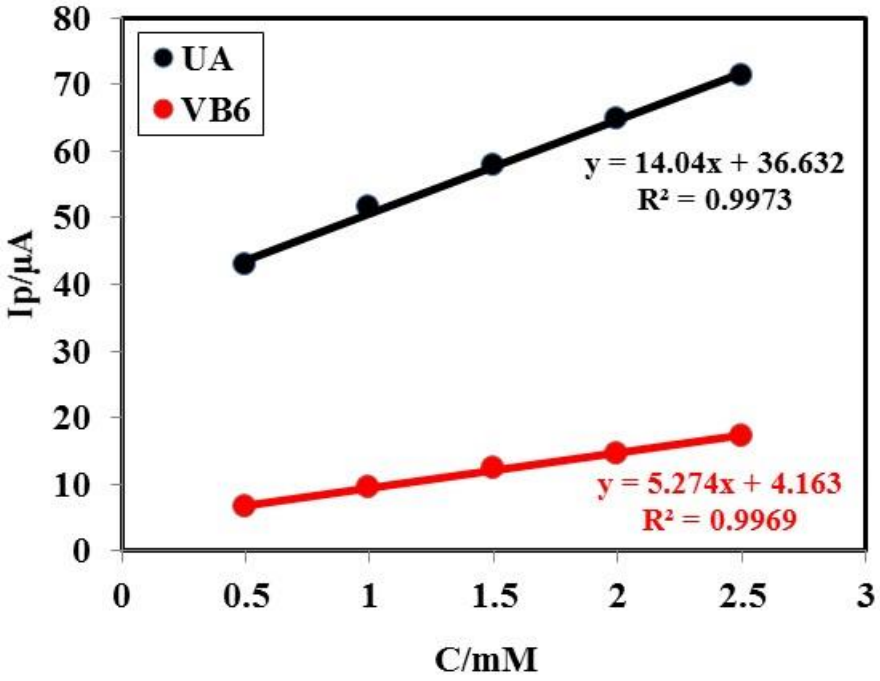

Figure 4.61: Plots of peak current (I_p) versus concentration (C) of UA (black line) and VB_6 (red line) in a binary mixture at SFL modified GC electrode.

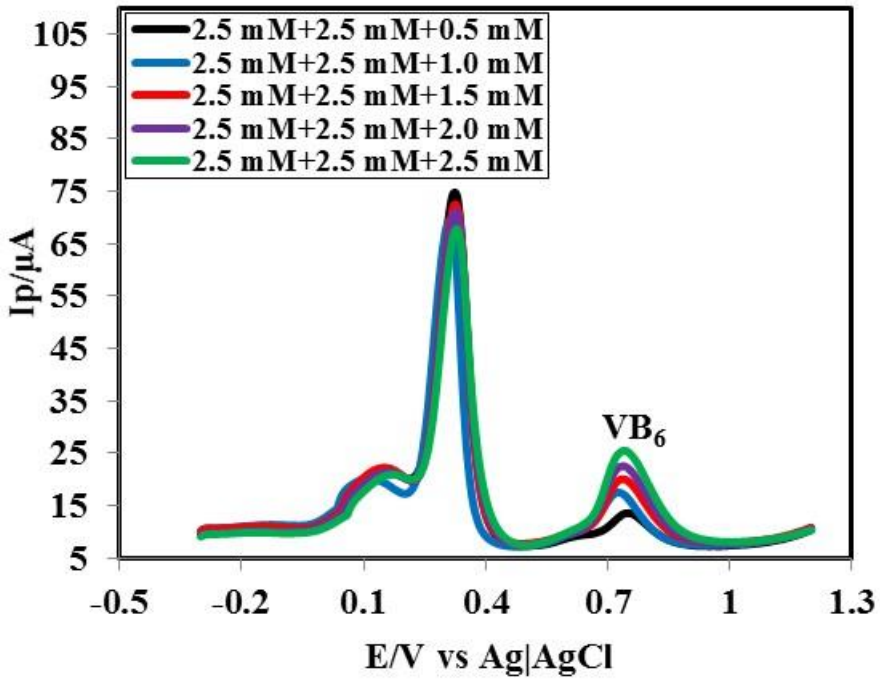

Figure 4.62: Differential pulse voltammogram (DPV) of different concentrations (0.5-2.5 mM) of VB_6 at constant concentration of VC and UA (2.5 mM) in ternary mixture at SFL modified GC electrode in PBS (pH 7) at scan rate 0.1 V/s.

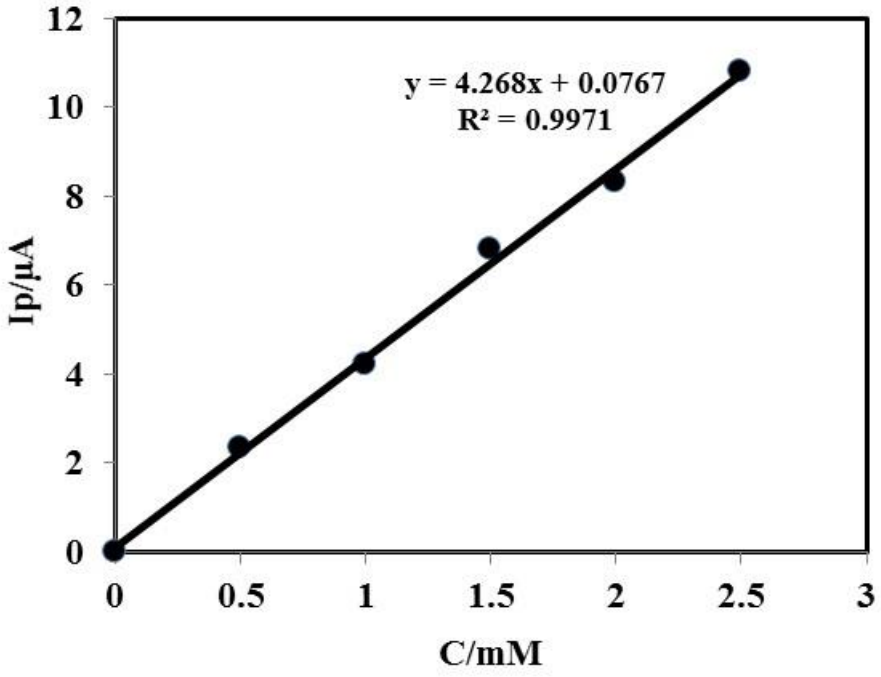

Figure 4.63: Plots of peak current (I_p) vs concentration (C) of VB_6 (0.5-2.5 mM) at constant concentration of VC and UA (2.5 mM) in a ternary mixture of VB_6+VC+UA at SFL modified GC electrode.

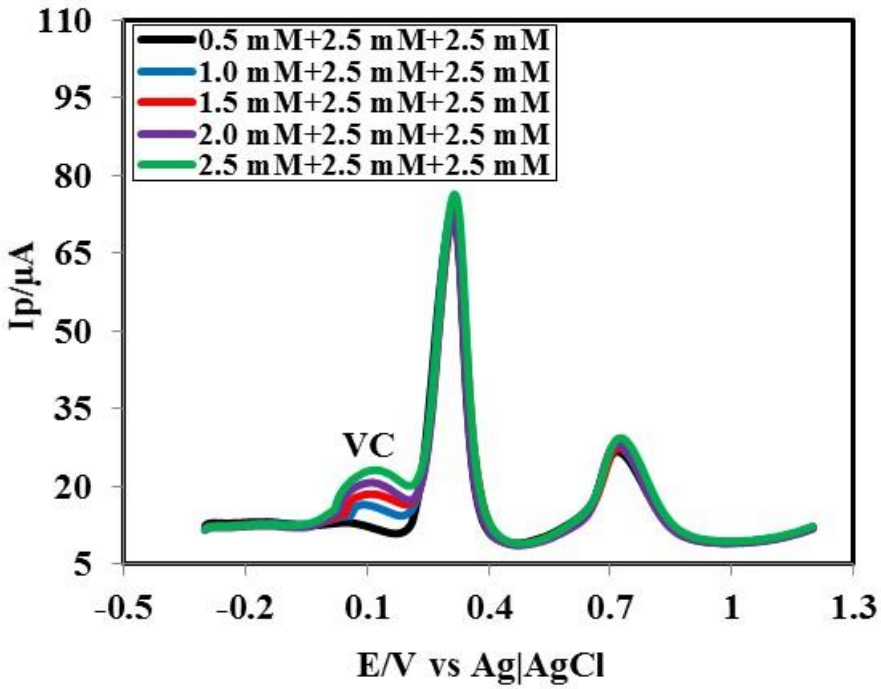

Figure 4.64: Differential pulse voltammogram (DPV) of different concentrations (0.5-2.5 mM) of VC at constant concentration of UA and VB_6 (2.5 mM) in ternary mixture at SFL modified GC electrode in PBS (pH 7) at scan rate 0.1 V/s.

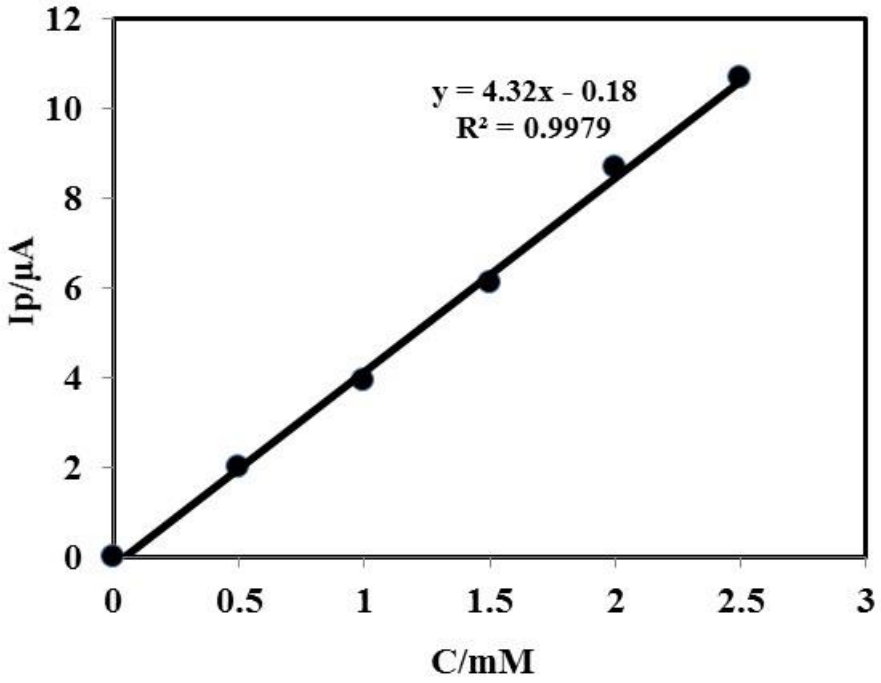

Figure 4.65: Plots of peak current (I_p) vs concentration (C) of VC (0.5-2.5 mM) at constant concentration of UA and VB_6 (2.5 mM) in a ternary mixture of VB_6+VC+UA at SFL modified GC electrode.

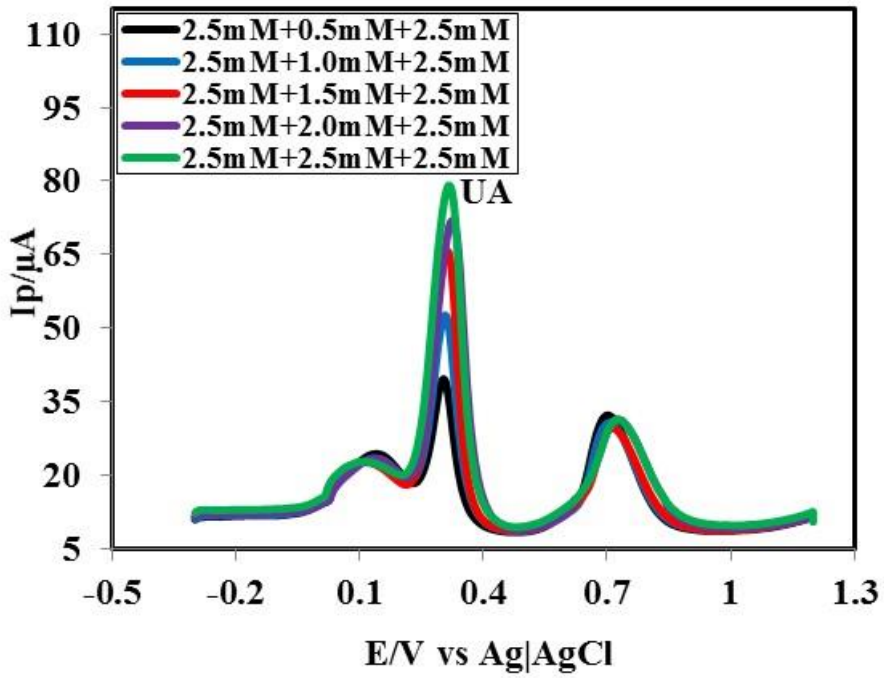

Figure 4.66: Differential pulse voltammogram (DPV) of different concentrations (0.5-2.5 mM) of UA at constant concentration of VC and VB_6 (2.5 mM) in ternary mixture at SFL modified GC electrode in PBS (pH 7) at scan rate 0.1 V/s.

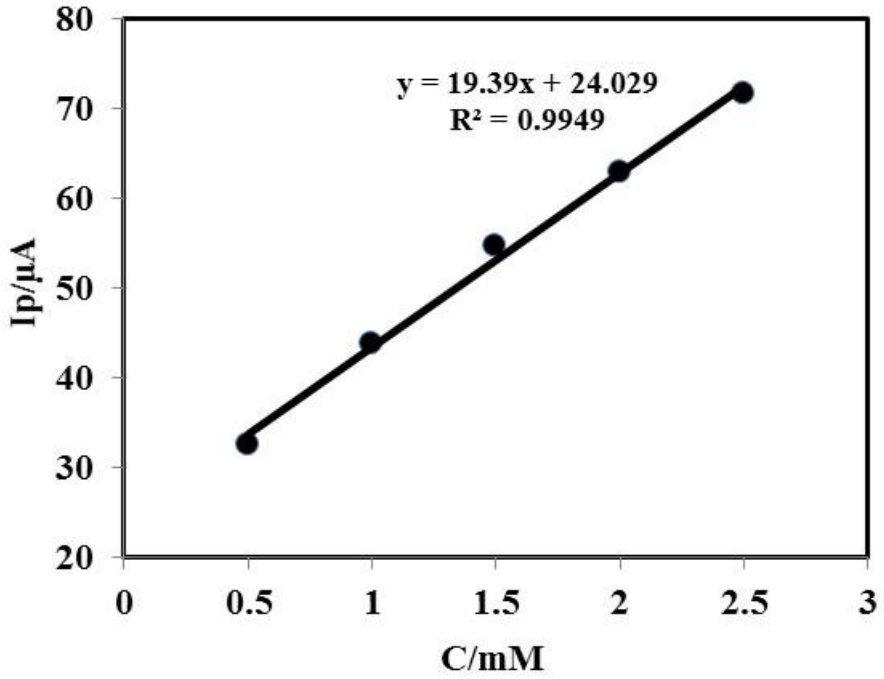

Figure 4.67: Plots of peak current (I_p) vs concentration (C) of UA (0-2.5 mM) at constant concentration of VC and VB_6 (2.5 mM) in a ternary mixture of VB_6+VC+UA at SFL modified GC electrode.

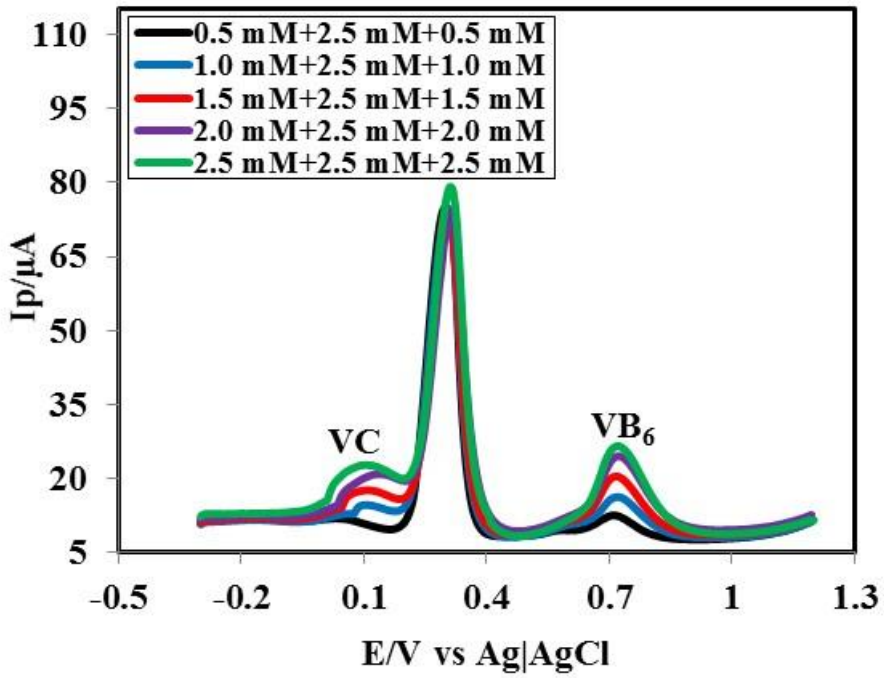

Figure 4.68: Differential pulse voltammogram (DPV) of different concentrations (0.5-2.5 mM) of VC and VB_6 at constant concentration of UA (2.5 mM) in ternary mixture at SFL modified GC electrode in PBS (pH 7) at scan rate 0.1 V/s.

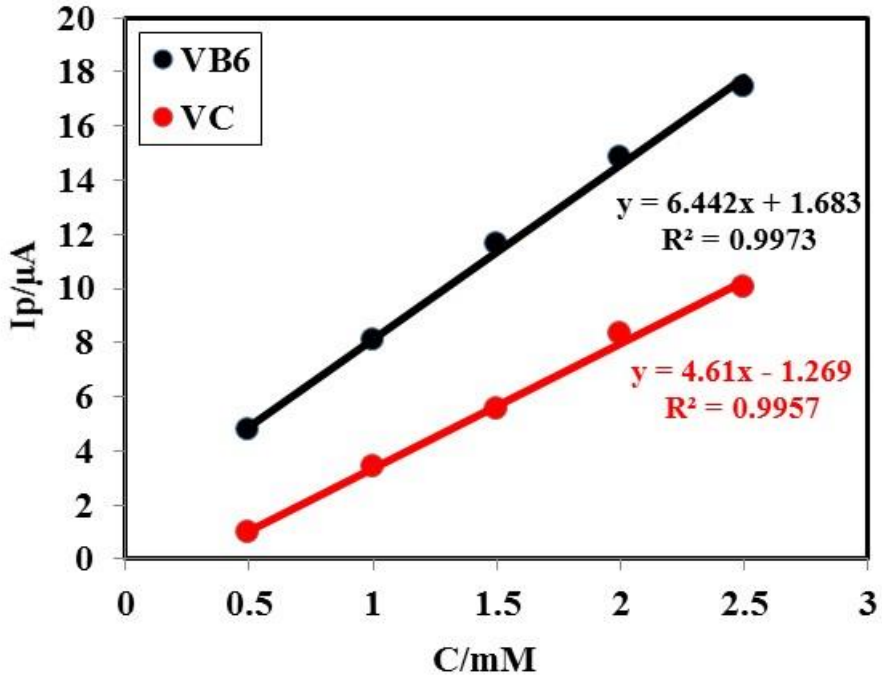

Figure 4.69: Plots of peak current (I_p) vs concentration (C) of VB_6 (black line) and VC (red line) (0.5-2.5 mM) at constant concentration of UA (2.5 mM) in a ternary mixture of VB_6+VC+UA at SFL modified GC electrode.

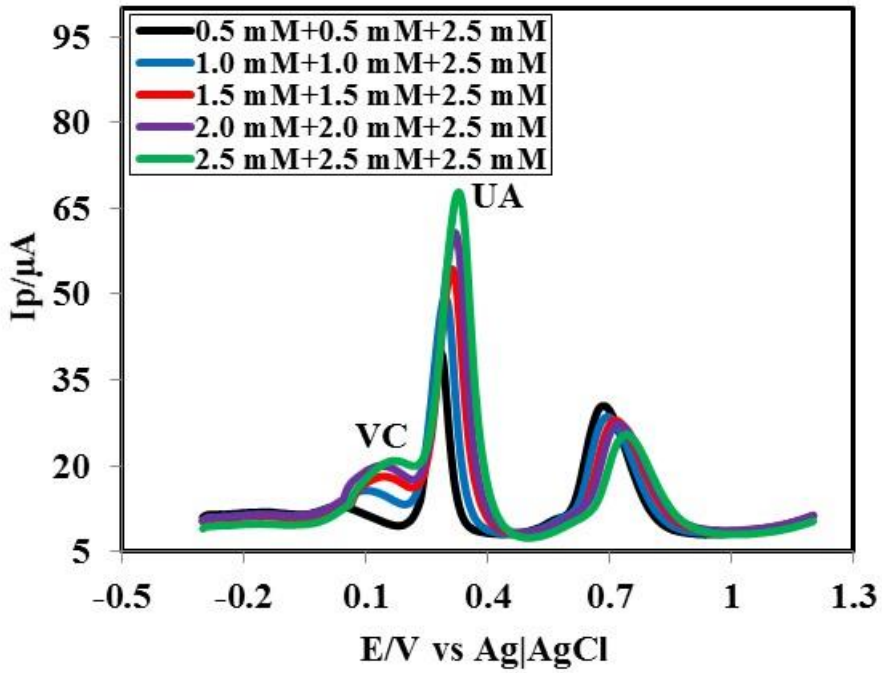

Figure 4.70: Differential pulse voltammogram (DPV) of different concentrations (0.5-2.5 mM) of VC and UA of at constant concentration of VB_6 (2.5 mM) in ternary mixture at SFL modified GC electrode in PBS (pH 7) at scan rate 0.1 V/s.

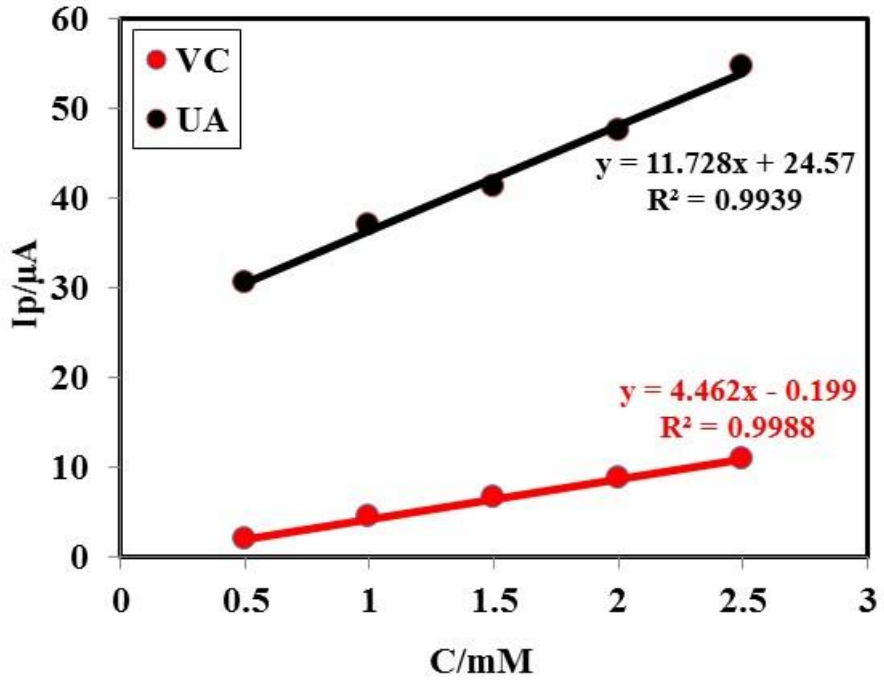

Figure 4.71: Plots of peak current (I_p) vs concentration (C) of VC (red line) and UA (black line) (0.5-2.5 mM) at constant concentration of VB_6 (2.5 mM) in a ternary mixture of VB_6+VC+UA at SFL modified GC electrode.

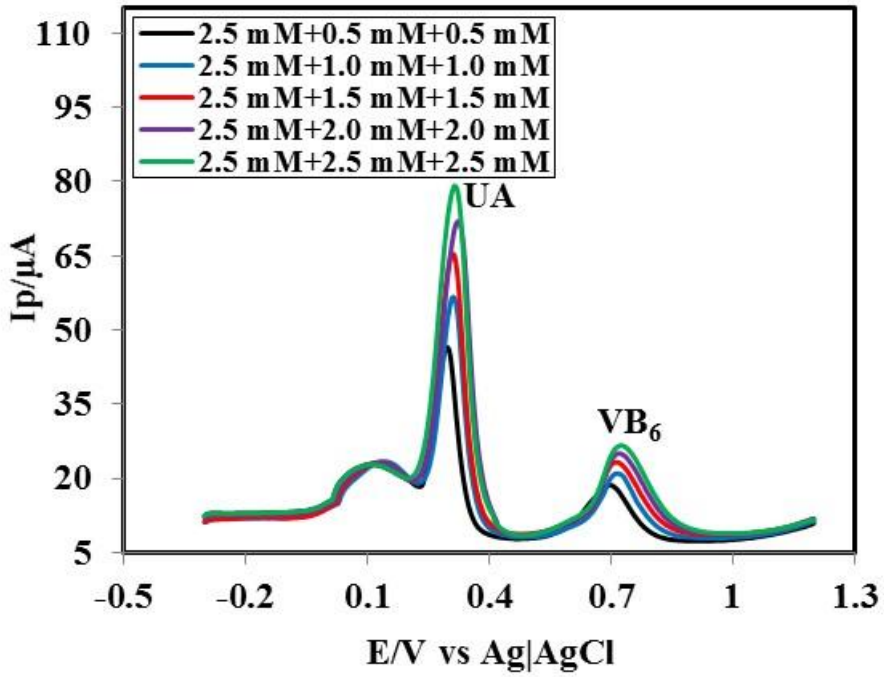

Figure 4.72: Differential pulse voltammogram (DPV) of different concentrations (0.5-2.5 mM) of UA and VB_6 at constant concentration of VC (2.5 mM) in ternary mixture at SFL modified GC electrode in PBS (pH 7) at scan rate 0.1 V/s.

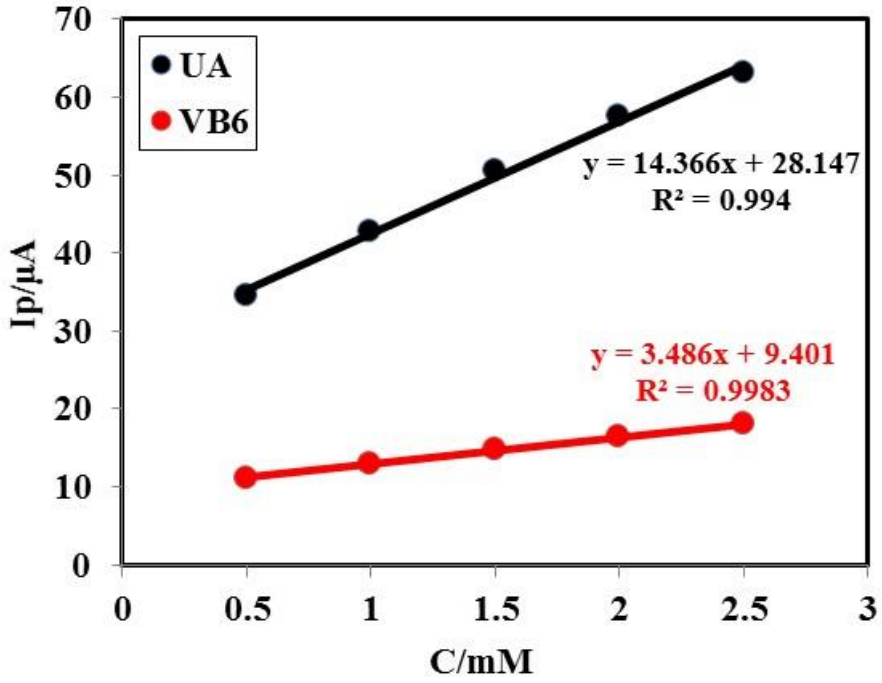

Figure 4.73: Plots of peak current (I_p) vs concentration (C) of UA (black line) and VB_6 (red line) (0.5-2.5 mM) at constant concentration of VC (2.5 mM) in a ternary mixture of VB_6+VC+UA at SFL modified GC electrode.

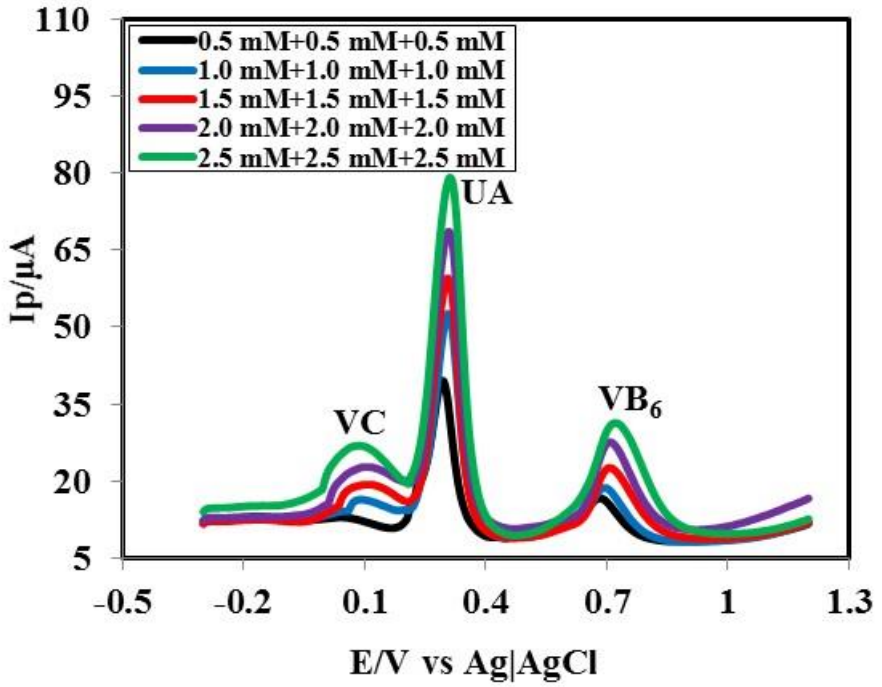

Figure 4.74: Differential pulse voltammogram (DPV) for different concentrations (0.5-2.5 mM) of VB_6, VC and UA in ternary mixture at SFL modified GC electrode in PBS (pH 7) at scan rate 0.1 V/s.

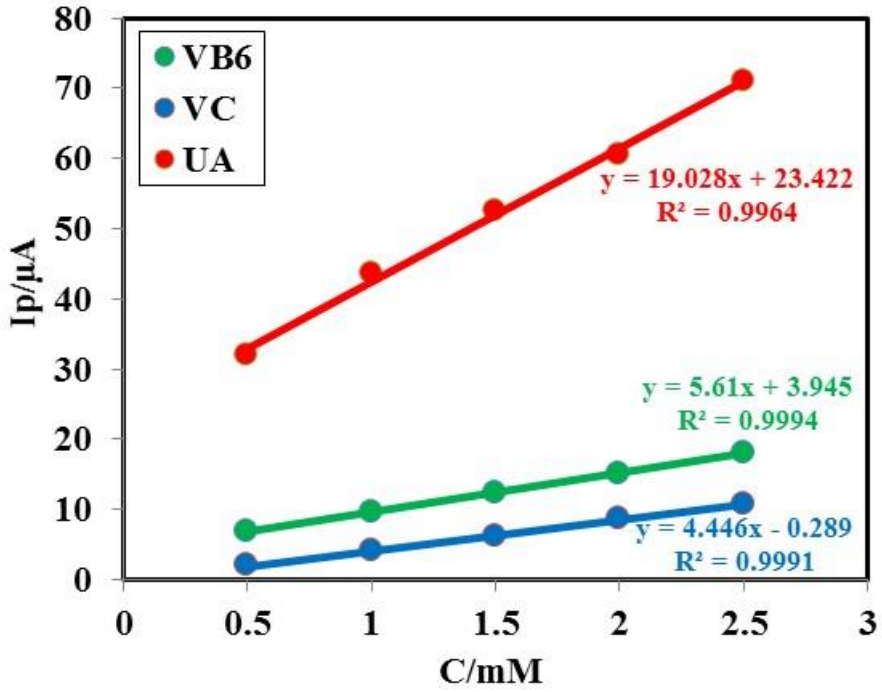

Figure 4.75: Plots of peak current (I_p) vs concentration (C) of VB_6 (green line), VC (blue line) and UA (red line) (0.5-2.5 mM) in a ternary mixture of VB_6+VC+UA at SFL modified GC electrode.

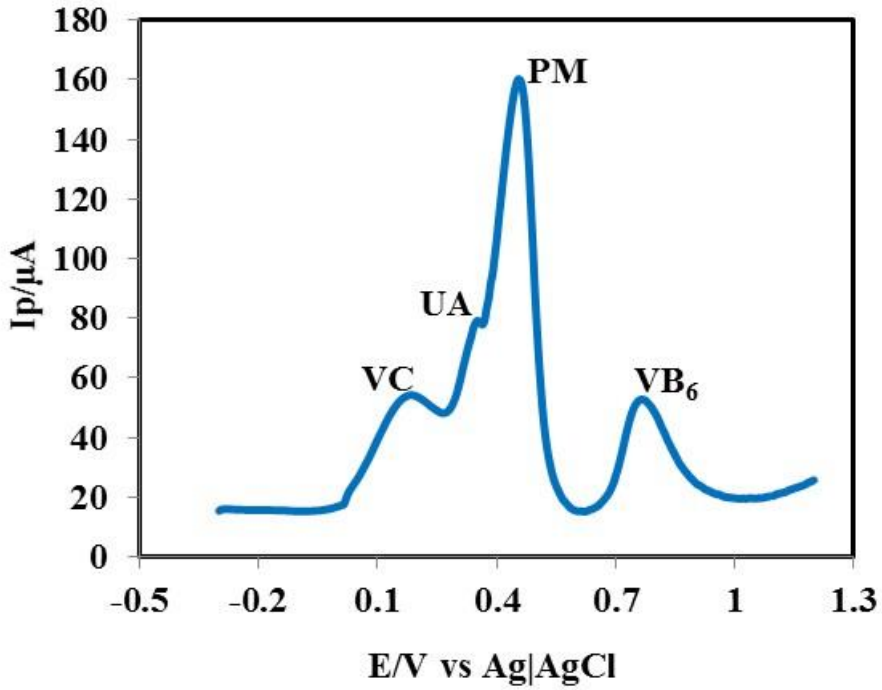

Figure 4.76: DPV of the ternary solution of VB_6, VC and UA in presence of paracetamol, thiamine (Vitamin B_1), nicotinamide (Vitamin B_3), histidine, aspargine, lysine, proline, phenylalanine and glucose in PBS (pH 7) at SFL modified GC electrode.

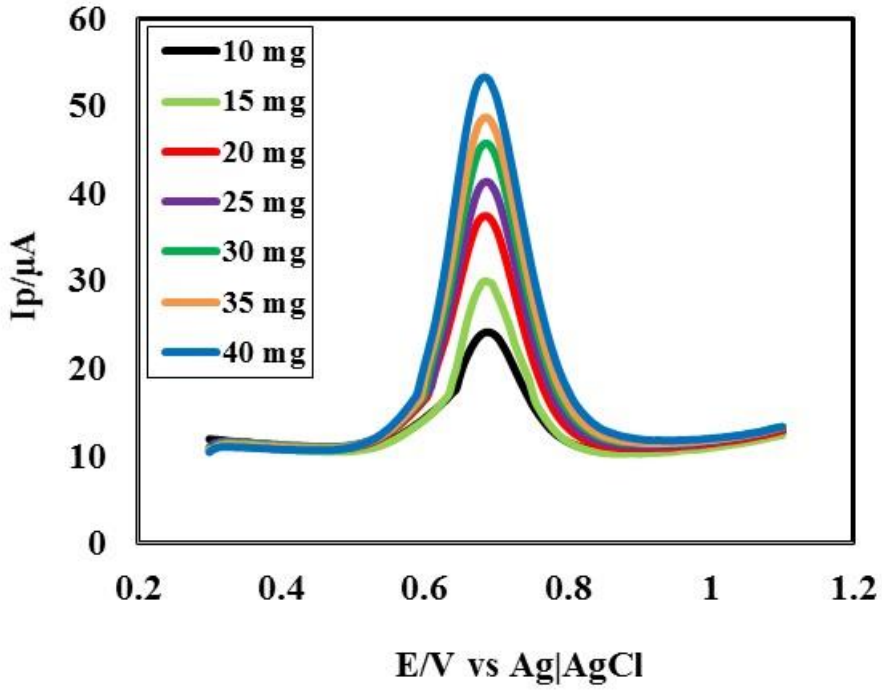

Figure 4.77: Differential pulse voltammogram (DPV) of different amount (10-40 mg) of standard VB_6 in 50 mL PBS (pH 7) at SFL modified GC electrode.

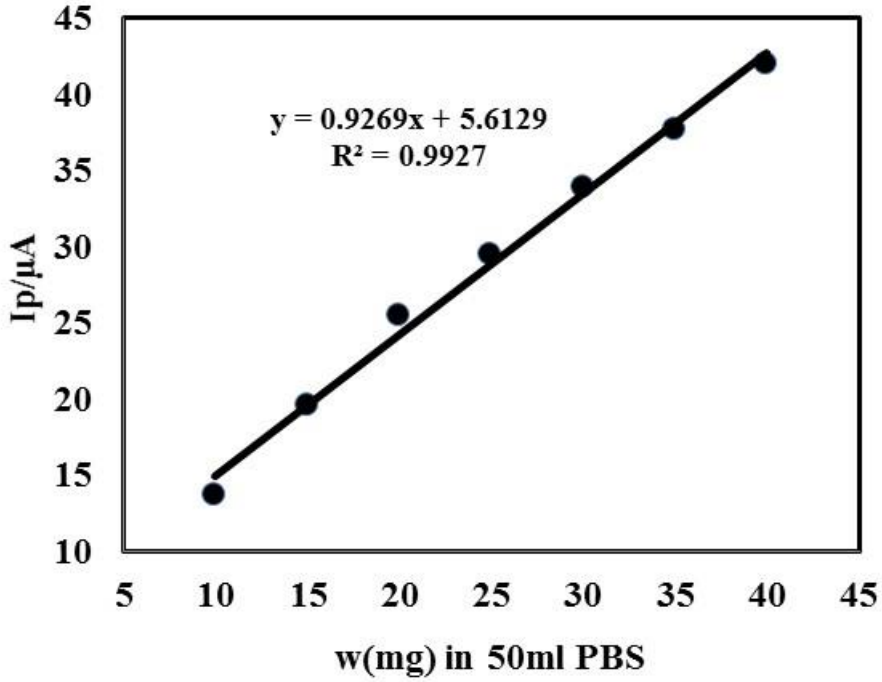

Figure 4.78: Calibration curve of VB_6 with response to different amount (10-40 mg) in 50 mL PBS (pH 7).

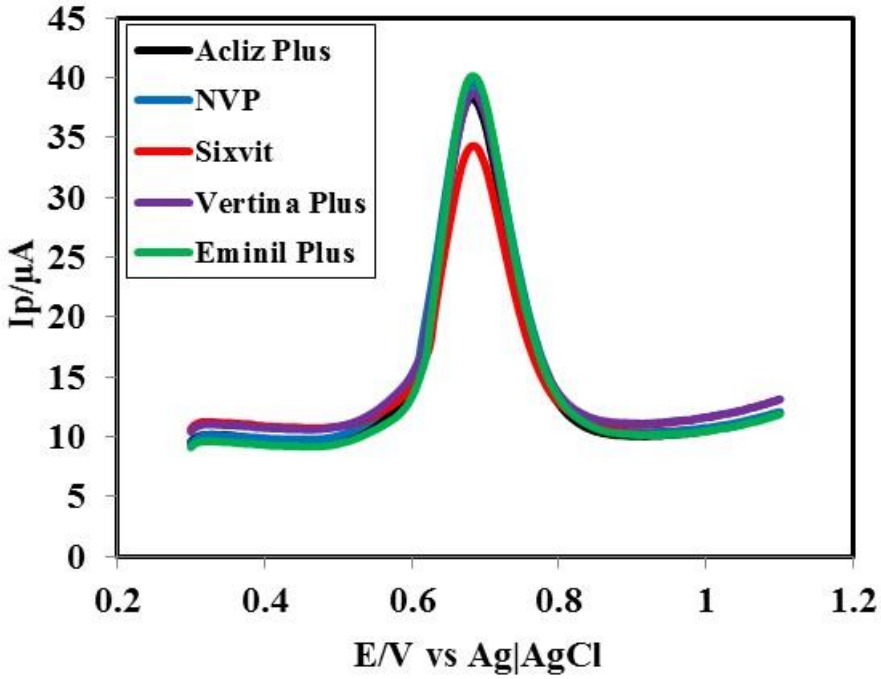

Fig 4.79: Differential pulse voltammogram (DPV) of VB_6 in Acliz Plus (black line), NVP (blue line), Sixvit (red line), Vertina Plus (purple line) and Eminil Plus (green line) tablets in PBS (pH 7) at SFL modified GC electrode.

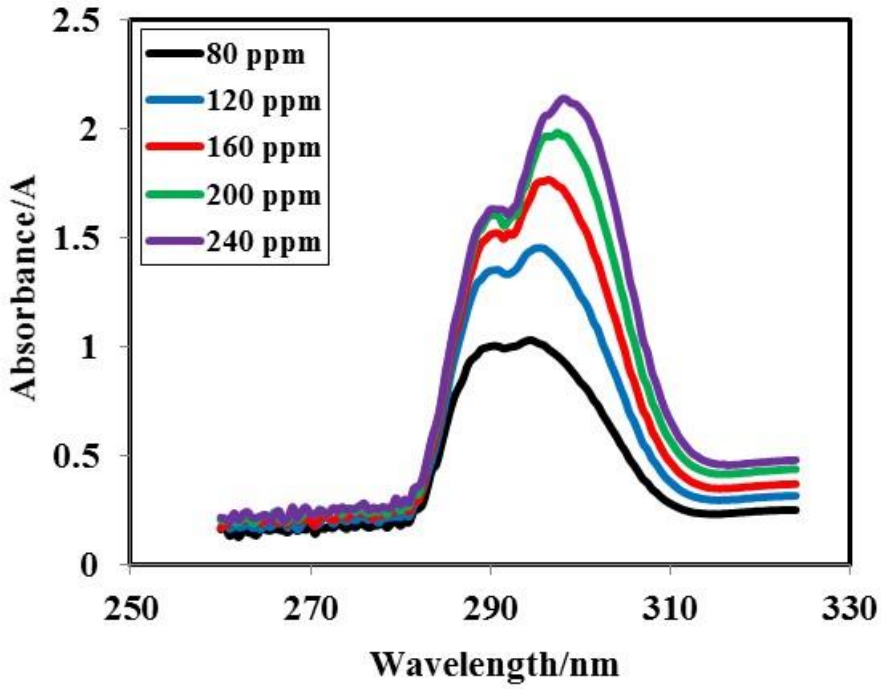

Figure 4.80: UV-Vis spectra of different concentrations (80-240 ppm) of standard VB_6 in water.

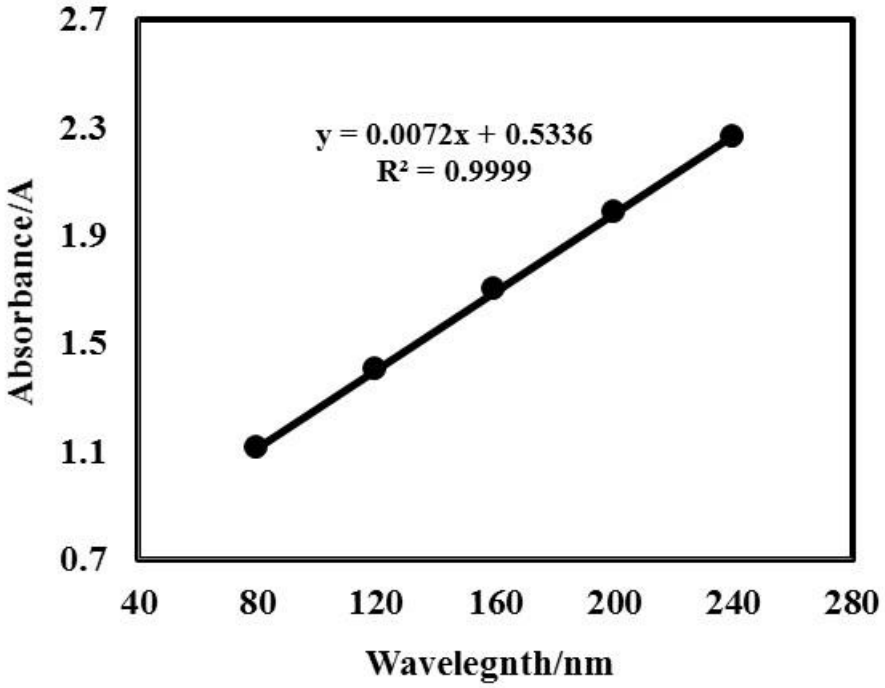

Figure 4.81: Calibration curve of standard VB_6 with response to different concentrations (80-240 ppm) in water.

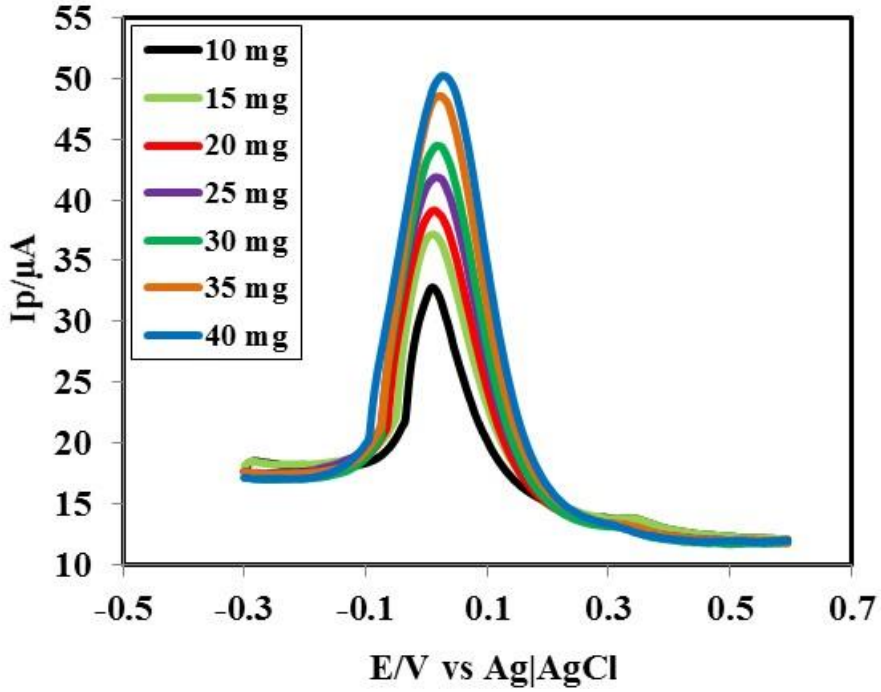

Figure 4.82: Differential pulse voltammogram (DPV) of different amount (10-40 mg) of standard VC in 50 mL PBS (pH 7) at SFL modified GC electrode.

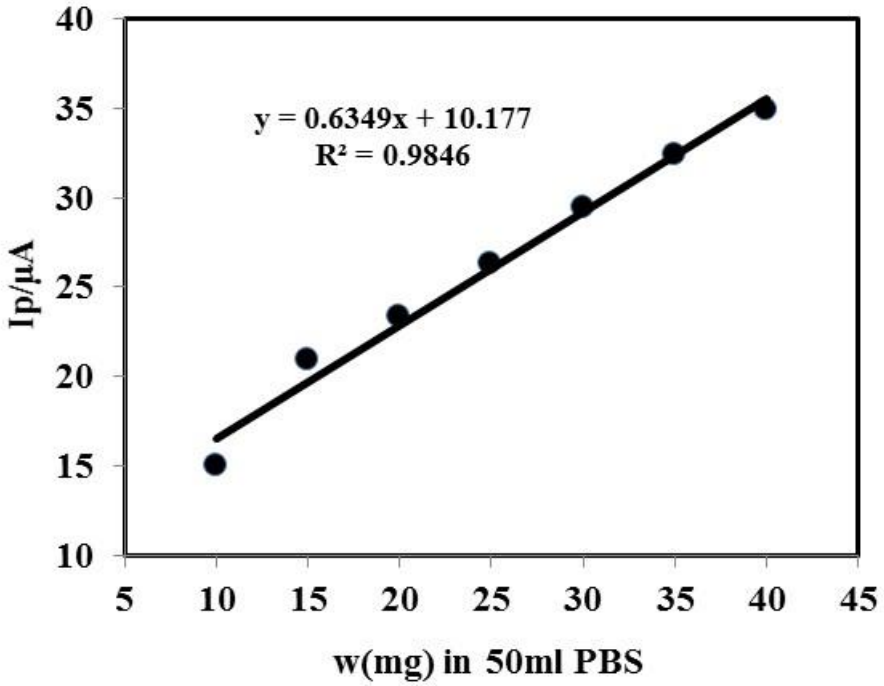

Figure 4.83: Calibration curve of VC with response to different amount (10-40 mg) in 50 mL PBS (pH 7).

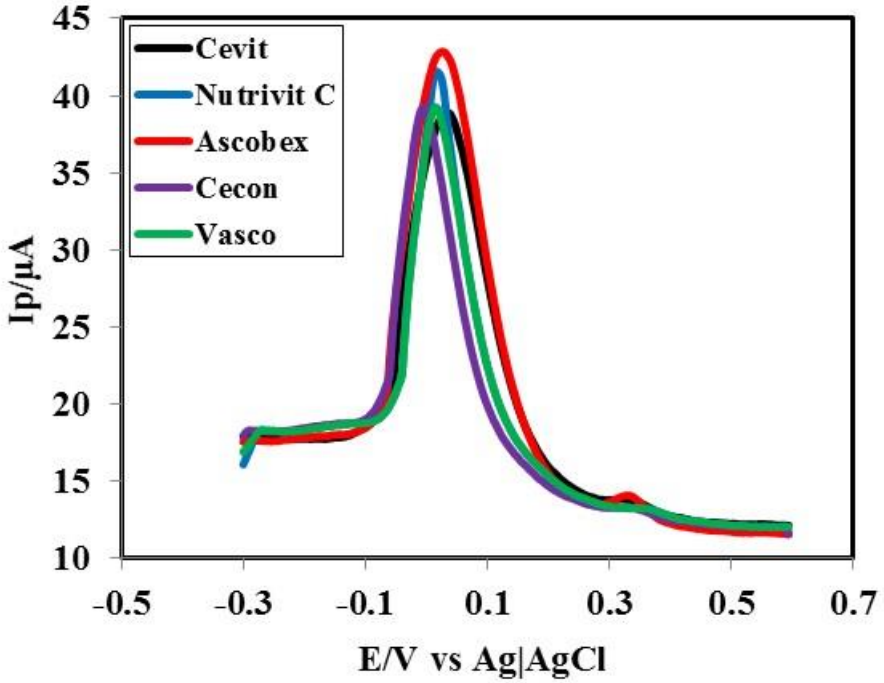

Fig 4.84: Differential pulse voltammogram (DPV) of VC in Cevit (black line), Nutrivit C (blue line), Ascobex (red line), Cecon (purple line) and Vasco (green line) tablets in PBS (pH 7) at SFL modified GC electrode.

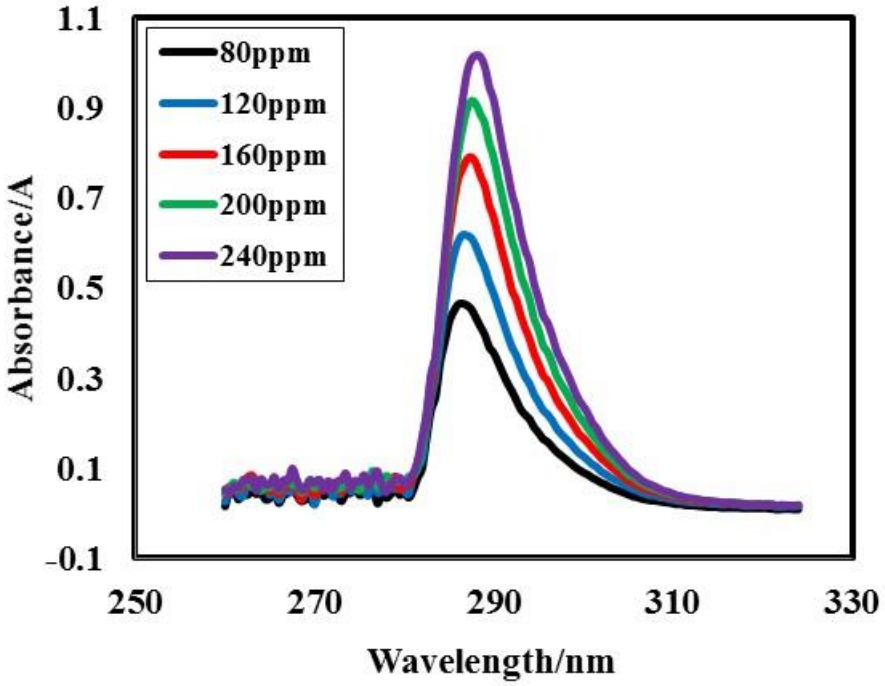

Figure 4.85: UV-Vis spectra of different concentrations (80-240 ppm) of standard VC in water.

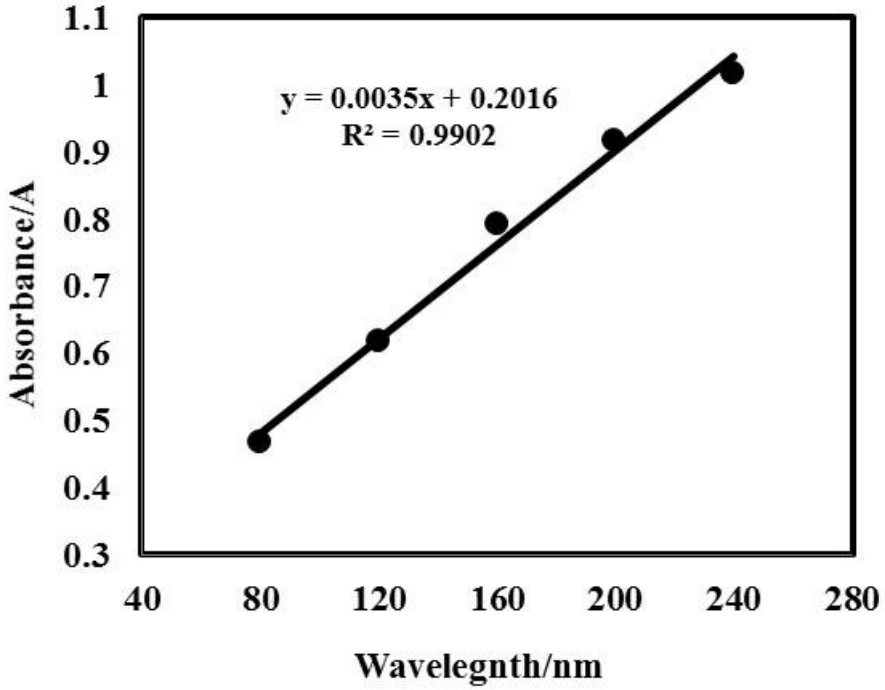

Figure 4.86: Calibration curve of standard VC with response to different concentrations (80-240 ppm) in water.

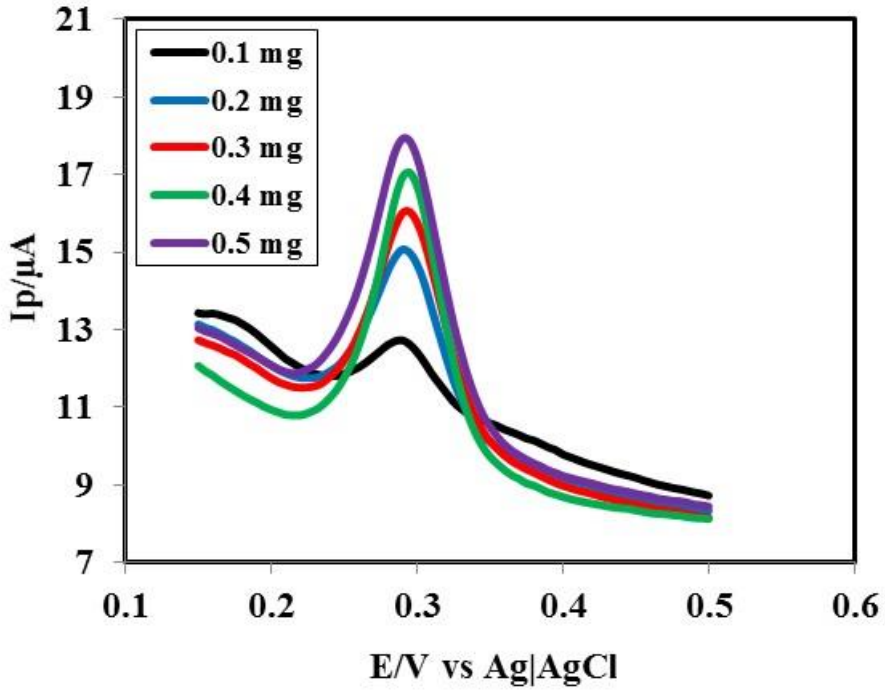

Figure 4.87: Differential pulse voltammogram (DPV) of different amount (0.1-0.5 mg) of standard UA in 50 mL PBS (pH 7) at SFL modified GC electrode.

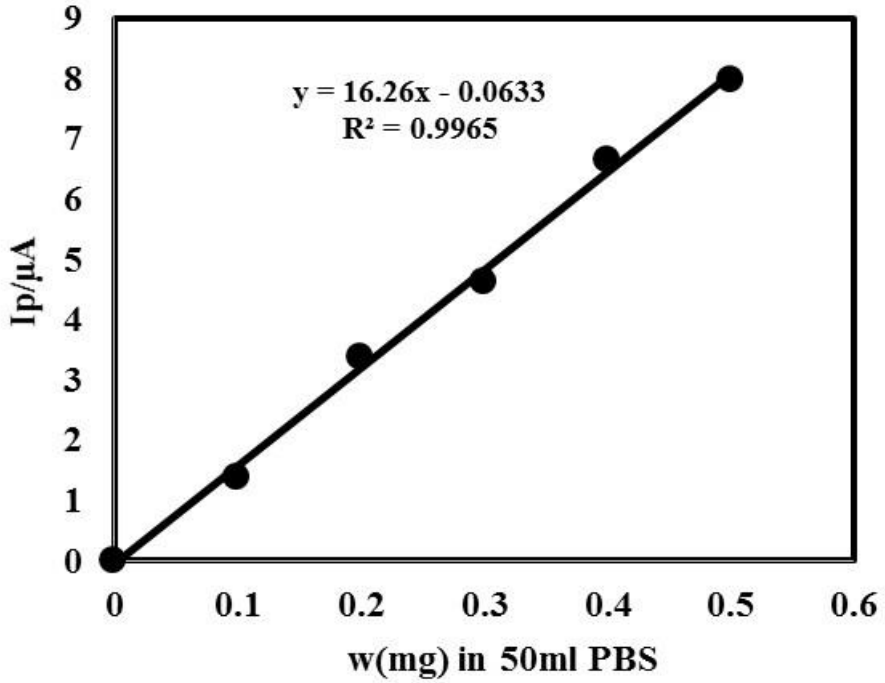

Figure 4.88: Calibration curve of UA with response to different amount (0.1-0.5 mg) in 50 mL PBS (pH 7).

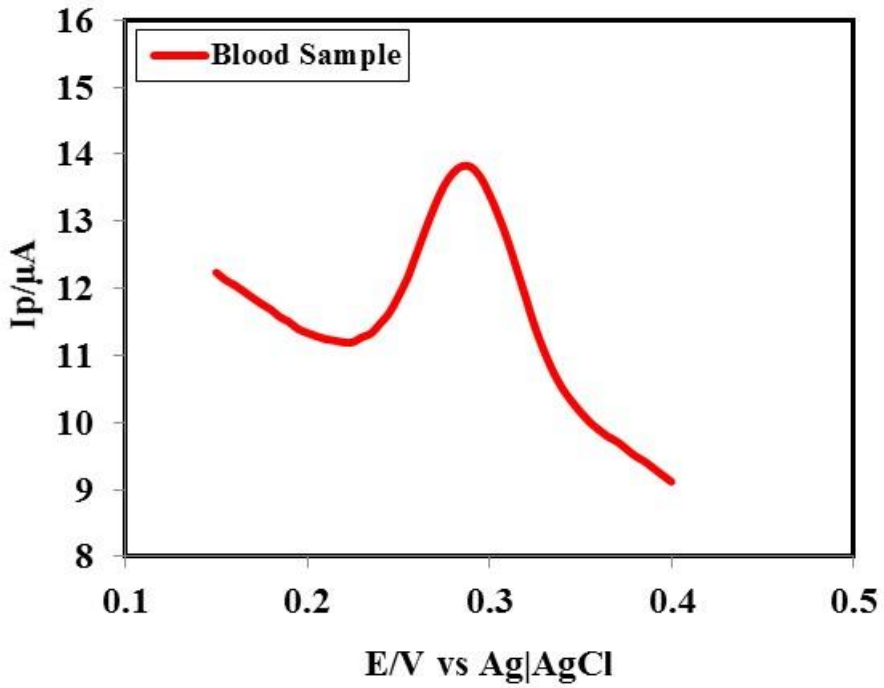

Fig 4.89: Differential pulse voltammogram (DPV) of UA in blood sample in PBS (pH 7) at SFL modified GC electrode at scan rate 0.1 V/s.

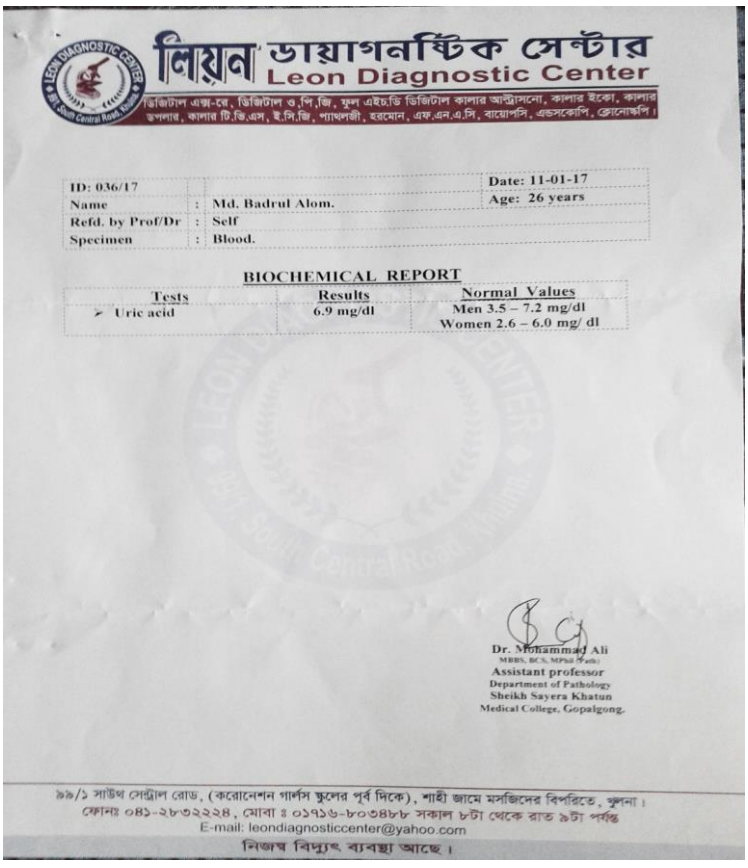
লিয়ন ডায়াগনষ্টিক সেন্টার
Leon Diagnostic Center

ডিজিটাল এক্স-রে, ডিজিটাল ও.পি.জি, ফুল এইচডি ডিজিটাল কালার আল্ট্রাসনো, কালার ইকো, কালার ডপলার, কালার টি.ডি.এস, ই.সি.জি, প্যাথলজী, হরমোন, এফ.এন.এ.সি, বায়োপসি, এন্ডসকোপি, কোলোস্কপি।

ID: 036/17			Date: 11-01-17
Name	:	Md. Badrul Alom.	Age: 26 years
Refd. by Prof/Dr	:	Self	
Specimen	:	Blood.	

BIOCHEMICAL REPORT

Tests	Results	Normal Values
➢ Uric acid	6.9 mg/dl	Men 3.5 – 7.2 mg/dl Women 2.6 – 6.0 mg/ dl

Dr. Mohammad Ali
MBBS, BCS, MPhil (Path)
Assistant professor
Department of Pathology
Sheikh Sayera Khatun
Medical College, Gopalgong.

৯৯/১ সাউথ সেন্ট্রাল রোড, (করোনেশন গার্লস স্কুলের পূর্ব দিকে), শাহী জামে মসজিদের বিপরিতে, খুলনা।
ফোনঃ ০৪১-২৮৩২২২৪, মোবাঃ ০১৭১৬-৮০৩৪৮৮ সকাল ৮টা থেকে রাত ৯টা পর্যন্ত
E-mail: leondiagnosticcenter@yahoo.com
নিজস্ব বিদ্যুৎ ব্যবস্থা আছে।

Fig 4.90: Pathological report for the determination of UA in human blood sample.

CHAPTER V

Conclusions

Vitamin B_6 (VB_6), Vitamin C (VC) and Uric acid (UA) are very important biological compounds which coexist in living systems such as blood and urine. The qualitative and quantitative determination of these three compounds have been carried out in this work. Cyclic voltammetry (CV) and Differential pulse voltammetry (DPV) techniques were used for the detection and UV-Vis spectroscopic method and pathological method was used for the validation of the quantitative determination.

A simple and sensitive electrochemical sensor based on Sulfolane (SFL) modified Glassy carbon (GC) electrode was developed for the determination of VB_6, VC and UA. The SFL modified GC electrode has been found to have sensing capability for the quantitative determination of VB_6, VC and UA.

The detection was mostly favorable at pH 7. SFL modified GC electrode shows very good sensitivity than bare GC electrode with considerable detection limit. In simultaneous detection, the LoD for VB_6, VC and UA are 0.8 μML^{-1}, 1.0 $\mu ML^{-1}$and 0.2 μML^{-1} respectively at SFL modified GC electrode. The sensitivity for VB_6, VC and UA are 41.84 $\mu A/mM/cm^2$, 31.12 $\mu A/mM/cm^2$ and 138.14 $\mu A/mM/cm^2$ respectively.

SFL modified GC electrode shows very good recovery value with minimum standard deviations. It was successfully used to determine the amount of VB_6 and VC in their relevant tablets of some different pharmaceutical companies of Bangladesh and UA in blood sample. The modified electrode sensor values are consistent with spectroscopic measurement value. SFL modified electrode is simple and rapid to fabricate. The sensor showed a stable output response and good selectivity in the presence of interfering species.

SFL modified GC electrode sensor is recommended to the pharmaceutical industries for the determination of VB_6 and VC. This sensor can also be recommended for the determination of UA in blood sample. It can save testing time and testing reagents to reduce the testing cost of the tablets and blood sample.

REFERENCES

1. P. Atkines and J. de Paul, 2010, “Physical Chemisty”, W. H. Freeman and Co., New York, 9th Ed.

2. R. Banerjee, D. Becker, M. Dickman, V. Gladyshev and S. Ragsdale, 2007, “Redox Biochemistry”, willey, New York, 2nd Ed.

3. P. T. Kissenger and W. R. Heineman, 1996, “Laboratory Techniques in Electroanalytical Chemistry”, Marcel Dekker, New York, 2nd Ed.

4. J. Wang, 2006, “Electroanalytical Chemistry”, Wiley-VCH Pub., New Jersey, 3rd Ed.

5. M. R. Smyth and J. G. Vos, 1992, “Analytical Voltammetry. XXVII”, Elsevier Science Pub., Amsterdam.

6. Holford, T. R. J., Davis, F. and Higson, S.P.J., 2012, “Recent trends in antibody based sensors”, Biosensors & Bioelectronics, Vol. 34, pp. 12-24.

7. Palchetti, I. and Mascini, M., 2012, “Electrochemical Nanomaterial Based Nucleic Acid Apta sensors”, Analytical and Bioanalytical Chemistry, Vol 402, pp. 3103-3114.

8. Perfezou, M., Turner, A. and Merkoci, A., 2012, “Cancer Detection Using Nanoparticle - Based Sensors”, Chemical Society Reviews, Vol. 41, pp. 2606-2622.

9. A. J. Bard and L. R. Faulkner, 2000, “Electrochemical Methods, Fundamentals and Applications”, John wiley & sons, inc., USA, 2nd Ed.

10. Skoog, D. A., West, D. M., Holler, F. J. and Crouch, S. R., 2007, “Principles of Instrumental Analysis”, Belmont, CA: Brooks/Cole, Thomson. p. 1. ISBN 0-495-01201-7.

11. Skoog, D. A., West, D. M. and Holler, F. J., 2014, Fundamentals of Analytical Chemistry, 7th Ed.). Harcourt Brace College Publishers, ISBN 0-03-005938-0.

12. X. Zhang, H. Ju and J. Wang, 2008, Electrochemical sensors, biosensors and their biomedical applications, Elsevier, Academic press.

13. Eggins, B. R., 2008, “Chemical Sensors and Biosensors (Google eBook)”, John Wiley & Sons.

14. Palchetti, I. and Mascini, M., 2012, “Electrochemical Nanomaterial Based Nucleic Acid Apta sensors”, Analytical and Bioanalytical Chemistry, Vol 402, pp. 3103-3114.

15. Murray, R. W., 1984, “Chemically Modified Electrodes”, Electroanalytical Chemistry, Vol. 13 pp. 379.

16. Buck, R. P., Freiser, H. and Plenum, N.Y., 1978, “Theory and Principles of Membrane Electrodes”, Chapt. 1, Ion-Selective Electrodes in Analytical Chemistry, Vol. 1.

17. Ross, J. W., Riseman, J. H. and J. A. Krueger., 1973, Pure Appl. Chem., Vol. 36(4), pp. 473.

18. Clark, L. C. Trans. Am. SOC. Artif, 1956, Int. Organs., Vol. 2, pp. 41.

19. Janata, J. and Huber, R. J., 1985, “Solid State Chemical Sensors,” Academic Press, Orlando, FL.

20. Ren, W., Luo, H. Q. and Li, N. B., 2006, Biosens. Bioelectron., Vol. 21, pp. 1086.

21. Duvall, S. H. and McCreery, R. L., 1999, Anal. Chem., Vol. 71, pp. 4594.

22. Murray, R. W., 1980, Acc. Chem. Res., Vol. 13, pp. 135.

23. Qi, H. L. and Zhang, C. X., 2005, Electroanal., Vol. 17, pp. 832.

24. Diab, N., Oni, J. and Schuhmann, W., 2005, Bioelectrochem., Vol. 66, pp. 105.

25. Deng, C., Li, M., Xie, Q. Liu, M. Tan, Y. Xu, X. and Yao, S., 2006, Anal. Chem. Act., Vol. 557, pp. 85.

26. Chen, Z., and Zhou, Y., 2006, Surface and Coatings Technology, Vol. 201, pp. 2419.

27. Pyun, S. and Bae, J. S., 1997, J. Power Sources, Vol. 68, pp. 669.

28. Sivakumar, C., Nian, J. N. and Teng, H., 2005, J. Power Sources, Vol. 144, pp. 295.

29. Munoz, E., Heras, M. A., Colina, A. I., Ruiz, V. and Lo’pez-Palacios, J., 2007, Electrochem. Acta, Vol. 52, pp. 4778.

30. Urray, R. W., 1980, Acc. Chem. Res., Vol. 13, pp. 135.

31. Qi, H. L. and Zhanh, C. X., 2005, Electroanal., Vol. 17, pp. 832.

32. Juan, L. and Xiaoli, Z., 2012, American Journal of Analytical Chemistry, Vol. 3, pp. 195-203.

33. Bensalah, N., Gadri, A., Canizares, P., Saez, C., Lobato, J. and Rodrigo, M. A., 2005, Environ. Sci. Technol., Vol. 39, pp. 7234.

34. Lau, O.W., Luk, S. F. and Cheung, Y. M., 1989, Analyst, Vol. 114, pp. 1047-1051.

35. Fernandes, D. M., Silva, N., Pereira, C., Moura, C., Magalhaes, J. M. C. S., Bachiller-Baeza, B., Rodriguez-Ramos, I., Guerrero-Ruiz, A., Delerue-Matos, C. and Freire, C., 2015, Sens. Actuators B, Vol. 218, pp. 128-136.

36. Sathisha, T. V., Kumara, S. B. E., Chandrashekar, B. N., Thomas, N. and Eswarappa, B., 2012, J. Electroanal. Chem., Vol. 674, pp. 57-64.

37. Wang, G., Meng, J., Liu, H., Jiao, S., Zhang, W., Chen, D. and Fang, B., 2008, Electrochimica Acta, Vol. 53, pp. 2837-2843.

38. Zhao, H., Zhang, Y. Z. and Yuan, Z. B., 2002, Electroanal., Vol. 14, pp. 1031.

39. Roy, P. R., Saha, M. S., Okajima, T., Park, S. G., Fujishima, A. and Ohsaka, T., 2004, Electroanal., Vol. 16, pp. 1777.

40. Roy, P. R., Saha, M. S., Okajima, T., and Ohsaka, T., 2004, Electroanal., Vol. 16, pp. 289.

41. Roy, R. R., Okajima, T. and Ohsaka, T., 2004, J. Electroanal. Chem., Vol. 75, pp. 561.

42. IUPAC Recommendation, 1997, Pure and Appl. Chem., Vol. 69, pp. 132.

43. Johannson, S., Lindstedt, S. and Tiselius, H., 1973, "Metabolic interconversions of different forms of Vitamin B_6", J. Biol. Chem., Vol. 249, pp. 6040–6046.

44. Yunhua, Wu. and Fajun, S., 2008 "Voltammetric Investigation of Vitamin B6 at a Glassy Carbon Electrode and Its Application in Determination", Bull. Korean Chem. Soc., Vol. 29, pp. 38-42.

45. Hai-Ying, G., Ai-Min Y. and Hong-Yuan C., 2001, "Electrochemical Behavior and Simultaneous Determination of Vitamin B_2, B_6 and C at Electrochemically Pretreated Glassy Carbon Electrode", Analytical Letters, Vol. 34, pp. 2361-2374.

46. L. A. Kaplan and A. J. Pesce, 1989, "Clinical Chemistry-Theory, analysis and correlation", The C.V. Mosby Company, St. Louis- USA, 2nd Ed., pp 808–819.

47. Afkhami-Ardekani M. and Shojaoddiny-Ardekani A., 2007, "Effect of vitamin C on blood glucose, serum lipids & serum insulin in type 2 diabetes patients", Indian J Med. Res., Vol. 126, pp. 471.

48. Antoon AY, Donovan DK. Burn Injuries. In: Behrman RE, Kliegman RM, Jenson HB., 2000, eds. Nelson Textbook of Pediatrics. Philadelphia, Pa: W. B. Saunders Company, pp. 287-294.

49. Aureda C, Patulny RV, Sander BH, Douglas RM., 2001, Mega-dose vitamin C in treatment of the common cold: a randomized controlled trial., Med. J Aust., Vol. 175(7), pp. 359-362.

50. "Ascorbic Acid". The American Society of Health-System Pharmacists. Retrieved 8 December 2016.

51. Vitart, V., Rudan, I. and Hayward, C., 2008, "SLC_2A_9 is a newly identified urate transporter influencing serum urate concentration, urate excretion and gout", Nature Genetics, Vol. 40(4), pp. 437–442.

52. Ping, J., Wu, J., Wang, Y. and Ying, Y., 2012, "Simultaneous determination of ascorbic acid, dopamine and uric acid using high-performance screen-printed graphene electrode", Biosensors and Bioelectronics, Vol. 34, pp. 70-76.

53. Glantzounis, G. K., Tsimoyiannis, E. C., Kappas, A. M. and Galaris, D. A., 2005, "Uric acid and oxidative stress", Current Pharmaceutical Design, Vol. 11(32), pp. 4145–4151.

54. Hayden, M. R. and Tyagi, S. C., 2004, "Uric acid: A new look at an old risk marker for cardiovascular disease, metabolic syndrome, and type 2 diabetes mellitus: The urate redox shuttle", Nutrition & Metabolism, Vol. 1(1), pp. 10.

55. Hillis O. Folkins, 2005, "Benzene" Ullmann's Encyclopedia of Industrial Chemistry, Wiley-VCH, Weinheim.

56. T. A. Nieman, D. A. Skoog and F. J. Holler, 1988, Principles of instrumental analysis, Pacific Grove, California.

57. J. A. Plambeck, 1982, Electroanalytical Chemistry, Basic Principles and Application, Wiley Inter science Pub., USA.

58. M. E. Hossain, 2014, "Electrochemical sensor simultaneous detection and estimation of environmental toxic pollutants", M.Phil Thesis, KUET.

59. http://www.drhuang.com/science/chemistry/electrochemistry/polar.doc.htm.

60. D.A. Skoog, F.J. Holler and T.A. Nieman, 2007, "Principles of Instrumental Analysis", Thomson Brooks/ Cole, 6^{th} Ed., pp. 349-351.

61 Skoog, D. A., Holler, F. J. and Neiman, T. A., 2007, Principles of Instrumental Analysis, 6th edn, Thomson Brooks/Cole., pp. 169-173.

62. https://www.google.com/?gws_rd=ssl#q=Definition+of+electrochemical+cell.

63. P.T. Kissinger and W.R. Heineman, 1996, "Laboratory Techniques in Electroanalytical Chemistry", Marcel Dekker, Inc.

64. Hai-Ying G., Ai-Min Y. and Hong-Yuan C., 2001, "Electrochemical Behavior and Simultaneous Determination of Vitamin B_2, B_6, and C at Electrochemically Pretreated Glassy Carbon Electrode", ANALYTICAL LETTERS, Vol. 34, pp. 2361–2374.

65. Marcos T. F. S., Segnini A., Moraes F. C., Marcolino L. H. J., Fatibello F. O. and Cavalheiro E. T. G., 2003, "Determination of Vitamin B6 (Pyridoxine) in Pharmaceutical Preparations by Cyclic Voltammetry at a Copper(II) Hexacyanoferrate(III) Modified Carbon Paste Electrode", J. Braz. Chem. Soc., Vol. 14, pp. 316-321.

66. Ahmed R., Qureshi S. A. and Nisa V. U., 2005, "Studies About the Determination of Ascorbic Acid by Differential Pulse Voltammetry", Jour. Chem. Soc. Pak., Vol. 27, pp. 168-173.

67. Zhao Y., Bai J., Wang L., XuHong E., Huang P., Wang H. and Zhang L., 2006, "Simultaneous Electrochemical Determination of Uric Acid and Ascorbic Acid Using L-Cysteine Self-Assembled Gold Electrode", Int. J. Electrochem. Sci., Vol. 1, pp. 363-371.

68. Wu Y. and Song F., 2008, "Voltammetric Investigation of Vitamin B6 at a Glassy Carbon Electrode and Its Application in Determination", Bull Korean Chem. Soc., Vol. 29, pp. 38-42.

69. Wang G., Meng J., Liu H., Jiao S., Zhang W., Chen D. and Fang B., 2008, "Determination of uric acid in the presence of ascorbic acid with hexacyanoferrate lanthanum film modified electrode", Electrochimica Acta, Vol. 53, pp. 2837-2843.

70. Yang G., Tan L., Shi Y., Wang S., Lu X., Bai H. and Yang Y., 2009, "Direct Determination of Uric Acid in Human Serum Samples Using Polypyrrole Nanoelectrode Ensembles", Bull. Korean Chem. Soc., Vol. 30, pp. 454-458.

71. Yuzhong, Z. and Yuehong, W., 2011, "Voltammetric Determination of Vitamin B_6 at Glassy Carbon Electrode Modified with Gold Nanoparticles and Multi-Walled Carbon Nanotubes", American Journal of Analytical Chemistry, Vol. 2, pp. 194-199.

72. Hadi, B, Hassan, K. M. and Iran, S., 2012, "Simultaneous Voltammetric Determination of Ascorbic Acid and Uric Acid Using a Modified Multiwalled Carbon Nanotube Paste Electrode", Caspian Journal of Chemistry, Vol. 1, pp. 17-29.

73. Shou-Qing, L, Wei-Hui, S, Li-Chun, L, Hua, L. and Xiu-Ling, W., 2012, " Electrocatalytic Oxidation and Voltammetric Determination of Vitamin B_6 by a ssDNA-modified Electrode", International Journal of Electrochemical Science, Vol. 7, pp. 324 – 337.

74. Sadikoglu M., Taskin G., Demirtas F. G., Selvi B., and Barut M., 2012, "Voltammetric Determination of UricAcid on Poly(p-Aminobenzene Sulfonic Acid)-Modified Glassy Carbon Electrode", Int. J. Electrochem. Sci., Vol. 7, pp. 11550 – 11557.

75. Fritea L., Tertiş M., Cristea C. and Sandulescu R., 2013, "New β-Cyclodextrin Entrapped in Polyethyleneimine Film-Modified Electrodes for Pharmaceutical Compounds Determination", Sensors, Vol. 13, pp. 16312-16329.

76. Ngai K. S., Tan W. T., Zainal Z., Zawawi R. M. and Zidan M., 2013, "Voltammetry Detection of Ascorbic Acid at Glassy Carbon Electrode Modified by Single-Walled Carbon Nanotube/Zinc Oxide", Int. J. Electrochem. Sci., Vol. 8, pp. 10557 – 10567.

77. Lamari A. S., Fattouh A. E., Qouatli S. E. E., Najih R. and Chtaini A., 2013, "Electrochemical Detection of Ascorbic Acid Using A Polymer Modified Carbon Paste Electrode", ACTA TECHNICA CORVINIENSIS-Bulletion of Engineering, Vol. 2, pp. 39-42

78. Bikila N. O., Shimeles A. K. and Tesfaye R. S., 2015, "Electrochemical determination of ascorbic acid at p-phenylenediamine film–holes modified glassy carbon electrodes", J. Serb. Chem. Soc., Vol. 80, pp. 1161-1175.

79. Afrasiabi M. and Kianipour S., 2015, "Simultaneous Determination of Ascorbic Acid, Uric Acid and Acetaminophen on a Glassy Carbon Electrode Coated with a Novel Single Walled Carbon Nanotubes/ Chitosan/ MCM-41 Composite", Anal. Bioanal. Electrochem., Vol. 7, pp. 331-343.

80. Eser, E, Serife, K, Derya, K. Z. and Bulent, Z., 2016, "Simultaneous electrochemical determination of ascorbic acid and uric acid using poly(glyoxal-bis(2-hydroxyanil)) modified glassy carbon electrode", Sensors and Actuators B, Vol. 224, pp. 55-64.

81. Shoup, D. and Szabo, A., 1982, Journal of Electroanalytical Chemistry, Vol. 140, pp. 237.

82. Ikeuchi, H. and Kanakubo, M., 2000, Journal of Electroanalytical Chemistry, Vol. 493, pp. 93.

83. Gavaghan, D.J. and Rollett, J.S., 1990, Journal of Electroanalytical Chemistry, Vol. 295, pp. 1.

84. Qian, W., Jin, B., Diao, G., Zhang, Z. and Shi, H., 1996, Journal of Electroanalytical Chemistry, Vol. 414, pp. 1.

85. Skoog, D. A., Holler, F. J. and Neiman, T. A., 2007, Principles of Instrumental Analysis, 6th Ed., Thomson Brooks/Cole., pp. 169-173.

86. Bland, J.M. and Altman, D.G., 1996, "Statistics notes: measurement error", BMJ, Vol. 312, pp. 1654.

87. M. Whitfield, and D. Jagner,, 1981, Marine electrochemistry: A practical introduction, John Wiley &Sons Inc.

88. Jr. D.K. Gosser, 1993, "Cyclic Voltammetry (Simulation and analysis of reaction mechanisms)", Wiley-VCH, Inc.

89. C.M.A. Brett and A.M.O. Brett, 1998, "Electroanalysis", Oxford University Press.

90. S. P. Kounaves, 1997, "Voltammetric Techniques" in Handbook of Instrumental Techniques for Analytical Chemistry, Upper saddle river, NJ.

91. Armada, P. G., Losada, J. and Perez, S. V., 1996, “Cation analysis scheme by differential pulse polarography”, Vol. 73(6), pp. 544-546.

92. E.R. Brown, R.F. Larg, A. Weissberger and B. (Eds.) Rossiter, 1971, Physical Methods of chemistry, Wiley-Inter science, New York, Vol.1-Part IIA.

93. F.M. Hawkridgein, P.T. Kissinger and W.R. Heieman, 1996, “Laboratory Techniques in Electroanalytical chemistry”, Marcel Dekker Inc., New York, 2nd Ed.